PhD

PROGRAM IN TRANSLATIONAL AND MOLECULAR MEDICINE

DIMET

UNIVERSITY OF MILANO-BICOCCA
SCHOOL OF MEDICINE AND SCHOOL OF SCIENCE

MYC acts as a tumor reprogramming factor in human mammary epithelial cells by inducing stem cell-like fate

Coordinator: Prof. Andrea Biondi
Tutor: Dr. Alessio Zippo

Dr. Vittoria POLI
Matr. No. 774795

XXVIII CYCLE
ACADEMIC YEAR
2014-2015

Table of contents

General introduction

Cancer biology

Cancer is a heterogeneous group of diseases caused by genetic and epigenetic changes. In addition, interactions between tumor cells and the stromal micro-environment are a crucial determinant of malignant growth (Tlsty and Coussens, 2006).

Tumorigenesis is a multistep process in which deregulation of the transcriptional program and disruption of molecular networks lead to the selective acquisition by cells of a number of functional characteristics that cause their transformation and further progression to a malignant phenotype (Hanahan and Weinberg, 2011). The most fundamental of these hallmarks is the ability of cancer cells to sustain chronic proliferation. This is generally achieved through deregulation of growth-promoting signals, that maintain normal tissue architecture and function (Bhowmick et al., 2004; Cheng et al., 2008; Hynes and MacDonald, 2009; Witsch et al., 2010), and inactivation of tumor suppressor genes (e.g. *RB* and *TP53*), that negatively regulate cell proliferation (Burkhart and Sage, 2008; Lowe et al., 2004; Sherr and McCormick, 2002). Another mechanism through which cancer cells resist to cell death and acquire unlimited replicative potential is the up-regulating expression of telomerase, the specialized DNA polymerase that, by adding telomere repeat segments to the ends of telomeric DNA, counters the progressive telomere erosion (Blasco, 2005).

In normal tissues, most blood vessels are quiescent, and angiogenesis (growth of new blood vessels from pre-existing ones) occurs only during the female reproductive cycle and under certain pathophysiological conditions (Carmeliet and Jain, 2011). An early event in the multistage development of cancer is the up-regulation of proangiogenic signals (e.g. VEGF-A, angiopoietin and members of the FGF family) that cause quiescent endothelial cells to enter in a cell-biological program consisting in a chronically activated angiogenesis necessary for tumor sustenance (Baeriswyl and Christofori, 2009; Bergers and Benjamin, 2003; Carmeliet, 2005; Hanahan and Folkman, 1996; Raica et al., 2009). Tumor-associated vessels are distinctly irregular and inherently unstable (De Bock et al., 2011; McDonald and Choyke, 2003).

The invasive and chaotic organization of tumor-associated neo-vasculature, combined with the chronic and uncontrolled cell proliferation, result in series of adjustments of energy metabolism. Under aerobic conditions, normal cells process glucose first to pyruvate, via glycolysis in the cytoplasm, and then to carbon dioxide in the mitochondria. Most cancer cells instead, even in the presence of oxygen, limit their energy metabolism largely to glycolysis, switching to a so called “aerobic glycolysis”. Since aerobic glycolysis is an inefficient way to generate ATP, respect to mitochondrial oxidative phosphorylation, cancer cells must compensate in part by upregulating glucose transporters (DeBerardinis et al., 2008; Hsu and Sabatini, 2008; Jones and Thompson, 2009). This reliance on aerobic glycolysis has been shown to be associated with activated oncogenes

(e.g. *RAS* and *MYC*) and mutant tumor suppressor (e.g. *TP53*) (DeBerardinis et al., 2008; Jones and Thompson, 2009) and can be further accentuated under the hypoxic conditions that operate within many tumors (DeBerardinis et al., 2008; Jones and Thompson, 2009; Semenza, 2010). Furthermore, increased glycolysis allows the employment of glycolytic intermediates into various biosynthetic pathways, including those involved in nucleoside and amino acid production, thus supporting the large-scale biosynthetic programs required for active proliferation (Vander Heiden et al., 2009).

For what concerns epithelial cancers, as the carcinoma progresses to higher grades of malignancies, cells acquire invasion and metastatic potential (Fidler, 2003). A means by which transformed epithelial cells can acquire the abilities to invade and disseminate is the epithelial-mesenchymal transition (EMT), a developmental process that can be reactivated in the adult during wound healing, fibrosis and cancer progression. During EMT, epithelial cells undergo a series of rapid changes during which they down-regulate cell-cell adhesion structures, lose their apical-basal polarity and reorganize their cytoskeleton (Fidler, 2003; Polyak and Weinberg, 2009; Thiery et al., 2009). This increases the motility of individual cells and enables the development of an invasive phenotype. This process can be activated transiently or stably by carcinogenic cells and is mediated by key transcription factors, including SNAIL, SLUG, TWIST and ZEB1/2, whose functions are finely regulated at the transcriptional, translational and post-translational levels.

It is well established that a fundamental part of cancer etiology is the stepwise accumulation of genetic mutations, including deletions, chromosomal rearrangements and gene amplifications (Hanahan and Weinberg, 2011). Cancer initiation and, more rarely, cancer progression can depend on the activation of certain oncogenes, most commonly *PI3K*, *MYC* and *RAS*, and on the inactivation of key tumor suppressor genes like *APC*, *TP53*, *PTEN*, *P21*, $P16^{INK4A}$ and *RB*. Such events are thought to be followed by a clonal selection of variant cells that show increasingly aggressive behaviours (Marusyk and Polyak, 2010).

Nevertheless, new models of oncogenic progression must consider the combined effect of genetic and epigenetic changes as determinant of tumor heterogeneity. Epigenetic alterations involve both losses and gains of DNA methylation, as well as altered patterns of histone modifications, that are linked to changes in gene expression and contribute to carcinogenesis, tumor invasion and metastasis (Feinberg, 2004). The best described epigenetic event in tumorigenesis is the transcriptional repression of tumor suppressor genes associated with hypermethylation at the CpG islands that lie in their promoter regions (Herman and Baylin, 2003; Jones and Baylin, 2002). These kind of events affect diverse genes, such as *RB* in retinoblastoma, $P16^{INK4A}$ in melanoma, *VHL* in renal cell carcinoma and *APC* in colorectal cancer (Gonzalez-Zulueta et al., 1995; Greger et al., 1994; Herman et al., 1994; Hiltunen et al., 1997). Another hallmark of tumors, both benign and malignant, is the global reduction of DNA methylation (Feinberg and Vogelstein, 1983). For

what concerns chromatin alterations, over production of key histone methyltransferases, that catalyze the methylation of either H3-K4 or H3-K27 residues, and global reductions in monoacetylated H4-K16 and trimethylated H4-K20 are common hallmark of human cancer (Fraga et al., 2005; Hess, 2004; Sellers and Loda, 2002).

In cancer initiation, genetic and epigenetic alterations may interact in that epigenetic alterations may render the cell more susceptible to subsequent genetic insults. For example, hypomethylation generally arises early during tumorigenesis and leads to chromosomal instability and increased tumor frequency (Eden et al., 2003; Gaudet et al., 2003), as well as activation of specific oncogenes, such as *RAS* and *Cyclin D2* in gastric cancer (Nishigaki et al., 2005; Oshimo et al., 2003; Sato et al., 2003). Furthermore, recent studies have shown that although the abnormal epigenetic silencing of genes can occur at any time during tumor progression, it occurs most frequently during the early stages of the neoplastic process, such as the precancerous stage (Feinberg and Tycko, 2004; Holst et al., 2003; Romanov et al., 2001). It has been proposed that these early epigenetic alterations could predispose cells to the acquisition of genetic abnormalities that would advance the neoplastic process. In some cases epigenetic changes and their interactions with genetic aberrations, can cause an addiction of neoplastic cells to certain oncogenic driving signaling. In fact, it is possible that epigenetic mechanisms induce constitutive activation of a signaling pathway even before the appearance of mutations in that pathway. As a consequence, cells that rely on the pathway for

proliferation, would start to expand abnormally and will be positively selected for their survival and proliferative advantages. This fact could enhance their probability to acquire subsequent mutations to the level of genes that lie downstream in the pathway, with consequent further increase of cellular addiction to the abnormalities and resultant tumor progression (DeAngelo et al., 2002; Gregorieff and Clevers, 2005; Hao et al., 2001; Mori et al., 2004).

The existence of epigenetic precursor lesions could explain the relationship between environmental exposure or injury and cancer: environmental insults, such as chronic inflammation, injury and nutrition, might influence disease onset by epigenetically affecting gene expression. For example, diet has a strong influence on DNA methylation and can increase the risk of cancer development (Pogribny and James, 2002; Poirier, 2002). Furthermore, environmental agents might lead to cancer by epigenetically disrupting key signaling pathways (Ruden et al., 2005).

It is now evident that tumor biology does not only rely on the individual specialized cell types within it, but also on the tumor microenvironment (TME), constituted by the non-cancerous cells present in the tumor (Hanahan and Weinberg, 2011). These include fibroblasts, myofibroblasts, neuroendocrine cells, adipose cells, immune and inflammatory cells, cells that comprise the blood and lymphatic vessels and the extracellular matrix (ECM), but also the proteins produced by all of the cells present in the tumor that support the growth of the cancer cells (Chen et al., 2015). The stroma of healthy individuals has a critical role in maintaining tissue

physiological homeostasis and recent studies indicate a specific anticancer activity of certain stromal components (Ozdemir et al., 2014; Rhim et al., 2014). Nevertheless, normal stroma also possesses the capacity to rapidly respond to evolving environmental conditions and oncogenic signals from growing tumors and, in concert with the adjacent epithelium, induces the emergence of a “reactive stroma”. Under such conditions, the stromal cells co-evolve with the cancer cells by being induced by the latter to synthesize a wide variety of cytokines, chemokines, growth factors and proteinases, that have a dramatic accelerating effect on tumor progression (Junttila and de Sauvage, 2013).

Prominent among the TME constituents are the endothelial cells implicated in tumor-associated angiogenesis and those forming the lymphatic vessels located at the peripheries of tumors and in the adjacent normal tissues, which likely serve as channels for the seeding of metastasis. Generic constituents of tumors are also infiltrating cells of both the innate and adaptive immune system. Such immune response represents in part an attempt by the immune system to eradicate tumors, but also have functionally important tumor-promoting effects (Colotta et al., 2009; DeNardo et al., 2010; Grivennikov et al., 2010; Qian and Pollard, 2010). Indeed, inflammation can contribute to neoplastic progression through the supply of bioactive molecules to the TME, including growth factors, survival factors, proangiogenic factors, ECM-modifying enzymes, that facilitate angiogenesis, invasion and metastasis, and inductive signals that lead to activation of EMT (DeNardo et al., 2010; Grivennikov et

al., 2010; Karnoub and Weinberg, 2006; Qian and Pollard, 2010). Inflammatory cells can also release reactive oxygen species that are actively mutagenic for nearby cancer cells, therefore accelerating their evolution toward state of enhanced malignancy (Grivennikov et al., 2010).

Cancer stem cells

Evidence is accumulating that many if not most tumors harbor subpopulations of so called "cancer stem cells" (CSCs): a subclass of neoplastic stem cells able to propagate malignant clones indefinitely and to produce an overt cancer (Valent et al., 2012).

Notably, whereas normal stem cells (SCs) self-renew in a highly regulated manner, CSCs do so in a poorly controlled way, and while SCs generate normal, mature cells, CSCs often differentiate abnormally. The existence of CSCs was first proven in the context of the acute myeloid leukemia (AML), where surface markers were used to distinguish the SC subpopulation from the remaining AML cells (Bonnet and Dick, 1997; Lapidot et al., 1994). Ten years later, CSCs were isolated also in solid tumors, in particular in breast carcinomas and glioblastoma, using appropriate cell surface markers (Al-Hajj et al., 2003; Singh et al., 2003).

Although CSCs express markers that are also expressed by normal SCs in the tissue of origin, it is not sufficient to define a CSC based solely on surface markers, in the absence of linking marker expression to a self-renewal assay. Indeed, none of the markers used to isolate SCs in various normal and cancerous tissues is expressed exclusively by SCs.

CSCs can thus only be defined experimentally by their potential to show both self-renewal and tumor propagation (Pardal et al., 2003) and the gold standard assay that fulfils these criteria is the serial transplantation in animal models (Figure 1).

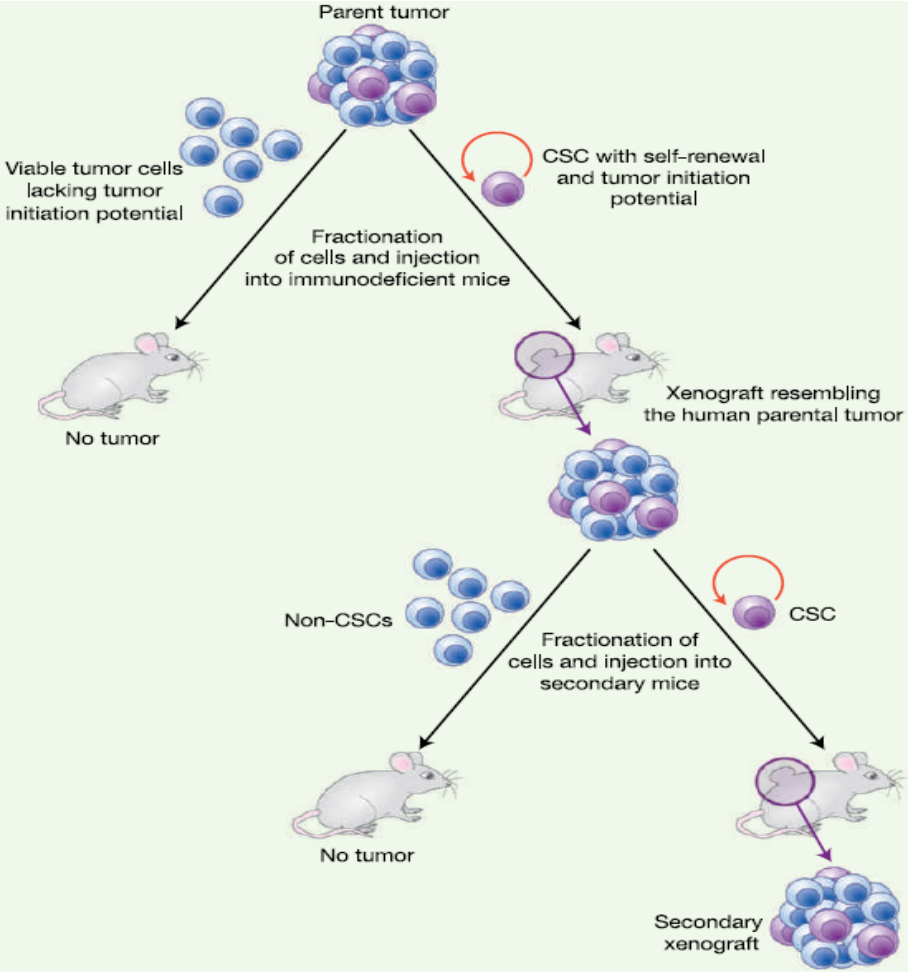

Figure 1. Features of human CSCs as assayed in immunodeficient mice (O'Brien et al., 2010).

In transplantation assays, cells are xenografted into an orthotopic site of immunocompromised mice, that are assayed for their capacity to

form tumors resembling the immune-pathological features of the primary cancer. The tumorigenic self-renewal potential is determined by measuring the capability of xenograft-derived cancer cells to engraft in secondary recipient mice. In addition to *in vivo* experiments, also several *in vitro* functional assays have been used to identify CSCs, including sphere assays, serial colony forming unit (CFU) assays and label retention assays.

The experimental demonstration of CSCs presence in several human tumors indicates the existence of a cancer cell hierarchy that contributes to the determination of intra-tumor heterogeneity. Current failure with cancer treatment is not usually due to a lack of primary response, but to relapse or tumor recurrence after therapy. This can be explained by the fact that CSCs seem to be more resistant to chemotherapy and radiotherapy than other cancer cells and can therefore escape from the conventional cytotoxic treatments, driving tumor growth that presents as clinically relapsed disease (Hoey et al., 2009; LaBarge, 2010; Varnat et al., 2010; Vermeulen et al., 2010). CSCs resistance to chemotherapeutics can be due to various reasons, including their quiescent or slowly dividing nature (Gottesman, 2002), the high expression level of ATP-binding cassette (ABC) drug pumps (Zhou et al., 2001), the intrinsic high levels of anti-apoptotic molecules, their relative resistance to oxidative or DNA damage and their efficiency of DNA repair (Bao et al., 2006; Diehn et al., 2009; Ito et al., 2004). On the basis of these observations, it has been hypothesized that treatments targeting the CSCs subpopulation could be more effective than existing therapies.

CSCs are known to have one or more aberrations in various signaling pathway. Notably, the abnormal activity of pathways that control normal SCs self-renewal and have important roles in embryonic development and differentiation, is probably most crucial to the tumorigenicity of CSCs. Increasing evidence demonstrates that these embryonic pathways can interact with other cellular signaling, such as those involving NFkB, MAPK and PI3K, and with additional signals like bone morphogenetic proteins (BMPs) and growth factors produced by cancer cells and the TME. All these signals converge to generate the CSCs distinct features and represent therefore important therapeutic (Merchant and Matsui, 2010; Takebe et al., 2011). Other potential strategies to kill CSCs include inhibiting their survival mechanisms, targeting CSCs surface markers through antibody-based cytotoxic approaches or inducing tumor cell differentiation, which can potentially be achieved by inhibiting developmental pathways or epigenetic programs. Moreover, as many CSCs can depend on a niche to maintain their identity, targeting their microenvironment could represent a strategy to indirectly inhibit or induce differentiation of CSCs (Zhou et al., 2009).

The term “cancer stem cell” does not imply that the cell necessarily derived from a normal SC: the phenotype of the cell of origin, the normal cell that acquired the first cancer-promoting insult, can deeply differ from that of the CSC (Visvader, 2011). Indeed, increasing evidence indicate that tumors may originate from SCs, progenitor cells, as well as from the dedifferentiation of mature cells. Moreover, although a SC may acquire the first oncogenic hit, the

subsequent alterations required for the onset of CSC traits can occur in descendent cells (Jamieson et al., 2004). It has been proposed that progressive accumulation of genetic and epigenetic alterations in a differentiated cell may induce the re-acquisition of self-renewal capacity and prevent the differentiation to a post-mitotic state (Friedmann-Morvinski et al., 2012; Koren et al., 2015; Nishi et al., 2014; Schroeder et al., 2014; Schwitalla et al., 2013; Southall et al., 2014; Van Keymeulen et al., 2015). CSC condition can also be induced by specific environmental cues (growth factor signaling) or in stress-related conditions (Vermeulen et al., 2010). Moreover, recent studies have linked the acquisition of CSC traits with the EMT, since induction of this program can induce many SC features, including self-renewal and the expression of markers that are common to SCs and CSCs (Mani et al., 2008; Morel et al., 2008; Singh and Settleman, 2010). In this view, not all cancer show a fixed hierarchical organization, that resembles that of the corresponding healthy tissue, but can be characterized by a "tumor cell plasticity" in which a cell dedifferentiation process from a non-SC to a CSC can happened. In a process similar to reprogramming of somatic cells induced by exogenous transcription factors, the cell of origin has to undergo a series of alterations, that would alter the epigenetic state that stabilizes its original identity, in order to gain a new epigenetic program responsible for the acquisition of a CSC phenotype (Apostolou and Hochedlinger, 2013). The molecular mechanism that regulates this dynamic processes in tumorigenesis, whether this

plasticity is restricted to certain type of cancer and the frequency with which dedifferentiation events can occur *in vivo* is still unclear.

Breast cancer cell of origin

The adult mammary gland is an epithelial organ characterized by a branching network of ducts formed by two main cell lineages, represented by basal and luminal cells. The majority of the basal cells are differentiated myoepithelial cells, namely specialized, contractile cells, located at the basal surface of the epithelium, adjacent to the basement membrane (Sleeman et al., 2007). However, it has been demonstrated that this layer also includes the mammary stem cells (MaSCs) population (Shackleton et al., 2006; Sleeman et al., 2006; Stingl et al., 2006; Taddei et al., 2008). Luminal cell lineage includes ductal epithelial cells, that line the ducts, and alveolar epithelial cells, that constitute the alveolar units that arise during pregnancy and synthesize milk proteins. MaSCs are important for both organ development and maintenance of tissue homeostasis, and give rise to mature epithelium of the two lineages, through a series of intermediate progenitors (Visvader and Stingl, 2014).

Breast cancer is a very heterogeneous disease at both the histological and molecular levels, which can be subdivided into clinical subtypes based on the expression of estrogen (ER) and progesterone (PR), as well as the expression of the growth factor receptor HER2 (Erb-B2). By this classification, combined with gene expression profiles, tumors have been classified as “luminal-like A” and “B” (which express ER and/or PR), “HER2-positive” (characterized by amplification of the *HER2* gene) or “basal-like/triple-negative”

(which do not express ER, PR or HER2) (Perou et al., 2000; Sorlie et al., 2001). The histological appearance and marker expression can predict the response of the tumor to therapy, but they are not necessarily correlated to the cell of origin. For example, it has been demonstrated that basal-like breast cancers developed in women with mutations in the *BRCA1* tumor suppressor gene, generally associated with a poor prognosis, the cell of origin is not represented by a basal stem cell, but by a luminal progenitor (Lim et al., 2009). Notably, inactivation of the gene in either luminal or basal progenitors in the mouse mammary gland showed that only luminal cells are able to give rise to basal-like breast cancers, suggesting that both the cell of origin and the specific oncogenic insult contribute to the diversity of breast cancer molecular subtypes (Molyneux et al., 2010). The cell of origin of most other breast cancer has not been identified yet. In particular, it is yet unclear the role that MaSCs have in tumorigenesis, although they are primarily affected by alterations of the WNT signaling. Recent studies showed that their expression profile has strong similarities with a newly identified "claudin-low" subtype, characterized by low expression of genes involved in tight junctions and cell-cell adhesion (Lim et al., 2009; Prat et al., 2010).

Wnt signaling

WNTs are a family of 19 secreted proteins with a crucial role in the regulation of cell proliferation, survival, migration and polarity, cell fate determination and self-renewal during embryonic development and in adult tissues homeostasis (Logan and Nusse,

2004). Aberrant Wnt signaling activation results in the expansion of SCs and progenitor cells populations and is therefore strongly related to tumor initiation and progression in many tissues, including mammary gland and colon. Currently, three different pathways are believed to signal upon Wnt receptor activation: the canonical Wnt/β-Catenin cascade, the non-canonical planar cell polarity (PCP) pathway, and the Wnt/Ca_2^+ pathway (Katoh, 2005; Kohn and Moon, 2005; Veeman et al., 2003). Of these three, the canonical pathway is the best understood and numerous studies indicate that it can contributes to cancer progression through the maintenance of CSCs (Nguyen et al., 2012) (Figure 2).

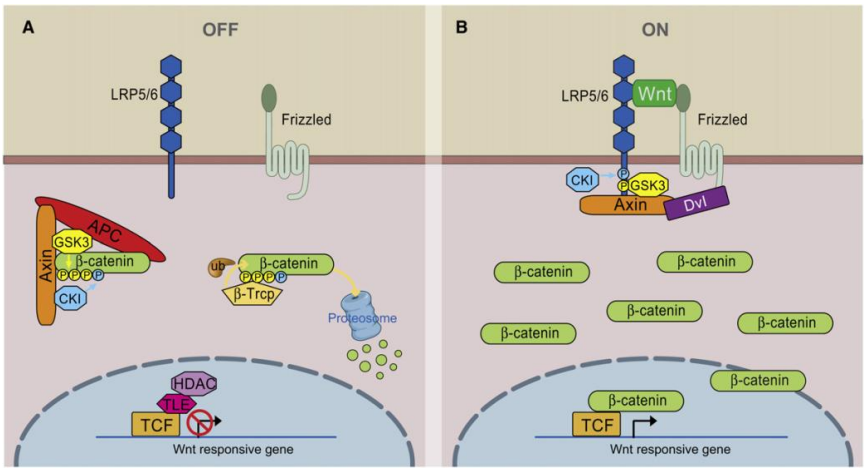

Figure 2. Wnt/β-Catenin signaling (MacDonald et al., 2009). (A) In the absence of WNT, cytoplasmic β-Catenin forms a complex with AXIN, APC, GSK3, and CK1, and is phosphorylated by CK1 and subsequently by GSK3. Phosphorylated β-Catenin is recognized by the E3 ubiquitin ligase β-TrCP, which targets β-Catenin for proteosomal degradation. Wnt target genes are repressed by TCF-TLE/Groucho and histone deacetylases (HDAC). (B) In the presence of WNT ligand, a receptor complex forms between FZ and LRP5/6. DVL recruitment by FZ leads to LRP5/6 phosphorylation and AXIN recruitment. This disrupts AXIN-mediated phosphorylation/degradation of β-Catenin, allowing β-Catenin to accumulate in the nucleus where it serves as a coactivator for TCF to activate Wnt-responsive genes.

In the presence of extracellular inhibitors, which act at the cell surface to inhibit Wnt signaling through its receptors, the stability of cytoplasmic β-Catenin is regulated by a "destruction complex" that contains two scaffolding proteins, the tumor suppressor proteins adenomatous polyposis coli (APC) and AXIN. APC and AXIN bind newly synthesized β-Catenin and facilitate its sequential phosphorylation to the level of a set of conserved Ser and Thr residues, by casein kinase 1 (CK1) and glycogen synthase kinase 3 (GSK3), two kinases residing in the destruction complex. Phosphorilated β-Catenin is then recognized by the F box/WD repeat protein β-TrCP, a component of a E3 ubiquitin ligase complex and targeted for ubiquitination and subsequent proteasomal degradation. In the nucleus, prospective target genes of the pathway are kept in a repressed state by T-cell factor (TCF) and lymphoid enhancer-binding protein (LEF) transcription factors. TCF represses gene expression by interacting with the repressor TLE1, which promotes histone deacetylation and chromatin compaction. So, in the "off state", cells maintain low cytoplasmic and nuclear levels of β-Catenin, although it is also associated with cadherins as a component of adherens junctions, an association that spares it from the degradative pathway (Nelson and Nusse, 2004). Mutations of β-Catenin at and surrounding its phosphorilation sytes are frequently found in cancers, generating mutant β-Catenin that escapes phosphorylation and degradation. Extracellular WNT ligands can interact with several secreted protein families that antagonize or modulate Wnt/β-Catenin signaling. Secreted Frizzled-related protein

(sFRP) and Wnt inhibitory protein (WIF) bind directly to WNT and, in the case of sFRP, also to FZ (Bovolenta et al., 2008). Dickkopf (DKK) proteins inhibit Wnt signaling by direct binding to LRP5/6 and causing the disruption of Wnt-induced FZ-LRP6 complexes (Semenov et al., 2001). Another class of secreted Wnt inhibitors, Wise and SOST, also act by binding to LRP5/6 (Itasaki et al., 2003; Li et al., 2005; Semenov et al., 2005). If the local concentration of WNTs exceeds the buffering capacity of inhibitors, WNTs engage their cognate receptor complex, consisting of members of the Frizzled (FZ) family of seven-pass transmembrane receptors, and a member of the single-pass transmembrane protein LDL-receptor family, the LDL-related proteins 5 and 6 (LRP5 and LRP6) (He et al., 2004; Tolwinski and Wieschaus, 2004). The binding of WNT to FZ inhibits the kinase activity of the destruction complex by a mechanism that leads to the activation and membrane recruitment of the cytoplasmic scaffolding protein Dishevelled (DSH or DVL), that may directly interact with FZ. This event induces the recruitement of AXIN and the destruction complex to the plasma membrane and the consequent phosphorilation of the cytoplasmic tail of LRP5/6 mediated by GSK3 and CK1, which constitute a docking site for AXIN (Davidson et al., 2005; Zeng et al., 2005). Recruitment to the plasma membrane induces AXIN degradation and also leads to the inhibition of GSK3, which further reduces the phosphorylation and degradation of β-Catenin (Tolwinski and Wieschaus, 2004). So, the “on state” involves cytoplasmic β-Catenin accumulation and its displacement to the nucleus, where it interacts with TCF/LEF factors, and recruits multiprotein complexes

such as the histone acetylase CBP and Brg-1 (Stadeli et al., 2006); this event displaces TLE1 and transiently converts TCF/LEF factors into transcriptional activators (MacDonald et al., 2009).

In addition to FZ family proteins, other reported transmembrane Wnt receptor are the RTK-like protein RYK and the tyrosine kinase receptors ROR1 and ROR2 (Lu et al., 2004)ˈ(Mikels and Nusse, 2006). Among Wnt antagonists, at least two families that are unrelated to WNT factors, represented by Norrin and R-spondin (Rspo) proteins, are able to activate the Frizzled/LRP receptors (Kim et al., 2005; Xu et al., 2004).

Notable, Wnt signaling is autoregulated at many levels, since the expression of a variety of positive and negative regulators of the pathway, such as *FZ*, *LRP*, *AXIN2*, and *TCF/LEF* genes, is under the control of the β-Catenin/TCF complex (Logan and Nusse, 2004). Most Wnt pathway mutations that are observed in cancer result in hyperactivation of Wnt/β-Catenin signaling. For example, mutations in APC activate the pathway and are responsible for the initial progression of almost all cases of human colorectal cancer (Gregorieff and Clevers, 2005). WNTs and Wnt pathway components are also frequently over- or under-expressed in different human cancers and these changes in the expression profiles often correlate with epigenetic activation or inactivation of gene promoters (Aguilera et al., 2006; Chim et al., 2007; Kansara et al., 2009; Klarmann et al., 2008).

Wnt pathway alteration in breast cancer

In the mammary gland, Wnt/β-Catenin signaling supports the self-renewal of both normal and malignant mammary stem cells (MaSCs). β-Catenin stabilization and nuclear localization has been observed in 50% of human breast tumors, with an enrichment in the aggressive basal-like subtype (Khramtsov et al., 2010); this finding has been associated with poor prognosis (Lin et al., 2000; Ozaki et al., 2005; Ryo et al., 2001). In addition to β-Catenin, other downstream targets, such as *cyclin D1*, *LEF1* and the proto-oncogene *MYC*, are reported to be upregulated in over 40% of breast cancers (Ayyanan et al., 2006; Chrzan et al., 2001; Lin et al., 2000). Nevertheless, contrary to colon cancer, active genetic mutations in Wnt pathway members are rare (van de Wetering et al., 2001). Instead, various lines of evidence suggest the Wnt pathway may be de-regulated by epigenetic loss of expression of negative pathway regulators. For example, loss of various antagonists of WNT ligands (SFRPs, WIF1 and DKK1) as well as loss of APC tumor suppressor, through promoter methylation, leads to overactivation of the pathway, promoting tumorigenesis in the mammary tissue (Ai et al., 2006; Suzuki et al., 2008; Veeck et al., 2006; Virmani et al., 2001; Wissmann et al., 2003).

cMYC

The *cMYC* (*MYC*) proto-oncogene encodes for a transcription factor that is broadly expressed during embryogenesis and in tissue compartments of the adult that possess high proliferative capacity. It

can regulate up to 22% of human genes (Perna et al., 2012) and its expression strongly correlates with cell growth and metabolism, proliferation, inhibition of terminal differentiation and apoptosis (Dang et al., 2006). MYC activates transcription as part of a heteromeric complex with MYC-associated factor X (MAX), which binds to specific DNA sequences, such as the E-box element CACGTG (Blackwood and Eisenman, 1991). MYC-MAX heterodimers regulate gene activation through the recruitment of multiple coactivators and protein complexes, including TRRAP, GCN5 and TBP, that cause chromatin remodeling (Fladvad et al., 2005; Liu et al., 2003; McMahon et al., 2000; Nikiforov et al., 2002). For example, the association with the co-activator TRRAP, that recruits the histone acetyltransferase GCN5, causes histones acetylation, permitting transcription of target genes (Bouchard et al., 2001).

MYC can also act as a transcriptional repressor via different mechanisms, often involving interaction with MYC-interacting zinc finger protein-1 (MIZ-1). By binding to MIZ-1, MYC indirectly represses transcriptional activation of genes that are activated by MIZ-1 (Adhikary and Eilers, 2005). For example, in the absence of TGF-β, MYC can repress *CDKN2B* gene by displacing MIZ-1. With TGF-β, MYC expression is suppressed, and the SMAD transcription factor cooperates with MIZ-1 to recruit NPM1 as a Miz-1 cofactor to stimulate *CDKN2B* transcription and induce cell-cycle arrest (Seoane et al., 2001; Wanzel et al., 2008). MYC can also inhibit MIZ-1 activity indirectly, by activating Rp123 ribosomal gene, which retain NPM1 in the nucleous (Li et al., 2008). Another critical mode for MYC-

mediated gene repression is through its ability to activate microRNAs (miRNAs) (Chang et al., 2008; O'Donnell et al., 2005).

One of the key biological functions of MYC is the regulation of cell proliferation (Amati et al., 1998; Dang, 1999; Eilers, 1999). An essential event in the G1-S progression is the MYC-induced activation of *CCND2* (cyclin D2) and *CDK4* (Cyclin-dependent Kinase 4) genes, which leads to sequestration and proteasomal degradation of the CDK inhibitor KIP1 (Bouchard et al., 1999; Coller et al., 2000; Hermeking et al., 2000). In doing so, KIP1 is not available for binding and inhibiting cyclin E-CDK2 complexes, which therefore can be activated by the cyclin-activating kinase (CAK) and promote cell cycle progression (Perez-Roger et al., 1999). Furthermore, MYC directly targets and activate the expression of the translation initiation factors eiF4 and eiF2, important in cell growth (Coller et al., 2000). Activation of MYC and cell-cycle entry is generally incompatible with terminal differentiation. MYC can block cell differentiation through repression of differentiation-induced $p21^{CIP1}$ expression, by interacting with MIZ-1 at $p21^{CIP1}$ core promoter (Wu et al., 2003). Moreover, in the absence of survival factors or in stress conditions, MYC can induce apoptosis (Askew et al., 1991; Evan et al., 1992; Harrington et al., 1994). This can happen through the induction of $p19^{ARF}$ expression, which leads to the stabilization of P53 (Zindy et al., 1998). MYC can also induce apoptosis by promoting the release of cytochrome c from mitochondria, in a $p19^{ARF}$ and P53-independent manner (Juin et al., 1999). This can be both mediated by MYC-induced expression of the pro-apoptotic BH3-only protein BIM, and

by block of the anti-apoptotic factors BCL2 and BCL-X_L expression, caused by MYC (Egle et al., 2004; Eischen et al., 2001).

In physiological conditions, MYC functions as a key integrator of many signaling cascade, included the Wnt/β-Catenin pathway, and its expression is strictly correlated to cell proliferation (Dang, 2012). In quiescent cells, MYC is virtually absent, but is rapidly induced by mitogens, during cell reentry into the cell cycle (Iyer et al., 1999). Thereafter, both mRNA and protein decline to a low, constant level and its expression and activity are maintained tightly regulated (Chung and Levens, 2005; Hanson et al., 1994; Liu and Levens, 2006; Oster et al., 2002). Nevertheless, the presence of anti-proliferative signals results in MYC immediate down-regulation (Dean et al., 1986; Lachman and Skoultchi, 1984). MYC is regulated by multiple signals that control promoter activity, transcriptional elongation and translation and post-translational modifications that control MYC's protein stability. One of the mechanisms by which MYC protein levels are regulated is a RAS-dependent signaling pathway, which controls MYC phosphorylation at two highly conserved residues: Ser62 (S62) and Thr58 (T58) (Sears et al., 2000; Yeh et al., 2004) (Figure 3).

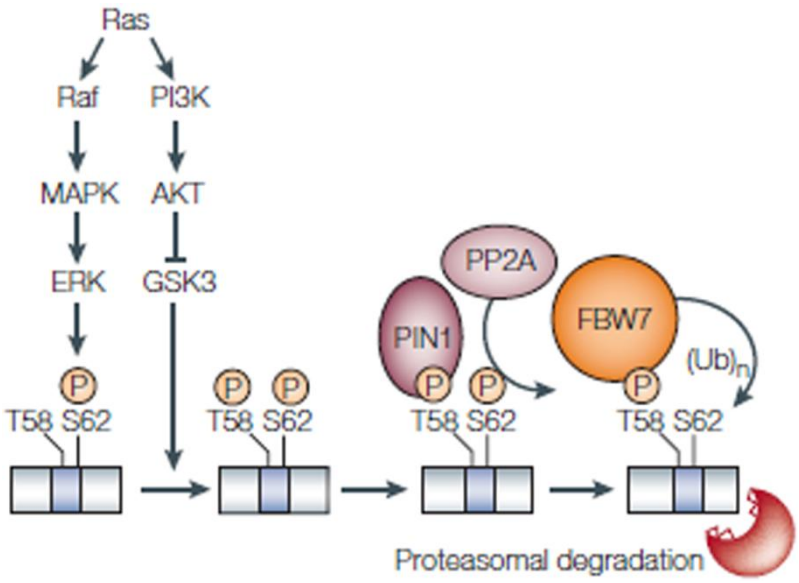

Figure 3. Regulation of MYC function by RAS-dependent signaling pathway (Adhikary and Eilers, 2005).

These two phosphorylation sites have opposite effects: while phospho-S62 stabilizes MYC, the presence of phospho-T58 induces its degradation. Phosphorylation at S62 is induced by RAS, through the MAPK/ERK pathway, and can serve as a platform for phosphorylation of T58 by GSK3 (Gregory et al., 2003). Phosphorylated T58 is recognized by the prolyl isomerase (PIN1), which enables phosphatase-2A (PP2A) to remove the phosphate residue from S62. The ubiquitin E3 ligase SCF^{FWB7} recognizes the remaining phospho-T58 and labels MYC for proteasomal degradation (Welcker et al., 2004a; Welcker et al., 2004b; Yada et al., 2004). In the presence of proliferative stimuli, RAS phosphorylates S62 and inhibits GSK3 through the PI3K signaling, therefore leading to MYC stabilization.

Unlike what has been observed for other oncogenes (RAS), MYC deregulation in cancer is generally not caused by genetic mutations in the coding sequence (Schulein and Eilers, 2009), but from large genetic changes in the *MYC* locus such as amplification and chromosomal translocation. Notably, its alteration can also be caused by any of the several mechanisms and signals that target its expression and/or control its activity. MYC has been found to be overexpressed in up to 50% of all human cancers and is often associated with aggressive and poorly differentiated tumors. The cellular response to MYC overexpression is dependent on the cellular context. In addition to causing uncontrolled cell proliferation and loss of terminal differentiation (Pelengaris et al., 2002a), deregulated expression of MYC can drive cell growth (Barna et al., 2008; Dang, 1999), angiogenesis (Baudino et al., 2002), reduced cell adhesion (Arnold and Watt, 2001; Frye et al., 2003) and promote metastasis (Pelengaris et al., 2002b). Nevertheless, the only MYC deregulated expression is not sufficient to transform either mouse or human cells, and tumors derived from MYC transgenic mice are characterized by a long latency, suggesting that additional mutagenic events are necessary for tumor formation (Beer et al., 2004; D'Cruz et al., 2001; Eischen et al., 1999).

In addition to its role in tumorigenesis, *MYC* has also been identified as one of four genes, including *OCT4*, *SOX2* and *KLF4*, that could collectively reprogram fibroblasts to a pluripotent SC state (known as OSKM factors) (Takahashi and Yamanaka, 2006). Although not essential for induced pluripotent stem cells (iPSCs) formation,

ectopic MYC expression strongly enhances and accelerates the process (Nakagawa et al., 2008; Wernig et al., 2008). MYC expression functions during the first transcriptional wave of the reprogramming process, characterized by cells de-differentiation and up-regulation of proliferating genes. In this phase, OSKM factors occupy accessible chromatin and MYC down-regulates fibroblast-specific genes, while activating many ES cells specific genes, mostly involved in metabolism (Brambrink et al., 2008; Sridharan et al., 2009; Stadtfeld et al., 2008). Moreover, MYC recruits chromatin remodeling factors, thus globally regulating chromosomal accessibility and enhancing the initial OSK engagement with chromatin (Soufi et al., 2012).

MYC and breast cancer

Considering breast cancer, *MYC* amplification is the most described alteration. It is found in a high proportion of tumors with *BRCA1* alterations and appears to be a basal-like characteristic, being amplified in 40% of the cases (Cancer Genome Atlas, 2012; Chandriani et al., 2009; Chen and Olopade, 2008; Nikolsky et al., 2008).

MYC oncogene has been assayed for mammary tumorigenic potential using different systems to drive its overexpression. Although tumor incidence is high, tumors form with variable latency, suggesting that additional mutagenic events are necessary for tumor formation (Sandgren et al., 1995; Schoenenberger et al., 1988; Stewart et al., 1984). In support to this hypothesis, a more recent study show that mammary carcinomas triggered by transgenic MYC expression

acquire KRAS mutations that induce tumor aggressiveness (D'Cruz et al., 2001).

Among the pathways that impact on MYC expression or activity in breast cancer, the Wnt pathway effectors directly bind the *MYC* promoter, thereby stimulating its transcription. Deregulating MYC might enforce autocrine Wnt pathway activity in human tumors by repressing negative regulators such as SFRP1 (Cowling et al., 2007). Nevertheless, while MYC deletion in intestine tumors was shown to reverse the tumor phenotype induced by APC loss, the dependency of Wnt-driven mouse mammary tumors on MYC up-regulation has not been determined yet (Sansom et al., 2007; Walz et al., 2014).

Considering these observations, MYC role in mammary gland tumorigenesis and tumor maintenance is still unclear.

Scope of the thesis

In the present study we investigated the role of MYC in mammary epithelial cells tumor initiation. We hypothesized that MYC may act as an oncogenic reprogramming factor that drives tumor initiation by inducing an epigenetic plasticity that predisposes differentiated cells to re-acquisition of stem cell characteristics and, after further oncogenic insults, to neoplastic transformation.

References

Adhikary, S., and Eilers, M. (2005). Transcriptional regulation and transformation by Myc proteins. Nature reviews Molecular cell biology *6*, 635-645.

Aguilera, O., Fraga, M.F., Ballestar, E., Paz, M.F., Herranz, M., Espada, J., Garcia, J.M., Munoz, A., Esteller, M., and Gonzalez-Sancho, J.M. (2006). Epigenetic inactivation of the Wnt antagonist DICKKOPF-1 (DKK-1) gene in human colorectal cancer. Oncogene *25*, 4116-4121.

Ai, L., Tao, Q., Zhong, S., Fields, C.R., Kim, W.J., Lee, M.W., Cui, Y., Brown, K.D., and Robertson, K.D. (2006). Inactivation of Wnt inhibitory factor-1 (WIF1) expression by epigenetic silencing is a common event in breast cancer. Carcinogenesis *27*, 1341-1348.

Al-Hajj, M., Wicha, M.S., Benito-Hernandez, A., Morrison, S.J., and Clarke, M.F. (2003). Prospective identification of tumorigenic breast cancer cells. Proceedings of the National Academy of Sciences of the United States of America *100*, 3983-3988.

Amati, B., Alevizopoulos, K., and Vlach, J. (1998). Myc and the cell cycle. Frontiers in bioscience : a journal and virtual library *3*, d250-268.

Apostolou, E., and Hochedlinger, K. (2013). Chromatin dynamics during cellular reprogramming. Nature *502*, 462-471.

Arnold, I., and Watt, F.M. (2001). c-Myc activation in transgenic mouse epidermis results in mobilization of stem cells and differentiation of their progeny. Current biology : CB *11*, 558-568.

Askew, D.S., Ashmun, R.A., Simmons, B.C., and Cleveland, J.L. (1991). Constitutive c-myc expression in an IL-3-dependent myeloid cell line suppresses cell cycle arrest and accelerates apoptosis. Oncogene *6*, 1915-1922.

Ayyanan, A., Civenni, G., Ciarloni, L., Morel, C., Mueller, N., Lefort, K., Mandinova, A., Raffoul, W., Fiche, M., Dotto, G.P.*, et al.* (2006). Increased Wnt signaling triggers oncogenic conversion of human breast epithelial cells by a Notch-dependent mechanism. Proceedings of the National Academy of Sciences of the United States of America *103*, 3799-3804.

Baeriswyl, V., and Christofori, G. (2009). The angiogenic switch in carcinogenesis. Seminars in cancer biology *19*, 329-337.

Bao, S., Wu, Q., McLendon, R.E., Hao, Y., Shi, Q., Hjelmeland, A.B., Dewhirst, M.W., Bigner, D.D., and Rich, J.N. (2006). Glioma stem cells promote radioresistance by preferential activation of the DNA damage response. Nature *444*, 756-760.

Barna, M., Pusic, A., Zollo, O., Costa, M., Kondrashov, N., Rego, E., Rao, P.H., and Ruggero, D. (2008). Suppression of Myc oncogenic activity by ribosomal protein haploinsufficiency. Nature *456*, 971-975.

Baudino, T.A., McKay, C., Pendeville-Samain, H., Nilsson, J.A., Maclean, K.H., White, E.L., Davis, A.C., Ihle, J.N., and Cleveland, J.L. (2002). c-Myc is essential for vasculogenesis and angiogenesis during development and tumor progression. Genes & development *16*, 2530-2543.

Beer, S., Zetterberg, A., Ihrie, R.A., McTaggart, R.A., Yang, Q., Bradon, N., Arvanitis, C., Attardi, L.D., Feng, S., Ruebner, B.*, et al.* (2004). Developmental context determines latency of MYC-induced tumorigenesis. PLoS biology *2*, e332.

Bergers, G., and Benjamin, L.E. (2003). Tumorigenesis and the angiogenic switch. Nature reviews Cancer *3*, 401-410.

Bhowmick, N.A., Neilson, E.G., and Moses, H.L. (2004). Stromal fibroblasts in cancer initiation and progression. Nature *432*, 332-337.

Blackwood, E.M., and Eisenman, R.N. (1991). Max: a helix-loop-helix zipper protein that forms a sequence-specific DNA-binding complex with Myc. Science *251*, 1211-1217.

Blasco, M.A. (2005). Telomeres and human disease: ageing, cancer and beyond. Nature reviews Genetics *6*, 611-622.

Bonnet, D., and Dick, J.E. (1997). Human acute myeloid leukemia is organized as a hierarchy that originates from a primitive hematopoietic cell. Nature medicine *3*, 730-737.

Bouchard, C., Dittrich, O., Kiermaier, A., Dohmann, K., Menkel, A., Eilers, M., and Luscher, B. (2001). Regulation of cyclin D2 gene expression by the Myc/Max/Mad network: Myc-dependent TRRAP recruitment and histone acetylation at the cyclin D2 promoter. Genes & development *15*, 2042-2047.

Bouchard, C., Thieke, K., Maier, A., Saffrich, R., Hanley-Hyde, J., Ansorge, W., Reed, S., Sicinski, P., Bartek, J., and Eilers, M. (1999). Direct induction of cyclin D2 by Myc contributes to cell cycle progression and sequestration of p27. The EMBO journal *18*, 5321-5333.

Bovolenta, P., Esteve, P., Ruiz, J.M., Cisneros, E., and Lopez-Rios, J. (2008). Beyond Wnt inhibition: new functions of secreted Frizzled-related proteins in development and disease. Journal of cell science *121*, 737-746.

Brambrink, T., Foreman, R., Welstead, G.G., Lengner, C.J., Wernig, M., Suh, H., and Jaenisch, R. (2008). Sequential expression of pluripotency markers during direct reprogramming of mouse somatic cells. Cell stem cell *2*, 151-159.

Burkhart, D.L., and Sage, J. (2008). Cellular mechanisms of tumour suppression by the retinoblastoma gene. Nature reviews Cancer *8*, 671-682.

Cancer Genome Atlas, N. (2012). Comprehensive molecular portraits of human breast tumours. Nature *490*, 61-70.

Carmeliet, P. (2005). VEGF as a key mediator of angiogenesis in cancer. Oncology *69 Suppl 3*, 4-10.

Carmeliet, P., and Jain, R.K. (2011). Molecular mechanisms and clinical applications of angiogenesis. Nature *473*, 298-307.

Chandriani, S., Frengen, E., Cowling, V.H., Pendergrass, S.A., Perou, C.M., Whitfield, M.L., and Cole, M.D. (2009). A core MYC gene expression signature is prominent in basal-like breast cancer but only partially overlaps the core serum response. PloS one *4*, e6693.

Chang, T.C., Yu, D., Lee, Y.S., Wentzel, E.A., Arking, D.E., West, K.M., Dang, C.V., Thomas-Tikhonenko, A., and Mendell, J.T. (2008). Widespread microRNA repression by Myc contributes to tumorigenesis. Nature genetics *40*, 43-50.

Chen, F., Zhuang, X., Lin, L., Yu, P., Wang, Y., Shi, Y., Hu, G., and Sun, Y. (2015). New horizons in tumor microenvironment biology: challenges and opportunities. BMC medicine *13*, 45.

Chen, Y., and Olopade, O.I. (2008). MYC in breast tumor progression. Expert review of anticancer therapy *8*, 1689-1698.

Cheng, N., Chytil, A., Shyr, Y., Joly, A., and Moses, H.L. (2008). Transforming growth factor-beta signaling-deficient fibroblasts enhance hepatocyte growth factor signaling in mammary carcinoma cells to promote scattering and invasion. Molecular cancer research : MCR *6*, 1521-1533.

Chim, C.S., Pang, R., Fung, T.K., Choi, C.L., and Liang, R. (2007). Epigenetic dysregulation of Wnt signaling pathway in multiple myeloma. Leukemia *21*, 2527-2536.

Chrzan, P., Skokowski, J., Karmolinski, A., and Pawelczyk, T. (2001). Amplification of c-myc gene and overexpression of c-Myc protein in breast cancer and adjacent non-neoplastic tissue. Clinical biochemistry *34*, 557-562.

Chung, H.J., and Levens, D. (2005). c-myc expression: keep the noise down! Molecules and cells *20*, 157-166.

Coller, H.A., Grandori, C., Tamayo, P., Colbert, T., Lander, E.S., Eisenman, R.N., and Golub, T.R. (2000). Expression analysis with oligonucleotide microarrays reveals that MYC regulates genes involved in growth, cell cycle, signaling, and adhesion. Proceedings of the National Academy of Sciences of the United States of America *97*, 3260-3265.

Colotta, F., Allavena, P., Sica, A., Garlanda, C., and Mantovani, A. (2009). Cancer-related inflammation, the seventh hallmark of cancer: links to genetic instability. Carcinogenesis *30*, 1073-1081.

Cowling, V.H., D'Cruz, C.M., Chodosh, L.A., and Cole, M.D. (2007). c-Myc transforms human mammary epithelial cells through repression of the Wnt inhibitors DKK1 and SFRP1. Molecular and cellular biology *27*, 5135-5146.

D'Cruz, C.M., Gunther, E.J., Boxer, R.B., Hartman, J.L., Sintasath, L., Moody, S.E., Cox, J.D., Ha, S.I., Belka, G.K., Golant, A.*, et al.* (2001). c-MYC induces mammary tumorigenesis by means of a preferred pathway involving spontaneous Kras2 mutations. Nature medicine *7*, 235-239.

Dang, C.V. (1999). c-Myc target genes involved in cell growth, apoptosis, and metabolism. Molecular and cellular biology *19*, 1-11.

Dang, C.V. (2012). MYC on the path to cancer. Cell *149*, 22-35.

Dang, C.V., O'Donnell, K.A., Zeller, K.I., Nguyen, T., Osthus, R.C., and Li, F. (2006). The c-Myc target gene network. Seminars in cancer biology *16*, 253-264.

Davidson, G., Wu, W., Shen, J., Bilic, J., Fenger, U., Stannek, P., Glinka, A., and Niehrs, C. (2005). Casein kinase 1 gamma couples Wnt receptor activation to cytoplasmic signal transduction. Nature *438*, 867-872.

De Bock, K., Cauwenberghs, S., and Carmeliet, P. (2011). Vessel abnormalization: another hallmark of cancer? Molecular mechanisms and therapeutic implications. Current opinion in genetics & development *21*, 73-79.

Dean, M., Levine, R.A., Ran, W., Kindy, M.S., Sonenshein, G.E., and Campisi, J. (1986). Regulation of c-myc transcription and mRNA abundance by serum growth factors and cell contact. The Journal of biological chemistry *261*, 9161-9166.

DeAngelo, A.B., Geter, D.R., Rosenberg, D.W., Crary, C.K., and George, M.H. (2002). The induction of aberrant crypt foci (ACF) in the colons of rats by trihalomethanes administered in the drinking water. Cancer letters *187*, 25-31.

DeBerardinis, R.J., Lum, J.J., Hatzivassiliou, G., and Thompson, C.B. (2008). The biology of cancer: metabolic reprogramming fuels cell growth and proliferation. Cell metabolism *7*, 11-20.

DeNardo, D.G., Andreu, P., and Coussens, L.M. (2010). Interactions between lymphocytes and myeloid cells regulate pro- versus anti-tumor immunity. Cancer metastasis reviews *29*, 309-316.

Diehn, M., Cho, R.W., Lobo, N.A., Kalisky, T., Dorie, M.J., Kulp, A.N., Qian, D., Lam, J.S., Ailles, L.E., Wong, M.*, et al.* (2009). Association of reactive

oxygen species levels and radioresistance in cancer stem cells. Nature *458*, 780-783.

Eden, A., Gaudet, F., Waghmare, A., and Jaenisch, R. (2003). Chromosomal instability and tumors promoted by DNA hypomethylation. Science *300*, 455.

Egle, A., Harris, A.W., Bouillet, P., and Cory, S. (2004). Bim is a suppressor of Myc-induced mouse B cell leukemia. Proceedings of the National Academy of Sciences of the United States of America *101*, 6164-6169.

Eilers, M. (1999). Control of cell proliferation by Myc family genes. Molecules and cells *9*, 1-6.

Eischen, C.M., Weber, J.D., Roussel, M.F., Sherr, C.J., and Cleveland, J.L. (1999). Disruption of the ARF-Mdm2-p53 tumor suppressor pathway in Myc-induced lymphomagenesis. Genes & development *13*, 2658-2669.

Eischen, C.M., Woo, D., Roussel, M.F., and Cleveland, J.L. (2001). Apoptosis triggered by Myc-induced suppression of Bcl-X(L) or Bcl-2 is bypassed during lymphomagenesis. Molecular and cellular biology *21*, 5063-5070.

Evan, G.I., Wyllie, A.H., Gilbert, C.S., Littlewood, T.D., Land, H., Brooks, M., Waters, C.M., Penn, L.Z., and Hancock, D.C. (1992). Induction of apoptosis in fibroblasts by c-myc protein. Cell *69*, 119-128.

Feinberg, A.P. (2004). The epigenetics of cancer etiology. Seminars in cancer biology *14*, 427-432.

Feinberg, A.P., and Tycko, B. (2004). The history of cancer epigenetics. Nature reviews Cancer *4*, 143-153.

Feinberg, A.P., and Vogelstein, B. (1983). Hypomethylation distinguishes genes of some human cancers from their normal counterparts. Nature *301*, 89-92.

Fidler, I.J. (2003). The pathogenesis of cancer metastasis: the 'seed and soil' hypothesis revisited. Nature reviews Cancer *3*, 453-458.

Fladvad, M., Zhou, K., Moshref, A., Pursglove, S., Safsten, P., and Sunnerhagen, M. (2005). N and C-terminal sub-regions in the c-Myc transactivation region and their joint role in creating versatility in folding and binding. Journal of molecular biology *346*, 175-189.

Fraga, M.F., Ballestar, E., Villar-Garea, A., Boix-Chornet, M., Espada, J., Schotta, G., Bonaldi, T., Haydon, C., Ropero, S., Petrie, K.*, et al.* (2005). Loss of acetylation at Lys16 and trimethylation at Lys20 of histone H4 is a common hallmark of human cancer. Nature genetics *37*, 391-400.

Friedmann-Morvinski, D., Bushong, E.A., Ke, E., Soda, Y., Marumoto, T., Singer, O., Ellisman, M.H., and Verma, I.M. (2012). Dedifferentiation

of neurons and astrocytes by oncogenes can induce gliomas in mice. Science *338*, 1080-1084.

Frye, M., Gardner, C., Li, E.R., Arnold, I., and Watt, F.M. (2003). Evidence that Myc activation depletes the epidermal stem cell compartment by modulating adhesive interactions with the local microenvironment. Development *130*, 2793-2808.

Gaudet, F., Hodgson, J.G., Eden, A., Jackson-Grusby, L., Dausman, J., Gray, J.W., Leonhardt, H., and Jaenisch, R. (2003). Induction of tumors in mice by genomic hypomethylation. Science *300*, 489-492.

Gonzalez-Zulueta, M., Bender, C.M., Yang, A.S., Nguyen, T., Beart, R.W., Van Tornout, J.M., and Jones, P.A. (1995). Methylation of the 5' CpG island of the p16/CDKN2 tumor suppressor gene in normal and transformed human tissues correlates with gene silencing. Cancer research *55*, 4531-4535.

Gottesman, M.M. (2002). Mechanisms of cancer drug resistance. Annual review of medicine *53*, 615-627.

Greger, V., Debus, N., Lohmann, D., Hopping, W., Passarge, E., and Horsthemke, B. (1994). Frequency and parental origin of hypermethylated RB1 alleles in retinoblastoma. Human genetics *94*, 491-496.

Gregorieff, A., and Clevers, H. (2005). Wnt signaling in the intestinal epithelium: from endoderm to cancer. Genes & development *19*, 877-890.

Gregory, M.A., Qi, Y., and Hann, S.R. (2003). Phosphorylation by glycogen synthase kinase-3 controls c-myc proteolysis and subnuclear localization. The Journal of biological chemistry *278*, 51606-51612.

Grivennikov, S.I., Greten, F.R., and Karin, M. (2010). Immunity, inflammation, and cancer. Cell *140*, 883-899.

Hanahan, D., and Folkman, J. (1996). Patterns and emerging mechanisms of the angiogenic switch during tumorigenesis. Cell *86*, 353-364.

Hanahan, D., and Weinberg, R.A. (2011). Hallmarks of cancer: the next generation. Cell *144*, 646-674.

Hanson, K.D., Shichiri, M., Follansbee, M.R., and Sedivy, J.M. (1994). Effects of c-myc expression on cell cycle progression. Molecular and cellular biology *14*, 5748-5755.

Hao, X.P., Pretlow, T.G., Rao, J.S., and Pretlow, T.P. (2001). Beta-Catenin expression is altered in human colonic aberrant crypt foci. Cancer research *61*, 8085-8088.

Harrington, E.A., Bennett, M.R., Fanidi, A., and Evan, G.I. (1994). c-Myc-induced apoptosis in fibroblasts is inhibited by specific cytokines. The EMBO journal *13*, 3286-3295.

He, X., Semenov, M., Tamai, K., and Zeng, X. (2004). LDL receptor-related proteins 5 and 6 in Wnt/beta-Catenin signaling: arrows point the way. Development *131*, 1663-1677.

Herman, J.G., and Baylin, S.B. (2003). Gene silencing in cancer in association with promoter hypermethylation. The New England journal of medicine *349*, 2042-2054.

Herman, J.G., Latif, F., Weng, Y., Lerman, M.I., Zbar, B., Liu, S., Samid, D., Duan, D.S., Gnarra, J.R., Linehan, W.M.*, et al.* (1994). Silencing of the VHL tumor-suppressor gene by DNA methylation in renal carcinoma. Proceedings of the National Academy of Sciences of the United States of America *91*, 9700-9704.

Hermeking, H., Rago, C., Schuhmacher, M., Li, Q., Barrett, J.F., Obaya, A.J., O'Connell, B.C., Mateyak, M.K., Tam, W., Kohlhuber, F.*, et al.* (2000). Identification of CDK4 as a target of c-MYC. Proceedings of the National Academy of Sciences of the United States of America *97*, 2229-2234.

Hess, J.L. (2004). Mechanisms of transformation by MLL. Critical reviews in eukaryotic gene expression *14*, 235-254.

Hiltunen, M.O., Alhonen, L., Koistinaho, J., Myohanen, S., Paakkonen, M., Marin, S., Kosma, V.M., and Janne, J. (1997). Hypermethylation of the APC (adenomatous polyposis coli) gene promoter region in human colorectal carcinoma. International journal of cancer *70*, 644-648.

Hoey, T., Yen, W.C., Axelrod, F., Basi, J., Donigian, L., Dylla, S., Fitch-Bruhns, M., Lazetic, S., Park, I.K., Sato, A.*, et al.* (2009). DLL4 blockade inhibits tumor growth and reduces tumor-initiating cell frequency. Cell stem cell *5*, 168-177.

Holst, C.R., Nuovo, G.J., Esteller, M., Chew, K., Baylin, S.B., Herman, J.G., and Tlsty, T.D. (2003). Methylation of p16(INK4a) promoters occurs in vivo in histologically normal human mammary epithelia. Cancer research *63*, 1596-1601.

Hsu, P.P., and Sabatini, D.M. (2008). Cancer cell metabolism: Warburg and beyond. Cell *134*, 703-707.

Hynes, N.E., and MacDonald, G. (2009). ErbB receptors and signaling pathways in cancer. Current opinion in cell biology *21*, 177-184.

Itasaki, N., Jones, C.M., Mercurio, S., Rowe, A., Domingos, P.M., Smith, J.C., and Krumlauf, R. (2003). Wise, a context-dependent activator and inhibitor of Wnt signalling. Development *130*, 4295-4305.

Ito, K., Hirao, A., Arai, F., Matsuoka, S., Takubo, K., Hamaguchi, I., Nomiyama, K., Hosokawa, K., Sakurada, K., Nakagata, N.*, et al.* (2004). Regulation of oxidative stress by ATM is required for self-renewal of haematopoietic stem cells. Nature *431*, 997-1002.

Iyer, V.R., Eisen, M.B., Ross, D.T., Schuler, G., Moore, T., Lee, J.C., Trent, J.M., Staudt, L.M., Hudson, J., Jr., Boguski, M.S*., et al.* (1999). The transcriptional program in the response of human fibroblasts to serum. Science *283*, 83-87.

Jamieson, C.H., Ailles, L.E., Dylla, S.J., Muijtjens, M., Jones, C., Zehnder, J.L., Gotlib, J., Li, K., Manz, M.G., Keating, A*., et al.* (2004). Granulocyte-macrophage progenitors as candidate leukemic stem cells in blast-crisis CML. The New England journal of medicine *351*, 657-667.

Jones, P.A., and Baylin, S.B. (2002). The fundamental role of epigenetic events in cancer. Nature reviews Genetics *3*, 415-428.

Jones, R.G., and Thompson, C.B. (2009). Tumor suppressors and cell metabolism: a recipe for cancer growth. Genes & development *23*, 537-548.

Juin, P., Hueber, A.O., Littlewood, T., and Evan, G. (1999). c-Myc-induced sensitization to apoptosis is mediated through cytochrome c release. Genes & development *13*, 1367-1381.

Junttila, M.R., and de Sauvage, F.J. (2013). Influence of tumour micro-environment heterogeneity on therapeutic response. Nature *501*, 346-354.

Kansara, M., Tsang, M., Kodjabachian, L., Sims, N.A., Trivett, M.K., Ehrich, M., Dobrovic, A., Slavin, J., Choong, P.F., Simmons, P.J*., et al.* (2009). Wnt inhibitory factor 1 is epigenetically silenced in human osteosarcoma, and targeted disruption accelerates osteosarcomagenesis in mice. The Journal of clinical investigation *119*, 837-851.

Karnoub, A.E., and Weinberg, R.A. (2006). Chemokine networks and breast cancer metastasis. Breast disease *26*, 75-85.

Katoh, M. (2005). WNT/PCP signaling pathway and human cancer (review). Oncology reports *14*, 1583-1588.

Khramtsov, A.I., Khramtsova, G.F., Tretiakova, M., Huo, D., Olopade, O.I., and Goss, K.H. (2010). Wnt/beta-Catenin pathway activation is enriched in basal-like breast cancers and predicts poor outcome. The American journal of pathology *176*, 2911-2920.

Kim, K.A., Kakitani, M., Zhao, J., Oshima, T., Tang, T., Binnerts, M., Liu, Y., Boyle, B., Park, E., Emtage, P*., et al.* (2005). Mitogenic influence of human R-spondin1 on the intestinal epithelium. Science *309*, 1256-1259.

Klarmann, G.J., Decker, A., and Farrar, W.L. (2008). Epigenetic gene silencing in the Wnt pathway in breast cancer. Epigenetics *3*, 59-63.

Kohn, A.D., and Moon, R.T. (2005). Wnt and calcium signaling: beta-Catenin-independent pathways. Cell calcium *38*, 439-446.

Koren, S., Reavie, L., Couto, J.P., De Silva, D., Stadler, M.B., Roloff, T., Britschgi, A., Eichlisberger, T., Kohler, H., Aina, O*., et al.* (2015). PIK3CA(H1047R) induces multipotency and multi-lineage mammary tumours. Nature *525*, 114-118.

LaBarge, M.A. (2010). The difficulty of targeting cancer stem cell niches. Clinical cancer research : an official journal of the American Association for Cancer Research *16*, 3121-3129.

Lachman, H.M., and Skoultchi, A.I. (1984). Expression of c-myc changes during differentiation of mouse erythroleukaemia cells. Nature *310*, 592-594.

Lapidot, T., Sirard, C., Vormoor, J., Murdoch, B., Hoang, T., Caceres-Cortes, J., Minden, M., Paterson, B., Caligiuri, M.A., and Dick, J.E. (1994). A cell initiating human acute myeloid leukaemia after transplantation into SCID mice. Nature *367*, 645-648.

Li, X., Zhang, Y., Kang, H., Liu, W., Liu, P., Zhang, J., Harris, S.E., and Wu, D. (2005). Sclerostin binds to LRP5/6 and antagonizes canonical Wnt signaling. The Journal of biological chemistry *280*, 19883-19887.

Li, Z., Boone, D., and Hann, S.R. (2008). Nucleophosmin interacts directly with c-Myc and controls c-Myc-induced hyperproliferation and transformation. Proceedings of the National Academy of Sciences of the United States of America *105*, 18794-18799.

Lim, E., Vaillant, F., Wu, D., Forrest, N.C., Pal, B., Hart, A.H., Asselin-Labat, M.L., Gyorki, D.E., Ward, T., Partanen, A*., et al.* (2009). Aberrant luminal progenitors as the candidate target population for basal tumor development in BRCA1 mutation carriers. Nature medicine *15*, 907-913.

Lin, S.Y., Xia, W., Wang, J.C., Kwong, K.Y., Spohn, B., Wen, Y., Pestell, R.G., and Hung, M.C. (2000). Beta-Catenin, a novel prognostic marker for breast cancer: its roles in cyclin D1 expression and cancer progression. Proceedings of the National Academy of Sciences of the United States of America *97*, 4262-4266.

Liu, J., and Levens, D. (2006). Making myc. Current topics in microbiology and immunology *302*, 1-32.

Liu, X., Tesfai, J., Evrard, Y.A., Dent, S.Y., and Martinez, E. (2003). c-Myc transformation domain recruits the human STAGA complex and requires TRRAP and GCN5 acetylase activity for transcription activation. The Journal of biological chemistry *278*, 20405-20412.

Logan, C.Y., and Nusse, R. (2004). The Wnt signaling pathway in development and disease. Annual review of cell and developmental biology *20*, 781-810.

Lowe, S.W., Cepero, E., and Evan, G. (2004). Intrinsic tumour suppression. Nature *432*, 307-315.

Lu, W., Yamamoto, V., Ortega, B., and Baltimore, D. (2004). Mammalian Ryk is a Wnt coreceptor required for stimulation of neurite outgrowth. Cell *119*, 97-108.

MacDonald, B.T., Tamai, K., and He, X. (2009). Wnt/beta-Catenin signaling: components, mechanisms, and diseases. Developmental cell *17*, 9-26.

Mani, S.A., Guo, W., Liao, M.J., Eaton, E.N., Ayyanan, A., Zhou, A.Y., Brooks, M., Reinhard, F., Zhang, C.C., Shipitsin, M.*, et al.* (2008). The epithelial-mesenchymal transition generates cells with properties of stem cells. Cell *133*, 704-715.

Marusyk, A., and Polyak, K. (2010). Tumor heterogeneity: causes and consequences. Biochimica et biophysica acta *1805*, 105-117.

McDonald, D.M., and Choyke, P.L. (2003). Imaging of angiogenesis: from microscope to clinic. Nature medicine *9*, 713-725.

McMahon, S.B., Wood, M.A., and Cole, M.D. (2000). The essential cofactor TRRAP recruits the histone acetyltransferase hGCN5 to c-Myc. Molecular and cellular biology *20*, 556-562.

Merchant, A.A., and Matsui, W. (2010). Targeting Hedgehog--a cancer stem cell pathway. Clinical cancer research : an official journal of the American Association for Cancer Research *16*, 3130-3140.

Mikels, A.J., and Nusse, R. (2006). Purified Wnt5a protein activates or inhibits beta-Catenin-TCF signaling depending on receptor context. PLoS biology *4*, e115.

Molyneux, G., Geyer, F.C., Magnay, F.A., McCarthy, A., Kendrick, H., Natrajan, R., Mackay, A., Grigoriadis, A., Tutt, A., Ashworth, A.*, et al.* (2010). BRCA1 basal-like breast cancers originate from luminal epithelial progenitors and not from basal stem cells. Cell stem cell *7*, 403-417.

Morel, A.P., Lievre, M., Thomas, C., Hinkal, G., Ansieau, S., and Puisieux, A. (2008). Generation of breast cancer stem cells through epithelial-mesenchymal transition. PloS one *3*, e2888.

Mori, H., Yamada, Y., Kuno, T., and Hirose, Y. (2004). Aberrant crypt foci and beta-Catenin accumulated crypts; significance and roles for colorectal carcinogenesis. Mutation research *566*, 191-208.

Nakagawa, M., Koyanagi, M., Tanabe, K., Takahashi, K., Ichisaka, T., Aoi, T., Okita, K., Mochiduki, Y., Takizawa, N., and Yamanaka, S. (2008). Generation of induced pluripotent stem cells without Myc from mouse and human fibroblasts. Nature biotechnology *26*, 101-106.

Nelson, W.J., and Nusse, R. (2004). Convergence of Wnt, beta-Catenin, and cadherin pathways. Science *303*, 1483-1487.

Nguyen, L.V., Vanner, R., Dirks, P., and Eaves, C.J. (2012). Cancer stem cells: an evolving concept. Nature reviews Cancer *12*, 133-143.

Nikiforov, M.A., Chandriani, S., Park, J., Kotenko, I., Matheos, D., Johnsson, A., McMahon, S.B., and Cole, M.D. (2002). TRRAP-dependent and TRRAP-independent transcriptional activation by Myc family oncoproteins. Molecular and cellular biology *22*, 5054-5063.

Nikolsky, Y., Sviridov, E., Yao, J., Dosymbekov, D., Ustyansky, V., Kaznacheev, V., Dezso, Z., Mulvey, L., Macconaill, L.E., Winckler, W.*, et al.* (2008). Genome-wide functional synergy between amplified and mutated genes in human breast cancer. Cancer research *68*, 9532-9540.

Nishi, M., Sakai, Y., Akutsu, H., Nagashima, Y., Quinn, G., Masui, S., Kimura, H., Perrem, K., Umezawa, A., Yamamoto, N.*, et al.* (2014). Induction of cells with cancer stem cell properties from nontumorigenic human mammary epithelial cells by defined reprogramming factors. Oncogene *33*, 643-652.

Nishigaki, M., Aoyagi, K., Danjoh, I., Fukaya, M., Yanagihara, K., Sakamoto, H., Yoshida, T., and Sasaki, H. (2005). Discovery of aberrant expression of R-RAS by cancer-linked DNA hypomethylation in gastric cancer using microarrays. Cancer research *65*, 2115-2124.

O'Brien, C.A., Kreso, A., and Jamieson, C.H. (2010). Cancer stem cells and self-renewal. Clinical cancer research : an official journal of the American Association for Cancer Research *16*, 3113-3120.

O'Donnell, K.A., Wentzel, E.A., Zeller, K.I., Dang, C.V., and Mendell, J.T. (2005). c-Myc-regulated microRNAs modulate E2F1 expression. Nature *435*, 839-843.

Oshimo, Y., Nakayama, H., Ito, R., Kitadai, Y., Yoshida, K., Chayama, K., and Yasui, W. (2003). Promoter methylation of cyclin D2 gene in gastric carcinoma. International journal of oncology *23*, 1663-1670.

Oster, S.K., Ho, C.S., Soucie, E.L., and Penn, L.Z. (2002). The myc oncogene: MarvelouslY Complex. Advances in cancer research *84*, 81-154.

Ozaki, S., Ikeda, S., Ishizaki, Y., Kurihara, T., Tokumoto, N., Iseki, M., Arihiro, K., Kataoka, T., Okajima, M., and Asahara, T. (2005). Alterations and correlations of the components in the Wnt signaling pathway and its target genes in breast cancer. Oncology reports *14*, 1437-1443.

Ozdemir, B.C., Pentcheva-Hoang, T., Carstens, J.L., Zheng, X., Wu, C.C., Simpson, T.R., Laklai, H., Sugimoto, H., Kahlert, C., Novitskiy, S.V.*, et al.* (2014). Depletion of carcinoma-associated fibroblasts and fibrosis induces immunosuppression and accelerates pancreas cancer with reduced survival. Cancer cell *25*, 719-734.

Pardal, R., Clarke, M.F., and Morrison, S.J. (2003). Applying the principles of stem-cell biology to cancer. Nature reviews Cancer *3*, 895-902.

Pelengaris, S., Khan, M., and Evan, G. (2002a). c-MYC: more than just a matter of life and death. Nature reviews Cancer *2*, 764-776.

Pelengaris, S., Khan, M., and Evan, G.I. (2002b). Suppression of Myc-induced apoptosis in beta cells exposes multiple oncogenic properties of Myc and triggers carcinogenic progression. Cell *109*, 321-334.

Perez-Roger, I., Kim, S.H., Griffiths, B., Sewing, A., and Land, H. (1999). Cyclins D1 and D2 mediate myc-induced proliferation via sequestration of p27(Kip1) and p21(Cip1). The EMBO journal *18*, 5310-5320.

Perna, D., Faga, G., Verrecchia, A., Gorski, M.M., Barozzi, I., Narang, V., Khng, J., Lim, K.C., Sung, W.K., Sanges, R*., et al.* (2012). Genome-wide mapping of Myc binding and gene regulation in serum-stimulated fibroblasts. Oncogene *31*, 1695-1709.

Perou, C.M., Sorlie, T., Eisen, M.B., van de Rijn, M., Jeffrey, S.S., Rees, C.A., Pollack, J.R., Ross, D.T., Johnsen, H., Akslen, L.A*., et al.* (2000). Molecular portraits of human breast tumours. Nature *406*, 747-752.

Pogribny, I.P., and James, S.J. (2002). De novo methylation of the p16INK4A gene in early preneoplastic liver and tumors induced by folate/methyl deficiency in rats. Cancer letters *187*, 69-75.

Poirier, L.A. (2002). The effects of diet, genetics and chemicals on toxicity and aberrant DNA methylation: an introduction. The Journal of nutrition *132*, 2336S-2339S.

Polyak, K., and Weinberg, R.A. (2009). Transitions between epithelial and mesenchymal states: acquisition of malignant and stem cell traits. Nature reviews Cancer *9*, 265-273.

Prat, A., Parker, J.S., Karginova, O., Fan, C., Livasy, C., Herschkowitz, J.I., He, X., and Perou, C.M. (2010). Phenotypic and molecular characterization of the claudin-low intrinsic subtype of breast cancer. Breast cancer research : BCR *12*, R68.

Qian, B.Z., and Pollard, J.W. (2010). Macrophage diversity enhances tumor progression and metastasis. Cell *141*, 39-51.

Raica, M., Cimpean, A.M., and Ribatti, D. (2009). Angiogenesis in pre-malignant conditions. European journal of cancer *45*, 1924-1934.

Rhim, A.D., Oberstein, P.E., Thomas, D.H., Mirek, E.T., Palermo, C.F., Sastra, S.A., Dekleva, E.N., Saunders, T., Becerra, C.P., Tattersall, I.W*., et al.* (2014). Stromal elements act to restrain, rather than support, pancreatic ductal adenocarcinoma. Cancer cell *25*, 735-747.

Romanov, S.R., Kozakiewicz, B.K., Holst, C.R., Stampfer, M.R., Haupt, L.M., and Tlsty, T.D. (2001). Normal human mammary epithelial cells spontaneously escape senescence and acquire genomic changes. Nature *409*, 633-637.

Ruden, D.M., Xiao, L., Garfinkel, M.D., and Lu, X. (2005). Hsp90 and environmental impacts on epigenetic states: a model for the trans-

generational effects of diethylstibesterol on uterine development and cancer. Human molecular genetics *14 Spec No 1*, R149-155.

Ryo, A., Nakamura, M., Wulf, G., Liou, Y.C., and Lu, K.P. (2001). Pin1 regulates turnover and subcellular localization of beta-Catenin by inhibiting its interaction with APC. Nature cell biology *3*, 793-801.

Sandgren, E.P., Schroeder, J.A., Qui, T.H., Palmiter, R.D., Brinster, R.L., and Lee, D.C. (1995). Inhibition of mammary gland involution is associated with transforming growth factor alpha but not c-myc-induced tumorigenesis in transgenic mice. Cancer research *55*, 3915-3927.

Sansom, O.J., Meniel, V.S., Muncan, V., Phesse, T.J., Wilkins, J.A., Reed, K.R., Vass, J.K., Athineos, D., Clevers, H., and Clarke, A.R. (2007). Myc deletion rescues Apc deficiency in the small intestine. Nature *446*, 676-679.

Sato, N., Maitra, A., Fukushima, N., van Heek, N.T., Matsubayashi, H., Iacobuzio-Donahue, C.A., Rosty, C., and Goggins, M. (2003). Frequent hypomethylation of multiple genes overexpressed in pancreatic ductal adenocarcinoma. Cancer research *63*, 4158-4166.

Schoenenberger, C.A., Andres, A.C., Groner, B., van der Valk, M., LeMeur, M., and Gerlinger, P. (1988). Targeted c-myc gene expression in mammary glands of transgenic mice induces mammary tumours with constitutive milk protein gene transcription. The EMBO journal *7*, 169-175.

Schroeder, A., Herrmann, A., Cherryholmes, G., Kowolik, C., Buettner, R., Pal, S., Yu, H., Muller-Newen, G., and Jove, R. (2014). Loss of androgen receptor expression promotes a stem-like cell phenotype in prostate cancer through STAT3 signaling. Cancer research *74*, 1227-1237.

Schulein, C., and Eilers, M. (2009). An unsteady scaffold for Myc. The EMBO journal *28*, 453-454.

Schwitalla, S., Fingerle, A.A., Cammareri, P., Nebelsiek, T., Goktuna, S.I., Ziegler, P.K., Canli, O., Heijmans, J., Huels, D.J., Moreaux, G.*, et al.* (2013). Intestinal tumorigenesis initiated by dedifferentiation and acquisition of stem-cell-like properties. Cell *152*, 25-38.

Sears, R., Nuckolls, F., Haura, E., Taya, Y., Tamai, K., and Nevins, J.R. (2000). Multiple Ras-dependent phosphorylation pathways regulate Myc protein stability. Genes & development *14*, 2501-2514.

Sellers, W.R., and Loda, M. (2002). The EZH2 polycomb transcriptional repressor--a marker or mover of metastatic prostate cancer? Cancer cell *2*, 349-350.

Semenov, M., Tamai, K., and He, X. (2005). SOST is a ligand for LRP5/LRP6 and a Wnt signaling inhibitor. The Journal of biological chemistry *280*, 26770-26775.

Semenov, M.V., Tamai, K., Brott, B.K., Kuhl, M., Sokol, S., and He, X. (2001). Head inducer Dickkopf-1 is a ligand for Wnt coreceptor LRP6. Current biology : CB *11*, 951-961.

Semenza, G.L. (2010). HIF-1: upstream and downstream of cancer metabolism. Current opinion in genetics & development *20*, 51-56.

Seoane, J., Pouponnot, C., Staller, P., Schader, M., Eilers, M., and Massague, J. (2001). TGFbeta influences Myc, Miz-1 and Smad to control the CDK inhibitor p15INK4b. Nature cell biology *3*, 400-408.

Shackleton, M., Vaillant, F., Simpson, K.J., Stingl, J., Smyth, G.K., Asselin-Labat, M.L., Wu, L., Lindeman, G.J., and Visvader, J.E. (2006). Generation of a functional mammary gland from a single stem cell. Nature *439*, 84-88.

Sherr, C.J., and McCormick, F. (2002). The RB and p53 pathways in cancer. Cancer cell *2*, 103-112.

Singh, A., and Settleman, J. (2010). EMT, cancer stem cells and drug resistance: an emerging axis of evil in the war on cancer. Oncogene *29*, 4741-4751.

Singh, S.K., Clarke, I.D., Terasaki, M., Bonn, V.E., Hawkins, C., Squire, J., and Dirks, P.B. (2003). Identification of a cancer stem cell in human brain tumors. Cancer research *63*, 5821-5828.

Sleeman, K.E., Kendrick, H., Ashworth, A., Isacke, C.M., and Smalley, M.J. (2006). CD24 staining of mouse mammary gland cells defines luminal epithelial, myoepithelial/basal and non-epithelial cells. Breast cancer research : BCR *8*, R7.

Sleeman, K.E., Kendrick, H., Robertson, D., Isacke, C.M., Ashworth, A., and Smalley, M.J. (2007). Dissociation of estrogen receptor expression and in vivo stem cell activity in the mammary gland. The Journal of cell biology *176*, 19-26.

Sorlie, T., Perou, C.M., Tibshirani, R., Aas, T., Geisler, S., Johnsen, H., Hastie, T., Eisen, M.B., van de Rijn, M., Jeffrey, S.S*., et al.* (2001). Gene expression patterns of breast carcinomas distinguish tumor subclasses with clinical implications. Proceedings of the National Academy of Sciences of the United States of America *98*, 10869-10874.

Soufi, A., Donahue, G., and Zaret, K.S. (2012). Facilitators and impediments of the pluripotency reprogramming factors' initial engagement with the genome. Cell *151*, 994-1004.

Southall, T.D., Davidson, C.M., Miller, C., Carr, A., and Brand, A.H. (2014). Dedifferentiation of neurons precedes tumor formation in Lola mutants. Developmental cell *28*, 685-696.

Sridharan, R., Tchieu, J., Mason, M.J., Yachechko, R., Kuoy, E., Horvath, S., Zhou, Q., and Plath, K. (2009). Role of the murine reprogramming factors in the induction of pluripotency. Cell *136*, 364-377.

Stadeli, R., Hoffmans, R., and Basler, K. (2006). Transcription under the control of nuclear Arm/beta-Catenin. Current biology : CB *16*, R378-385.

Stadtfeld, M., Maherali, N., Breault, D.T., and Hochedlinger, K. (2008). Defining molecular cornerstones during fibroblast to iPS cell reprogramming in mouse. Cell stem cell *2*, 230-240.

Stewart, T.A., Pattengale, P.K., and Leder, P. (1984). Spontaneous mammary adenocarcinomas in transgenic mice that carry and express MTV/myc fusion genes. Cell *38*, 627-637.

Stingl, J., Eirew, P., Ricketson, I., Shackleton, M., Vaillant, F., Choi, D., Li, H.I., and Eaves, C.J. (2006). Purification and unique properties of mammary epithelial stem cells. Nature *439*, 993-997.

Suzuki, H., Toyota, M., Carraway, H., Gabrielson, E., Ohmura, T., Fujikane, T., Nishikawa, N., Sogabe, Y., Nojima, M., Sonoda, T.*, et al.* (2008). Frequent epigenetic inactivation of Wnt antagonist genes in breast cancer. British journal of cancer *98*, 1147-1156.

Taddei, I., Deugnier, M.A., Faraldo, M.M., Petit, V., Bouvard, D., Medina, D., Fassler, R., Thiery, J.P., and Glukhova, M.A. (2008). Beta1 integrin deletion from the basal compartment of the mammary epithelium affects stem cells. Nature cell biology *10*, 716-722.

Takahashi, K., and Yamanaka, S. (2006). Induction of pluripotent stem cells from mouse embryonic and adult fibroblast cultures by defined factors. Cell *126*, 663-676.

Takebe, N., Harris, P.J., Warren, R.Q., and Ivy, S.P. (2011). Targeting cancer stem cells by inhibiting Wnt, Notch, and Hedgehog pathways. Nature reviews Clinical oncology *8*, 97-106.

Thiery, J.P., Acloque, H., Huang, R.Y., and Nieto, M.A. (2009). Epithelial-mesenchymal transitions in development and disease. Cell *139*, 871-890.

Tlsty, T.D., and Coussens, L.M. (2006). Tumor stroma and regulation of cancer development. Annual review of pathology *1*, 119-150.

Tolwinski, N.S., and Wieschaus, E. (2004). Rethinking WNT signaling. Trends in genetics : TIG *20*, 177-181.

Valent, P., Bonnet, D., De Maria, R., Lapidot, T., Copland, M., Melo, J.V., Chomienne, C., Ishikawa, F., Schuringa, J.J., Stassi, G.*, et al.* (2012).

Cancer stem cell definitions and terminology: the devil is in the details. Nature reviews Cancer *12*, 767-775.

van de Wetering, M., Barker, N., Harkes, I.C., van der Heyden, M., Dijk, N.J., Hollestelle, A., Klijn, J.G., Clevers, H., and Schutte, M. (2001). Mutant E-cadherin breast cancer cells do not display constitutive Wnt signaling. Cancer research *61*, 278-284.

Van Keymeulen, A., Lee, M.Y., Ousset, M., Brohee, S., Rorive, S., Giraddi, R.R., Wuidart, A., Bouvencourt, G., Dubois, C., Salmon, I.*, et al.* (2015). Reactivation of multipotency by oncogenic PIK3CA induces breast tumour heterogeneity. Nature *525*, 119-123.

Vander Heiden, M.G., Cantley, L.C., and Thompson, C.B. (2009). Understanding the Warburg effect: the metabolic requirements of cell proliferation. Science *324*, 1029-1033.

Varnat, F., Siegl-Cachedenier, I., Malerba, M., Gervaz, P., and Ruiz i Altaba, A. (2010). Loss of WNT-TCF addiction and enhancement of HH-GLI1 signalling define the metastatic transition of human colon carcinomas. EMBO molecular medicine *2*, 440-457.

Veeck, J., Niederacher, D., An, H., Klopocki, E., Wiesmann, F., Betz, B., Galm, O., Camara, O., Durst, M., Kristiansen, G.*, et al.* (2006). Aberrant methylation of the Wnt antagonist SFRP1 in breast cancer is associated with unfavourable prognosis. Oncogene *25*, 3479-3488.

Veeman, M.T., Axelrod, J.D., and Moon, R.T. (2003). A second canon. Functions and mechanisms of beta-Catenin-independent Wnt signaling. Developmental cell *5*, 367-377.

Vermeulen, L., De Sousa, E.M.F., van der Heijden, M., Cameron, K., de Jong, J.H., Borovski, T., Tuynman, J.B., Todaro, M., Merz, C., Rodermond, H.*, et al.* (2010). Wnt activity defines colon cancer stem cells and is regulated by the microenvironment. Nature cell biology *12*, 468-476.

Virmani, A.K., Muller, C., Rathi, A., Zoechbauer-Mueller, S., Mathis, M., and Gazdar, A.F. (2001). Aberrant methylation during cervical carcinogenesis. Clinical cancer research : an official journal of the American Association for Cancer Research *7*, 584-589.

Visvader, J.E. (2011). Cells of origin in cancer. Nature *469*, 314-322.

Visvader, J.E., and Stingl, J. (2014). Mammary stem cells and the differentiation hierarchy: current status and perspectives. Genes & development *28*, 1143-1158.

Walz, S., Lorenzin, F., Morton, J., Wiese, K.E., von Eyss, B., Herold, S., Rycak, L., Dumay-Odelot, H., Karim, S., Bartkuhn, M.*, et al.* (2014). Activation and repression by oncogenic MYC shape tumour-specific gene expression profiles. Nature *511*, 483-487.

Wanzel, M., Russ, A.C., Kleine-Kohlbrecher, D., Colombo, E., Pelicci, P.G., and Eilers, M. (2008). A ribosomal protein L23-nucleophosmin circuit coordinates Mizl function with cell growth. Nature cell biology *10*, 1051-1061.

Welcker, M., Orian, A., Grim, J.E., Eisenman, R.N., and Clurman, B.E. (2004a). A nucleolar isoform of the Fbw7 ubiquitin ligase regulates c-Myc and cell size. Current biology : CB *14*, 1852-1857.

Welcker, M., Orian, A., Jin, J., Grim, J.E., Harper, J.W., Eisenman, R.N., and Clurman, B.E. (2004b). The Fbw7 tumor suppressor regulates glycogen synthase kinase 3 phosphorylation-dependent c-Myc protein degradation. Proceedings of the National Academy of Sciences of the United States of America *101*, 9085-9090.

Wernig, M., Meissner, A., Cassady, J.P., and Jaenisch, R. (2008). c-Myc is dispensable for direct reprogramming of mouse fibroblasts. Cell stem cell *2*, 10-12.

Wissmann, C., Wild, P.J., Kaiser, S., Roepcke, S., Stoehr, R., Woenckhaus, M., Kristiansen, G., Hsieh, J.C., Hofstaedter, F., Hartmann, A.*, et al.* (2003). WIF1, a component of the Wnt pathway, is down-regulated in prostate, breast, lung, and bladder cancer. The Journal of pathology *201*, 204-212.

Witsch, E., Sela, M., and Yarden, Y. (2010). Roles for growth factors in cancer progression. Physiology *25*, 85-101.

Wu, S., Cetinkaya, C., Munoz-Alonso, M.J., von der Lehr, N., Bahram, F., Beuger, V., Eilers, M., Leon, J., and Larsson, L.G. (2003). Myc represses differentiation-induced p21CIP1 expression via Miz-1-dependent interaction with the p21 core promoter. Oncogene *22*, 351-360.

Xu, Q., Wang, Y., Dabdoub, A., Smallwood, P.M., Williams, J., Woods, C., Kelley, M.W., Jiang, L., Tasman, W., Zhang, K.*, et al.* (2004). Vascular development in the retina and inner ear: control by Norrin and Frizzled-4, a high-affinity ligand-receptor pair. Cell *116*, 883-895.

Yada, M., Hatakeyama, S., Kamura, T., Nishiyama, M., Tsunematsu, R., Imaki, H., Ishida, N., Okumura, F., Nakayama, K., and Nakayama, K.I. (2004). Phosphorylation-dependent degradation of c-Myc is mediated by the F-box protein Fbw7. The EMBO journal *23*, 2116-2125.

Yeh, E., Cunningham, M., Arnold, H., Chasse, D., Monteith, T., Ivaldi, G., Hahn, W.C., Stukenberg, P.T., Shenolikar, S., Uchida, T.*, et al.* (2004). A signalling pathway controlling c-Myc degradation that impacts oncogenic transformation of human cells. Nature cell biology *6*, 308-318.

Zeng, X., Tamai, K., Doble, B., Li, S., Huang, H., Habas, R., Okamura, H., Woodgett, J., and He, X. (2005). A dual-kinase mechanism for Wnt co-receptor phosphorylation and activation. Nature *438*, 873-877.

Zhou, B.B., Zhang, H., Damelin, M., Geles, K.G., Grindley, J.C., and Dirks, P.B. (2009). Tumour-initiating cells: challenges and opportunities for anticancer drug discovery. Nature reviews Drug discovery *8*, 806-823.

Zhou, S., Schuetz, J.D., Bunting, K.D., Colapietro, A.M., Sampath, J., Morris, J.J., Lagutina, I., Grosveld, G.C., Osawa, M., Nakauchi, H*., et al.* (2001). The ABC transporter Bcrp1/ABCG2 is expressed in a wide variety of stem cells and is a molecular determinant of the side-population phenotype. Nature medicine *7*, 1028-1034.

Zindy, F., Eischen, C.M., Randle, D.H., Kamijo, T., Cleveland, J.L., Sherr, C.J., and Roussel, M.F. (1998). Myc signaling via the ARF tumor suppressor regulates p53-dependent apoptosis and immortalization. Genes & development *12*, 2424-2433.

MYC favors the onset of tumorigenesis by inducing epigenetic reprogramming of mammary epithelial cells towards a stem cell-like state

Vittoria Poli[1], Luca Fagnocchi[1#], Stefania Mazzoleni[1], Alessandro Cherubini[1], Alessandra Fasciani[1], Valeria Berno[1], Valentina Vaira[2], Alice Turdo[3], Antonella Benfante[3], Miriam Giaggianesi[3], Matilde Todaro[3], and Alessio Zippo[1#]

[1]Fondazione Istituto Nazionale di Genetica Molecolare *"Romeo ed Enrica Invernizzi",* Via F. Sforza 35, 20122 Milan, Italy.

[2] Fondazione Cà Granda Policlinico Maggiore.

[3] Dipartimento di Biotecnologie Mediche e Medicina Legale Sezione di Biochimica Medica, Facoltà di Medicina e Chirurgia, Policlinico "P.Giaccone", Università di Palermo.

[#] to whom correspondence should be addressed: zippo@ingm.org and fagnocchi@ingm.org

Abstract

Breast cancer is the most frequent cancer among women and it consists of highly heterogeneous tumors whose cell of origin resulted difficult to be defined. Recent finding highlighted the possibility that tumor-initiating cells (TICs) may arise from the dedifferentiation of lineage-committed cells by reactivation of multipotency in response to oncogenic insults. MYC is the most frequent amplified oncogene in breast cancer and the activation of MYC pathway has been associated with the basal-like subtype, which is characterized by poor survival, lacking of a specific therapeutic strategy. Although MYC has been considered a driver oncogene in breast cancer, its mechanism of action in tumor initiation has been poorly addressed. Here we show that MYC acts as tumor reprogramming factor by inducing an alternative epigenetic program, which triggers loss of cell identity and activation of oncogenic enhancers. Overexpression of MYC induces transcriptional repression of lineage-specific transcription factors, provoking decommissioning of luminal-specific regulatory elements. MYC-driven dedifferentiation supports the onset of a SC-like state by inducing the activation of *de novo* oncogenic enhancers, triggering the formation of TICs.

Highlights

- MYC induces dedifferentiation of mammary luminal epithelial cells by determining transcriptional repression of luminal-specific TFs
- Sustained MYC expression confers stem cell-like traits by re-activating oncogenic enhancers
- MYC-induced epigenetic reprogramming favors tumor initiation

Introduction

Tumorigenesis can be described as a succession of genetic and epigenetic alterations which turn in heritable changes in gene expression programs, ultimately leading to the formation of a cell population characterized by functional and phenotypic heterogeneity (Feinberg and Tycko, 2004; Hanahan and Weinberg, 2011). Cell transformation frequently involves activation of developmental signaling programs which endow cells with unlimited self-renewal potential and aberrant differentiation capability (Visvader and Lindeman, 2012; Zhou et al., 2009). Cancer cells that display stem-like properties are considered the driver of tumor initiation and propagation (Al-Hajj et al., 2003; Bonnet and Dick, 1997).

Somatic stem cells (SCs) have been considered putative candidates for targets of transformation because of their inherent capacity for self-renewal and their longevity, which would allow the acquisition of the combination of genetic and epigenetic aberrations sufficient for cell transformation (Barker et al., 2009; Schepers et al., 2012). Nevertheless, several recent studies demonstrated that, upon oncogenic alterations, progenitors or committed cells can serve as a tumor initiating cell (TIC) by dedifferentiating and re-acquiring stem cell-like traits (Chaffer et al., 2013; Friedmann-Morvinski et al., 2012; Schwitalla et al., 2013; Visvader, 2011).

In the context of mammary gland tumorigenesis, several studies, designed to elucidate the cell of origin of different molecular subtypes of breast cancer, have shown that the human basal-like breast cancer subtype may arise from luminal progenitor cells (Lim et

al., 2009; Molyneux et al., 2010; Shehata et al., 2012). More recently it has been shown that oncogenic PIK3CA^{H1047R} into normal lineage-restricted mouse mammary cells causes cell dedifferentiation and development of multi-lineage mammary tumors (Koren et al., 2015; Van Keymeulen et al., 2015). Although these findings highlighted a functional role for oncogenic-driven cell dedifferentiation in tumor initiation, the molecular mechanisms underlying cell reprogramming are incompletely understood.

Cell reprogramming requires overcoming those epigenetic barriers which are involved in maintaining cell-specific transcriptional program, thereby preserving cell identity (Apostolou and Hochedlinger, 2013; Buganim et al., 2013) (Fagnocchi et al., 2016). The activation of a specific repertoire of *cis*-regulatory elements -enhancers- is critical for cell specification. Cooperative binding of lineage-determining and signal-dependent transcription factors dictate the spatio-temporal pattern of gene expression, by recruiting on the enhancers chromatin modifiers, nucleosome remodelers and chaperones (Calo and Wysocka, 2013). Enhancers are characterized by accessible chromatin, marked by the deposition of H3K4me1, and their activation is associated with an increased of H3K27 acetylation. Given their pivotal role in the determination of cell identity, decommissioning of active enhancers represent a critical step towards cell reprogramming (Whyte et al., 2012). Of importance, several evidences indicated that deregulation of chromatin players responsible for enhancer regulation, could favor tumorigenesis by

driving the aberrant activation of oncogenic transcriptional programs (Shen et al., 2016).

Among the transcription factors with a documented function in somatic cell reprogramming (Singh and Dalton, 2009; Takahashi and Yamanaka, 2006), the proto-oncogene *MYC* has a pivotal role in growth control, differentiation and apoptosis and its expression level is tightly regulated in physiological conditions (Dang, 2012). In cancer, *MYC* overexpression has been associated with up to 70% of all human tumors and near 45% of breast cancers, in which MYC hyperactivation has been identified as key regulatory feature of the aggressive triple negative subtype (Cancer Genome Atlas, 2012; Chandriani et al., 2009; Dang, 2012; Palaskas et al., 2011; Vita and Henriksson, 2006).

Despite MYC proven oncogenic potential and its known function in the maintenance of self-renewing capacity and pluripotency (Fagnocchi L. et al., 2016), a causal link between MYC role as reprogramming factor and its tumorigenic effects has not been investigated yet.

In the present study, we aimed to understand whether MYC acts as an oncogenic reprogramming factor that drives tumor initiation by inducing a phenotypic plasticity that predisposes differentiated cells to re-acquisition of SCs characteristics and, after further oncogenic insults, to neoplastic transformation. We demonstrated that stable MYC overexpression makes human mammary luminal epithelial cells competent for tumor initiation, by inducing the reactivation of a progenitor-like transcriptional program. The isolation of single MYC

overexpressing cells allows the propagation of mammospheres that go further in the reprogramming process, gaining mammary SC-like traits. This process is mediated by the specific activation of a number of oncogenic enhancers, including regulatory elements related to the Wnt/β-Catenin signaling. In this scenario, the combination of MYC overexpression with the reinforcement of the PIK3CA pathway causes the onset of TICs.

Results

MYC alters cell polarity and mitotic spindle orientation in mammary luminal epithelial cells

In order to evaluate the role of MYC in perturbing the pattern of cell division of mammary epithelial cells, we transduced hTERT-immortalized human mammary epithelial cells (thereafter named HMEC) with a retroviral vector expressing low levels of the exogenous c-Myc (Figure 1A). MYC overexpression induced alteration of the epithelial (cobblestone-like) morphology with cells loosing polarity and adhesion to the basement membrane, growing in semi-adherent condition and forming fluctuating spheroids (Figure 1B). These phenotypic observations were corroborated by immunofluorescence staining, which showed disorganization of adherent junctions resulting in cytoskeleton alterations (Figure 1C). In addition, we measured a relative decrease of E-Cadherin at both the transcription and protein level, which was mirrored by a concomitant reduction of β-Catenin (Figure 1D-E), suggesting

destabilization of adherent junctions. Of note, we did not observed cadherin switching (Andrews et al., 2012) nor induction of epithelial-mesenchymal transition (EMT)-related transcription factors, indicating that the observed phenotype could not solely rely on induction of EMT (Figure 1E and Supplementary Figure S1A). Given that junctional complexes participate in the establishment of apical-basal cell polarity (Martin-Belmonte and Perez-Moreno, 2012), we determined whether the MYC-induced morphological changes could depend on mislocalization of polarity complexes. We assessed by immunofluorescence the localization of the atypical protein kinase C (aPKC), which is enriched at the apical cortex and is functionally associated with cell fate determination. We observed that, although MYC overexpression in HMEC did not affect the total protein level of PAR-related proteins (not shown), it caused changes of aPKC subcellular localization, which was not restricted to the apical membrane (Figure 1F). Considering that the PAR complex and adherent junctions orient cell division (Zimdahl et al., 2014) (Hao et al., 2010) (Taddei et al., 2008), we determined whether MYC overexpression may affect the mitotic spindle positioning in HMEC. By visualizing the centrosomal nucleation via γ-Tubulin staining of mitotic cells, we observed that in HMEC the spindle positioned parallel (0–10°) to the substrate in both metaphase and telophase, as expected (Figure 1G). In contrast, we determined that in at least 50% of the analyzed cells, HMEC-MYC (MYC) showed a tendency to divide with non-planar spindle orientations (10-25°), indicating that MYC overexpression induces mitotic spindle disorientation at high

frequency (Figure 1G). To further confirm these findings, we analyzed the pattern of cell division in living cells by performing continuous time-lapse imaging on HMEC expressing H2B-mCherry (Supplementary Movies S1 and S2). By imaging cell entering in mitosis at different focal plane, we observed that while HMEC always divided with a planar mitotic spindle, the MYC overexpressing cells positioned the separating chromosomes on different planes (Figure 1H and Supplementary Movie S1 and S2). By performing single cell tracking of the mis-oriented segregated cells, we measured a higher tendency to grow in non-adherent conditions, giving rise to the formation of mammospheres. Taken together, these data suggest that MYC overexpression in HMEC favors asymmetric division by inducing adherent junction disorganization, perturbation of cell polarity and mitotic spindle disorientation (Figure 1I).

MYC inhibits the transcriptional program of mature luminal epithelial cells

Considering that the establishment and maintenance of apical-basal polarity is critical for normal function and symmetric cell division of mammary epithelial cells, we sought to investigate whether MYC overexpression could subvert cell identity. Genome wide expression profile analyses showed that HMEC and HMEC-MYC differed for the expression of a specific subset of genes (Figure 2A). In order to gain insights on which cell processes are differentially regulated in cells overexpressing MYC, we performed gene ontology (GO) analyses, which indicated a relative enrichment for genes involved in metabolic

processes and cell transporter activity (Figure 2B and Supplementary Figure S2A). Moreover, gene enrichment analyses showed that these up-regulated genes were commonly target of both MYC and MAX and were generally marked with histone modifications associated with active transcription (Supplementary Figure S2A). At the same time, genes down-regulated in HMEC-MYC were enriched for genes involved in developmental processes, mechanisms of cell adhesion and extracellular matrix integrity (Figure 2B and Supplementary Figure S2A). These observations agree with the well known function of MYC in the induction of cell growth, metabolism and inhibition of cell adhesion (Gebhardt et al., 2006) (Dang et al., 2006). Of note, the gene expression profiling results corroborated the observed MYC-induced disorganization of adherence junctions (Figure 1C-E). Moreover, gene set enrichment analysis (GSEA) confirmed that genes involved in cell apical junction and mitotic spindle orientation were significantly down-regulated in HMEC-MYC respect to WT (Supplementary Figure S2B). In order to determine whether MYC-induced alterations at both the morphological and transcriptional level may trigger perturbation of cell identity, we compared the gene expression profile of HMEC WT and -MYC with available gene expression signatures of mature (ML) and progenitor luminal (LP) cells. GSEA analyses revealed a marked down-regulation of the ML program in cells overexpressing MYC, combined with a significant enrichment of the LP-specific signature (Figure 2C). Accordingly, HMEC-MYC down-regulated ML lineage markers (*GATA3*, *ESR1*, *MUC1* and *VEGFC*), while up-regulating mammary LP markers

(*EIF2S3*, *STAT5A/B* and *LETMD1*) (Figure 2D and Supplementary Figure S2C). Notably, GATA3 and ESR1 transcription factors are master regulators of mammary gland morphogenesis and luminal cell differentiation (Asselin-Labat et al., 2007; Mueller et al., 2002). We therefore asked whether GATA3 and ESR1 down-regulation in *MYC* overexpressing cells could be mediated by MYC binding to their *cis*-regulatory elements. Upon MYC overexpression, we measured a concomitant increased of MYC association and reduction of histone marks related to transcriptionally active genes (Figure 2E). In agreement with *GATA3* and *ESR1* down-regulation, also genes under the control of enhancer regulatory elements, bound by luminal lineage transcription factors, resulted specifically down-regulated in HMEC-MYC (Figure 2F). Together, these data indicate that MYC overexpression induced dedifferentiation of mature luminal cells, by down-regulating the expression of lineage-specific transcription factors, thereby supporting the acquisition of a progenitor-like cell identity.

Sustained MYC overexpression confers stem cell-like traits

On the basis of the observed MYC-induced transcriptional cell reprogramming versus a progenitor-like condition, we asked whether MYC overexpression could enrich for cells with functional stem cell properties. We therefore measured the ability of HMEC WT and -MYC to grow for subsequent passages in low adherence conditions as mammospheres, an in vitro system that allows the enrichment for progenitor/stem cells (Dontu et al., 2003). While WT cells formed

mammospheres with low efficiency and did not proliferate beyond the second passage, cells overexpressing MYC showed enhanced sphere formation efficiency (SFE) (Figure 3A-B). Of importance, we observed that MYC overexpression supported cell growth as mammospheres for several passages, indicating acquisition of long-term self-renewal capacity (Figure 3A-C and Supplementary Figure S3A-B). In addition, we observed that with the increment of cell passages, the dimension of MYC-derived mammospheres were reduced, suggesting a progressive enrichment for slow proliferating stem-like cells (Figure 3C). Furthermore, HMEC-MYC mammospheres contained a higher percentage of $ALDH1^{high}$ cells (Figure 3D), where expression of high ALDH1 levels is considered a distinctive marker of mammary SCs (Ginestier et al., 2007). Considering that different genetic alterations are commonly related to breast cancer (Cancer Genome Atlas, 2012), in order to verify whether the observed phenotype was a specific MYC-dependent effect, we set out to analyze cell behaviors carrying also other oncogenic hits. We therefore transduced HMEC with vectors expressing either oncogenic $PIK3CA^{H1047R}$, RAS or dominant negative P53 (P53DD) and measured their long-term capacity to propagate as mammospheres. Although HMEC-$PIK3CA^{H1047R}$ and -RAS showed an intermediate level of proliferation capacity in low adhesion, all conditions were characterized by lower proliferation and reduced SFE respect to HMEC-MYC, similarly to WT cells (Supplementary Figure S3A-C).

In order to verify a MYC-dependent enrichment in cells with SC properties, we analyzed the self-renewing capacity, by measuring the

potential of a single cell to form a mammosphere. While HMEC WT could give rise to a single cell-derived clone only with the addition of an extracellular support, such as Matrigel, MYC overexpression was always associated with higher self-renewing capability than PIK3CA^{H1047R}, RAS or P53DD (Figure 3E and Supplementary Figure S3E). Moreover, single cell-derived primary spheres (M1) originating from HMEC-MYC, turned out to be further enriched in cells with self-renewal capacity, showing higher SFE respect to parental heterogeneous population (Figure 3F). This phenotype could be maintained at least in two subsequent clonings, in which the time-window required for development of secondary (M2) and tertiary (M3) spheres became progressively shortened (Figure 3F). Of importance, similar results were obtained with freshly isolated primary HMEC: although a preliminary transduction with P53DD was necessary, in order to overcome MYC pro-apoptotic effects in primary cells, MYC-P53DD combination showed higher SFE respect to P53DD-only condition (Supplementary Figure S3F).

To determine whether the MYC-driven mammospheres were enriched for SC-like cells with differentiation potential, we analyzed the expression of lineage-restricted markers. For what concerns the expression of mammary gland luminal (Cytokeratin 8 and ESR1) and myoepithelial (Cytokeratin 14 and α-SMA) markers, single cell-derived mammospheres showed an undefined, not fully committed phenotype (Figure 3G). Furthermore, under differentiation conditions, they were able to modulate the expression of markers of both lineages, showing enhanced expression of luminal and

myoepithelial cytokeratins, reduction of α-SMA expression and nuclear localization of ESR1 (Figure 3G). Given the observed phenotype, we asked whether MYC supported the activation of stem cell-like transcriptional program. To this end, we profiled gene expression of single cell-derived mammospheres (M2), determining differentially expressed genes respect to HMEC-MYC. GO analyses showed that mammospheres were characterized by further up-regulation of genes involved in metabolic processes and down-regulation of genes involved in developmental processes (Figure 3H and 2B). This suggested a reinforcement of MYC-driven transcriptional program. Furthermore, as observed by both GO and GSEA analyses, M2 up-regulated genes involved in Wnt and Hippo signaling pathways, which are critical regulators of stem cell self-renewing (Reya and Clevers, 2005; Zhao et al., 2011) (Figure 3H and Supplementary Figure 3G). Notably, GSEA analysis also revealed that the core embryonic stem cell-like gene module (Core ESCS) was highly active in M2 clones respect to HMEC-MYC, and that genes codifying for MYC-related factors (MYC Module) significantly contributed to this transcriptional signature (Figure 3I and Supplementary S3H) (Kim et al., 2010). Collectively, the above data suggest that constitutive MYC overexpression in mature luminal cells induces a reprogramming process characterized by gaining of mammary SC-like traits, such as sustained self-renewing capacity, and re-activation of a pluripotency transcriptional program (Figure 3J).

MYC induces an alternative epigenetic program in mammary epithelial cells

To gain insights the mechanisms through which MYC induced cellular reprogramming, we performed ChIP-seq analyses to profile chromatin modifications and the binding of MYC in HMEC-WT, -MYC and mammospheres (Figure 4). We identified 1113 peaks for endogenous MYC, which were enriched at promoters of both coding and non-coding genes. Upon overexpression of MYC, we observed an increment of MYC-bound loci in both HMEC-MYC and M2 cells (3966 and 4629, respectively), in agreement with previous findings (Cancer Genome Atlas, 2012) (Sabo et al., 2014). However, the distribution of MYC-bound loci did not change in response to MYC overexpression, with nearly 50% of binding sites localized at promoters (Figure 4A). Considering that MYC binding has been associated with transcription activation, we analyzed the pattern of H3K4me3 on those promoters that resulted being MYC targets. ChIP-seq analyses showed that MYC occupancy at promoters increased in response to its overexpression and it correlated with an increment of H3K4me3 deposition. Gene expression profiling of MYC-bound genes showed that overall the augmented MYC association at their promoters correlated with an increased gene expression (Figure 4B and Supplementary Figure S4A). Importantly, GO analyses showed that MYC-target genes are involved in cell metabolism and cell cycle progression (Figure 4C). These analyses indicated that MYC activated a gene expression program related to cell growth by binding the proximal promoter of active genes, in accordance to what have been previously described.

Considering that MYC also associated to introns and intergenic regions (Figure 4A), we investigated whether MYC occupied and modulated the activation of enhancers in the three cellular conditions. By profiling the distribution of H3K4me1 in HMEC WT, -MYC and M2, we first mapped all the putative distal cis-regulatory elements, resulting in identifying more than 240.000 putative enhancers (Figure 4D). To investigate the dynamic changes occurring at the enhancers during the cellular transition from luminal epithelial cells towards SC-like state, we determined the relative enrichment for H3K27ac at these loci. Overall, the cellular reprogramming was mirrored by a highly dynamic modulation of the defined cis-regulatory elements giving rise to different enhancer states (Figure 4D). The comparative analyses showed that a subset of enhancers resulted repressed in the MYC-overexpressing cells, as they showed a consistent reduction of the H3K27ac level (Figure 4E). Importantly, the repressed enhancer resulted being target of MYC, which dissociated from these loci in response to its overexpression in both HMEC-MYC and M2 cells. In order to define whether these epigenetic changes caused perturbation of the transcriptional state, we sought to identify the set of genes that are most likely associated with the enhancers. Considering that most of the enhancer-promoter looping occurs within a distance of 50-100 kb, (Chepelev et al., 2012) we assigned each enhancer to the most proximal gene. Using this criterium of proximity and measuring the relative gene expression level, we observed that enhancer repression determined the down regulation of their related-genes (Figure 4E and Supplementary

Figure S4B). Of importance, this subset of enhancers modulated the expression level of many genes involved in the establishment of the transcriptionally regulatory network of luminal cells, such as ESR1, AP2-γ and ZNF217 (Figure 4F and Supplementary Figure S5A). In addition, the same group of repressed enhancers controlled the expression of a large set of genes involved in cell polarity, mitotic spindle orientation and cell adhesion (Figure 4E-F and Supplementary Figure S5B). GO analyses highlighted that the WT-specific activated enhancers were enriched for genes involved in the integrin, EGF and PI3K signaling pathways, indicating that some of the repressed genes in HMEC-MYC were controlled at the enhancer level (Figure 4F and Supplementary Figure S4C). In the same comparison, we detected enhancers in which the level of H3K27ac was transiently increased in the HMEC-MYC but not maintained in the mammospheres, suggesting that the specified epigenetic program was restricted to the progenitor-like state (Figure 4F and Supplementary Figure S4C). By focusing on the chromatin modulations occurring in the mammospheres, we identified a subset of enhancers, which were specifically activated in M2. (Figure 4D). These *de novo* enhancers were defined as distal genomic regions, which resulted unmarked for both H3K4me1 and H3K27ac in HMEC and gained these chromatin modifications upon the transition to a SC-like state (Figure 4E). In addition, the global analyses highlighted that the activation of the *de novo* enhancers was characterized by an increment of MYC association at these loci. Gene expression profiling showed that the activation of this class of enhancers was mirrored by an increased

expression of the associated genes, which were particularly enriched for transcription factors enriched in basal/SC-like state such as SOX9, ZEB1, FOXC1, TCF7L1 and TAZ (Figure 4F and Supplementary Figure S5C-D). In addition, we found that genes involved in activating the Wnt signaling were strongly enriched in this subset of enhancer, including receptor for both the canonical and the non-canonical pathway (Figure 4E). These findings were corroborated by performing GO analyses, which showed that the *de novo* enhancers were enriched for genes specifically involved in the Wnt signaling pathways (Figure 4F and Supplementary Figure S4C). Taken together, these results indicated that the MYC-induced transcriptional program is triggered by the repression of those enhancers that modulate the expression of lineage-specific transcription factors. In addition, the acquisition of a SC-like fate is driven by the activation of *de novo* enhancers that controlled the expression of transcription factors and signaling pathway which are specifically induced in both somatic and cancer stem cells.

Activation of *de novo* enhancers drives oncogenic pathways

To gain insight into the molecular mechanisms that may support the transcriptional activation of the *de novo* enhancer-related genes, we focused on those transcription factors that could be involved in this regulation. By ranking the *de novo* enhancer-related genes for their expression level, we observed a relative increment of MYC association to those enhancers associated with the overexpressed genes in mammospheres (Figure 5A). Importantly, GO analyses

showed that the enhancer-dependent regulated genes are associated with the modulation of Wnt pathways (Figure 5B). To better define the contribution of MYC binding to the transcriptional modulation of these targets we defined the set of genes whose *de novo* enhancers were bound by MYC and induced in mammospheres. This analysis showed that MYC associated with one third of the 289 regulated genes, suggesting a functional role of MYC in inducing gene expression by directly binding the enhancers of the associated-genes (Figure 5C and D). Specifically among the regulated targets which are enriched for MYC binding and increased of H3K27ac, we identified genes coding for oncogenic transcription factors as well as genes involved in regulating both the canonical and non-canonical Wnt pathway which are often deregulated in breast cancer. We then determined the direct contribution of MYC binding to the chromatin state of the *de novo* enhancers, by measuring the relative enrichment for H3K27ac and MYC at these loci (Figure 5E and F). These analyses showed that the M2-induced enhancers are characterized by a large distribution of both H3K27 and K4me1 marks, spanning as average regions over 3.1 kb. In addition, we found that MYC binding peaked at the center of the H3K27ac-enriched region, suggesting a direct contribution to the deposition of this active histone mark (Figure 5F). Considering that cooperative binding of different transcription factors modulate enhancer activation, we sought to define DNA binding elements enriched at the epicenter of the *de novo* enhancers. By performing motif discovery analyses we found enrichment for FOX- and SOX- family member as well as ETS1 motifs (Figure 5G).

Importantly, among the MYC-target *de novo* enhancers we found a specific enrichment for a non-canonical E-box, indicating that MYC association is mediated by its direct binding to the chromatin. In summary, these data strongly support the notion that *de novo* enhancers modulate the transcriptional activation of oncogenic pathways, and that MYC binding is enriched at the epicenter of these enhancers, suggesting a critical role in their activation.

Reactivation of Wnt pathway supports MYC-induced stem cell features

In order to verify whether the observed positive regulation of enhancers associated with the transcriptional activation of Wnt pathway-related genes, we performed qRT-PCR on selected genes. We confirmed that *FZD1* and *FZD8* receptors were strongly induced in M2 respect to HMEC-MYC, supporting the enhancer-driven transcriptional activation of these genes (Figure 6A). Interestingly the co-receptors *LRP5* and *LRP6* were induced with a different kinetics as they were up-regulated in response to MYC overexpression, suggesting a different mechanism of transcriptional regulation (Figure 6A). On the other hand, the two major inhibitors of the pathway, *DKK1* and *SFRP1*, were strongly down-regulated in cells overexpressing MYC, with further reduction in mammospheres (Figure 6A). These data supported the notion that MYC-driven SC state correlated with the transcriptional modulation of Wnt pathway-related genes. To determine whether these regulatory mechanisms determined the overall hyperactivation of the Wnt pathway we

transduced HMEC-MYC with a lentiviral vector containing a 7xTCF-eGFP reporter cassette (7TGP), that would allow to visualize cells positive for Wnt signaling activity. FACS analyses showed that the Wnt pathway was activated in mammospheres but not in HMEC-MYC. Furthermore, we observed that the level of Wnt activation augmented with increased cell passaging, as determined by measuring the median fluorescence intensity (MFI) (Figure 6B). This observation suggested that enrichment for cells overexpressing MYC, able to grow in low adhesion conditions, was related to induction of Wnt signaling activation. In order to determine whether such up-regulation could have a functional role in MYC-induced SC features, we proceeded by discerning between HMEC-MYC with the highest (GFP^{high}) and the lowest (GFP^{low}) signal of Wnt pathway activation. By performing dye retention assay, we observed that Wnt responsive cells (GFP^{high}) were enriched for slow-dividing cells as retained higher level of the cell tracer (Figure 6C). Given the cellular heterogeneity within the mammospheres population, these results suggested that GFP^{high} cells could be endowed with SC-like properties. We therefore performed single cell sorting of GFP^{high} and GFP^{low} cells, in order to compare the relative SFE (Figure 6D). On average, GFP^{high} sub-population showed enrichment in cells with self-renewing capacity (Figure 6E). We further characterized the GFP^{high}-derived primary spheres (GFP^{high}-derived M1) respect to the relative enrichment for Wnt pathway activation. The obtained results showed a concomitant increment of Wnt signaling in the GFP^{high}-derived mammospheres respect to the GFP^{low} cells (Figure 6E). Furthermore, by performing

serial clonogenic assay of both GFP^{high} and GFP^{low} cells (Figure 6D), we observed that the Wnt responsive population was further endowed with self-renewing capacity, giving rise to clones characterized by enhanced activation of the pathway (Figure 6E). To support these findings, we compared the gene expression profile of freshly isolated GFP^{high} and GFP^{low} cells with available gene expression signature of mammary stem cells (MaSCs). GSEA analyses revealed a marked enrichment of the MaSCs transcriptional signature in GFP^{high} respect to GFP^{low} cells (Figure 6F). In addition we observed that GFP^{high} subpopulation had also high correlation with different metastatic transcriptional signatures (Figure 6G). Altogether these results suggested a correlation between the reactivation of Wnt pathway and acquisition of a SC-like transcriptional program, which has been shown to associate with increased risk of developing recurrent cancer (Charafe-Jauffret et al., 2009; Friedmann-Morvinski and Verma, 2014; Merlos-Suarez et al., 2011). Furthermore our results suggest that, within the heterogeneous cell population, the hyperactivation of Wnt pathway could represent a functional marker for cells endowed with the highest self-renewing capacity.

MYC-induced reprogramming favors the onset of TICs

In order to determine whether MYC-induced transcriptional cell reprogramming could favor the onset of TICs *in vivo*, we challenged HMEC-MYC with an additional oncogenic insult by overexpressing $PIK3CA^{H1047R}$. $PIK3CA^{H1047R}$ expression induced enhanced MYC-related phenotype, with the majority of the cells growing in suspension, and

increased self-renewing capacity respect to HMEC-MYC and HMEC-PIK3CA^{H1047R} (Figure 7A-B). We then subjected HMEC-MYC, -PIK3CA^{H1047R} and -MYC-PIK3CA^{H1047R} to soft agar colony forming assay and transwell migration assay, in order to assess their *in vitro* tumorigenic potential and invasion capacity, respectively. We observed that HMEC-MYC-PIK3CA^{H1047R} cells formed about 3-fold more colonies and showed higher migration capacity than control cells (Figure 7C and Supplementary Figure 6A), suggesting that they could be enriched for transformed cells, with *in vivo* tumorigenic and invasion capacity. In order to address this aspect, we injected HMEC-MYC-PIK3CA^{H1047R} cells in the mammary fat pad of immunocompromised (*Nude*) mouse hosts. Within 30 days, all mice injected with HMEC-MYC-PIK3CA^{H1047R} cells formed tumors, while no tumors arose when an equal number of HMEC-MYC or HMEC-PIK3CA^{H1047R} were injected (Figure 7D). Immuno-histochemical analyses showed that all formed tumors presented a highly undifferentiated and proliferative phenotype (KI67^{+}), with high degree of vascularization and rare necrotic areas (Figure 7E). The xenografts resulted in highly heterogenous cell population bearing both luminal and epithelial phenotypes as illustrated by the double positive signal for both myoepithelial (Cytokeratins 5/6 and P63) and luminal markers (Cytokeratins 8/18 and progesterone receptor) (Supplementary Figure 6B). In addition we scored cells that were positive for vimentin mesenchymal marker and showed negativity for HER2 and estrogen receptor (Supplementary Figure 6B). We further characterized the MYC-PIK3CA^{H1047R}-tumors by isolating xenograft-

derived (XD) cells and performing functional assays. All XD cells showed a completely reprogrammed morphology, since they showed an even reduced capacity to adhere and form epithelial-like structures, respect to the parental population (Figure 7F). In addition soft agar assay showed that XD cells maintained capacity to form colonies, similarly to the parental HMEC-MYC-PIK3CA^{H1047R} (Supplementary Figure 6C). Many tumor types harbor a subpopulation of cancer stem cells (CSCs), endowed with tumorigenic potential, which are uniquely able to indefinitely propagate malignant clones (Valent et al., 2012). In order to assess whether HMEC-MYC-PIK3CA^{H1047R} neoplastic population could contain cells that had acquired properties of CSCs, we injected the XD cells into secondary recipient mice. Both the injected XD cell lines gave rise to secondary tumors with a similar kinetics respect to the parental cells, indicating maintenance of long-term tumorigenic capacity.

Discussion

MYC is as key oncogenic driver, able to interfere with normal as well as tumor cell differentiation (Dang, 2012). Despite its proven role in tumorigenesis, its mechanisms of action as tumor reprogramming factor are still not fully defined. It has been demonstrated that, in contrast to other transcription factors, that activate gene expression by recruiting the transcription apparatus to promoters, MYC does not regulate a specific cohort of target genes. Studies conducted on embryonic stem cells (ESCs) and tumor cells indicated that MYC acts as a general amplifier of gene expression, preferentially binding to E-

box sequences in the core promoter elements of most actively transcribed genes (Lin et al., 2012; Nie et al., 2012; Rahl et al., 2010).

In this work, we report the central role of MYC in initiating and sustaining a step-wise cell reprogramming process in differentiated mammary epithelial cells, toward a stem cell-like condition, which favors cell transformation and tumor initiation. We show that MYC overexpression in luminal cells induces dedifferentiation toward a progenitor-like state, achieved through down-regulation of the lineage-specific transcription factors . Our data showed enrichment of MYC binding at the level of key luminal transcription factors, such as *GATA3* and *ESR1* master regulators, to which correspond reduced histone marks related to active transcription. Although these observations suggested that MYC could directly mediate this process, we did not define the molecular mechanism through which it could act. MYC role as transcriptional repressor in cell reprogramming has been already observed in the formation of induced pluripotent stem cells (iPSCs), where ectopic *MYC* predominantly acts during the first transcriptional wave of the process, in which fibroblast-specific genes are down-regulated (Brambrink et al., 2008; Sridharan et al., 2009; Stadtfeld et al., 2008). Nevertheless, the mechanism through which MYC drives repression of the adult somatic transcriptional program is still not clear. We recently demonstrated that MYC can directly induce gene repression in ESCs, through recruitment of the Polycomb repressive complex 2 (PRC2) (Fagnocchi et al., 2016). Even if we cannot exclude a possible MYC/PRC2 interaction to drive gene silencing in HMEC, preliminary analysis did not show enrichment in

H3K27me3 signal at the regulatory elements of the down-regulated genes (data not shown), suggesting that MYC-induced gene repression could act through an alternative mechanism in this context. A recent work provided evidence for MYC binding to an additional repressor complex, the NuRD complex, through direct interaction with the Mbd3 subunit (Rais et al., 2013). Repression mediated by the NuRD complex has been demonstrated to be a critical step in the early phase of somatic cell reprogramming and to facilitate the induction of pluripotency in a context dependent manner (dos Santos et al., 2014; Rais et al., 2013). NuRD complex could be therefore a plausible candidate for mediating MYC-driven repression of the adult cell transcriptional program. Nevertheless, we cannot exclude that this could happen through an indirect mechanism, in which MYC binding to MIZ-1 could displace MIZ-1 cofactors and indirectly repress target genes (Schneider et al., 1997).

Morphology analysis indicated that MYC-induced reprogramming in HMEC corresponded to destabilization of adherence junctions, mis-localization of polarity complexes and mitotic spindle disorientation (Figure 1). These observations suggested us that stable MYC overexpression could confers on cells a large degree of phenotypic plasticity, that predisposes them to acquisition of stem cell characteristics. We demonstrated that, when cultured in low adhesion conditions, HMEC overexpressing MYC were uniquely endowed with sustained self-renewing capacity (Figure 3). The herein deciphered multistep reprogramming process consisted in the re-activation of a pluripotency transcriptional program, mirrored by the

establishment of a specific epigenetic landscape. Previous works showed that in highly overexpressing conditions, MYC binding to promoter elements of already active genes significantly increased and expanded to the related enhancers, through binding to additional low-affinity E-box-like sequences (Sabo et al., 2014) (Lin et al., 2012). In this view, MYC overexpression caused amplification of the already existing transcriptional program. Our data indicated that MYC overexpression not necessarily correlates with the spreading of MYC binding to additional regulatory elements, since in the comparison between HMEC WT and -MYC we only observed modulation of already existing enhancers. Instead, analysis of MYC-derived mammospheres showed activation of *de novo* enhancers characterized, for one third, by direct MYC binding through a non-canonical E-box sequence (Figure 4-5). We did not identify the mechanism through which chromatin at these regulatory elements switches from a close condition in HMEC-MYC to an open, transcriptionally active state, in M2. On the basis of our data we hypothesized that pioneer transcription factors, such as FOX family members, could engage closed chromatin and establish a positive feedback loop, in which they auto-stimulate their own transcription. This would induce a wave of chromatin remodeling that would allow MYC binding to open regions and the consequent recruitment of further chromatin remodelers. Interestingly, we observe enrichment for FOXC1 binding motifs at enhancers associated to those genes that are transcriptionally induced in M2. Given these observations, it could be interesting to verify whether FOXC1, which has been

demonstrated to be a pivotal biomarker specific for basal-like breast cancers (Ray et al., 2011; Ray et al., 2010; Wang et al., 2012), could also play a role as pioneer factor in MYC-induced oncogenic cell reprogramming.

We propose that such a wide remodeling of the cell epigenetic landscape represents a bottleneck in MYC-induced cell reprogramming process, whose orchestration could be essential for the establishment and maintenance of a stem cell-like state and allows the amplification of MYC oncogenic potential. Indeed, we provide evidences that activation of *de novo* enhancers corresponds to increased expression of the associated genes, which are particularly enriched for pro-self-renewing transcription factors, with established roles in tumorigenesis and enriched in basal/stem cell-like state, such as *SOX9*. Moreover, components of both canonical and non-canonical Wnt signaling resulted being re-activated at this cellular state., our data indicate that Wnt activation represent a bona fide functional marker of MYC-induced reprogramming in mammary epithelial cells. In-depth analysis will be further required to determine whether these observations will translate to chromatin remodeling processes that characterize MYC-guided cell transformation *in vivo*, and whether continuous active transcription of these regulated genes is mandatory for tumor maintenance.

Cell plasticity in which any cell in a tissue, regardless of its differentiation state, has the potential to acquire stem cell-like properties, following an appropriate oncogenic insult, has been suggested to be at the basis of intra- and inter-tumor heterogeneity

(Chaffer et al., 2013; Friedmann-Morvinski et al., 2012; Koren et al., 2015; Nishi et al., 2014; Schroeder et al., 2014; Schwitalla et al., 2013; Southall et al., 2014; Van Keymeulen et al., 2015). Analogous to reprogramming of differentiated cells into induced pluripotent cells (iPS), oncogenic transformation frequently involves de novo acquisition of developmental programs and yields cells with unlimited self-renewal potential. A resetting of the epigenetic landscape can be therefore considered a hallmark of tumor initiation, which allows the establishment of a new stem cell-like transcriptional program and predisposes cells to neoplastic transformation (Apostolou and Hochedlinger, 2013; Buganim et al., 2013). This epigenetic remodeling can indeed cause a susceptible state, in which cells are more prone to acquire genetic alterations, going through transformation and tumor progression. Clearly, the possibility that this chain of events occur is strictly related to the intrinsic features of a tissue: tissues characterized by recurrence of proliferative and remodeling cycles, such as the mammary gland, would more likely adhere to this model.

Experimental procedures

Cell culture and primary cells extraction. hTERT-immortalized human mammary epithelial cells (HMECs) were cultured at 37°C and 5% CO_2 in 1:1 DMEM/F-12 medium (gibco #11320-074) supplemented with insulin (Clonetics, MEGM SingleQuots #CC-4136), EGF (Clonetics, MEGM SingleQuots #CC-4136), bovine pituitary extract (BPE) (Clonetics, MEGM SingleQuots #CC-4136) and hydrocortisone (Clonetics, MEGM SingleQuots #CC-4136) (DiRenzo et al., 2002). HMEC-MYC, HMEC-PIK3CA^{H1047R}, HMEC-P53DD and HMEC-RAS were generated by transducing HMECs with pMXs-c-Myc, PGK-PIK3CA^{H1047R}, pBABE-RASV12 and MSCV-p53DD-iGFP respectively.

Primary cultures of normal human mammary epithelial cells (primary HMEC) were isolated from the normal breast tissue of breast cancer patients, according to Stemcell Technologies technical bulletin. In brief, human mammary tissue was digested for ~16 hoursat 37°C DMEM/F-12 with 2% bovine serum albumin (BSA) (Sigma #A7030), 300 U/ml collagenase III (Worthington #M3D14157) and 100 U/ml hyaluronidase (Worthington #P2E13472). The following day, a single cell suspension was obtained by sequential dissociation of the fragments by incubation at 37°C for 5 minutes in 0.25% Trypsin-EDTA (gibco #25200-056), and then 1 minute in 5 mg/ml dispase (Stemcell Technologies #07913) and 1 mg/ml DNase I (Sigma #D45I3). Thereafter, lysis of the red blood cells was performed with ACK Lysing Buffer (BioWhittaker #10-548E), followed by filtration through a 40

µm cell strainer (Falcon #352340). Viable cells were counted using Trypan Blue Solution (gibco #15250-061). Thereafter the single cells suspension was stained with CD31-V450 (BD Bioscience #561653) and CD45-V450 (BD Bioscience #560367), for the LIN^- exclusion, and with CD49f-FITC (BD Bioscience#555735) and EpCAM-APC (BD Bioscience #347200), to highlight the different cell subpopulations. All the antibodies were incubated for 30 minutes on ice. Primary HMEC-MYC, HMEC-P53DD and HMEC-P53DD-MYC were generated by transducing primary cells with MSCV-MycT58A-iCD2, MSCV-p53DD-iGFP and MSCV-p53DD-iGFP/MSCV-MycT58A-iCD2 combination, respectively.

Mammospheres culture. Mammospheres culture was performed as previously described (Dontu et al., 2003). Briefly, single cells were plated in ultralow attachment plates (Corning) at a density of $2x10^4$ viable cells/ml and mammospheres were collected after 6 days. For culture in Matrigel (BD Biosciences #354230), cells were plated in mammospheres medium, supplemented with 2% Matrigel. For long-term clonogenic assays, cells were transduced with PGK-H2BmCherry and single cells were plated in 96 well plates, in 6 technical replicates, at a density of $4x10^3$ viable cells in 100 µl. After 6 days, fluorescence images of the entire wells were acquired, then the cells were collected and passed in the same conditions. This was repeated for 4 subsequent passages. Images were acquired with an Eclipse T*i* fully automated system (Nikon); number of formed mammospheres and mammospheres area (μm^2) were measured using the NIS Element software (Nikon). Objects with an area <2000

μm^2 (diameter <50 μm) were excluded from the analysis. Single cell clonogenic assay was performed in 96 well plates, in at least 3 biological replicates. Single cells were sorted with a BD FACS Aria III sorter (BD Bioscieces), one cell/well and formed mammospheres were counted after 3 weeks (time window used for 1° Spheres formation).

Tumor injection. Xenografts were obtained using $2x10^6$ cells injected in the mammary fat pad of athymic nude mice. Secondary tumors were generated by the inoculation of $2x10^6$ primary xenograft-derived cells.

Soft agar assay. 0.4% Seaplaque soft agar (Lonza) was diluted with HMEC medium and was covered by a second 0.3% soft agar layer in which $1X10^3$ cells were embedded. After 21 days, colonies were stained with 0.005% crystal violet (Sigma) for 1 hour at 37°C.

Invasion assay. $2x10^3$ cells were plated into Matrigel-coated transwell of 8 μm pore size (Corning #3422) in HMEC medium without cytokines. Complete HMEC medium, supplemented with 10% Fetal Bovine Serum (FBS) (Euroclone #ECS0180L), was used as chemoattractant in the lower part of the transwell.

Immunohistochemical analysis. To assess tissue morphology, haematoxylin and eosin (H&E) staining was performed. Xenograft samples' immunoreactivity for cytokeratins 8/18 (clone B22.1&B23.1), cytokeratins 5/6 (clone D5/16B4), VIMENTIN (clone V9), P63 (clone 4A4), ER (clone SP1), PR (clone 1E2), KI67 (clone MIB-1, code M7240), c-erbB2 (clone A0485) was analyzed using an automated immunostainer (Benchmark ULTRA) after a blocking agent

to reduce endogenous mouse IgG was applied to each slide (Space srl #RBM961G rodent block). Reactions were revealed using the UltraView Universal DAB detection system. All instruments and reagents except KI67 and c-erb2 antibodies (DAKO) were from Ventana Medical Systems (part of Roche Group). Negative controls were prepared in the absence of primary antibody and included in each reaction. For quantification of proliferative activity, a Ki67 score was determined as the percentage of positive tumor cells out of 200 counted tumor nuclei. Immunoreactivity for CK8/18, CK5/6, VIMENTIN, P63, ESTROGEN, PROGESTERONE, was quantified as the percentage of positive tumor cells. c-erbB2 levels were determined using a standard guidelines in according to ASCO/CAP 2016 (Overcast et al., 2016).

Vectors. pMXs-c-Myc was a gift from Shinya Yamanaka (Addgene plasmid #13375); pBABE-RASV12/V12A; MSCV-p53DD-iGFP; MSCV-MycT58A-iGFP; MSCV-MycT58A-iCD2. PGK-H2BmCherry was a gift from Mark Mercola (Addgene plasmid # 21217); PIK3CA^{H1047R} was subcloned from pBabe-puro-HA-PIK3CA^{H1047R}, a gift from Jean Zhao (Addgene plasmid # 12524), into PGK-H2BmCherry.

Retrovirus and Lentivirus Transduction. Retrovirus and lentivirus were produced by transient calcium phosphate transfection of HEK-293T cells with viral plasmids (pMXs-cMyc, pBABE-RAS V12, MSCV-p53DD-iGFP, MSCV-Myc^{T58A}-iGFP, MSCV-MycT58A-iCD2, PGK-H2BmCherry, PGK-PIK3CA^{H1047R}, 7xTcf-eGFP//SV40-PuroR (7TGP)) and the corresponding packaging plasmids (pVSVG and pGAG/Pol for retroviral vectors, Pmd2g and DeltaR8.74 for lentiviral vectors). Virus

was harvested from the culture medium 30 hours later. Recipient cells were counted and seeded in 6 well culture dishes in complete medium 8 hours before infection. Subsequently, the medium was changed with fresh medium containing polybrene (Sigma #107689). Concentrated virus suspension was added to individual wells containing target cells at MOI of 1 and the cells were incubated at 37°C for 12 hours. The following day the medium was removed and replenished with fresh medium containing appropriate antibiotic for selection (Puromycin, 0.5 μg/ml).

Protein extraction and western blot analysis. Total protein extracts were obtained as follows. Cells were washed twice with cold PBS, harvested by scrapping in 1 ml cold PBS and centrifuged for 5 minutes at 1500 rpm. Harvested cell pellets were lysed by the addition of 5X v/v ice-cold F-buffer 30 minutes at 4°C. The chromosomal binding proteins were then separated using BioRuptor waterbath sonicator (Diagenode) at low setting for 5 minutes. Samples were sonicated in pulse of 30 seconds with 30 seconds intervals. Lysates were cleared by centrifugation for 10 minutes at 14.000 rpm at 4°C and supernatant was collected on ice. Protein concentration of lysates was determined using PierceTM BCA Protein Assay Kit 24 (Thermo Scientific, 574 #23227), according to manufacturer's instructions. The absorbance was measured at λ=595 using SAFAS spectrophotometer (SAFAS, Monaco). Values were compared to a standard curve obtained from the BSA dilution series. For western blots analysis, 20 μg of protein samples were boiled and loaded onto a pre-cast Bolt 4-12% Bis-Tris Plus gels (Novex

#NW04122BOX) and run in Bolt MES running buffer (Novex #B0002). After electrophoresis, proteins were transferred to a nitrocellulose membrane. Membranes were blocked in PBS-T containing 5% Blotting-Grade Blocker (BIO-RAD #170-6404) (blocking buffer), for 1 h at RT with constant agitation and incubated with indicated primary antibody O/N at 4°C with agitation. The membrane was then washed three times with PBS-T, each time for 5 min, followed by incubation with secondary antibody HRP-conjugated for 1 h at RT. ECL reagents (GE Healthcare #RPN2232) was used to initiate the chemiluminescence of HRP. The chemiluminescent signal was captured using LAS3000 system (GE Healthcare). Primary antibodies used are as follows: β-Actin (Sigma-Aldrich #A5441), c-Myc (Cell Signaling #5605), β-Catenin (BD Biosciences #610153), E-Cadherin (BD Biosciences #610182), Pan Cadherin (abcam #ab6528). Relative optical density was quantified with ImgeJ Software.

Immunofluorescence. Cells were plated on gelatin (Sigma-Aldrich #G1393)-coated glass coverslips and fixed 20 minutes at room temperature with 4% paraformaldehyde (Sigma-Aldrich #158127). For mammospheres analysis, cells were grown in mammospheres culture conditions for 6 days, than mammospheres were collected and left lay down on gelatin-coated glass coverslips and fixed 20 minutes at room temperature with 4% paraformaldehyde. Coverslips were processed for immunofluorescence according to the following conditions: permeabilization and blocking with PBS/1% BSA/0.3% Triton X-100 (blocking solution) for 1 hour at room temperature, followed by incubation with primary antibody (diluted in the blocking

solution) for 2 hours at RT, 3 washes in the blocking solution and incubation with secondary antibodies (diluted in the blocking solution) for 30 minutes at room temperature. For mammospheres differentiation assay, mammospheres were collected and left lay down on collagene I-coated glass coverslips, in mammospheres medium supplemented with 10% FBS for 7 days.

Images were acquired using a Leica TCS SP5 confocal microscope with HCX PL APO 63x/1.40 objective. Confocal z stacks were acquired with sections of 0.35 µm. In cases where image analysis was performed, image acquisition settings were kept constant. Spindle angle measurements were performed by measuring the three-dimensional distance (across the x, y and z planes) between the two spindle poles and the two-dimensional distance (across the x and y planes) of the spindle. The spindle angle was then calculated using the $\sin^{-1}$ (arcosine) (Figure 1). Image analysis was done using Volocity (PerkinElmer) software.

Primary antibodies are as follows: β-Catenin (Santa Cruz #sc-7199), Phalloidin-TRITC (Sigma-Aldrich #P1951), ϒ-Tubulin (Sigma # T6557), Keratin 8 (Covance #1E8-MMS-162P), Keratin 14 (Covance #AF64-155P), ESR1 (Merk Millipore #F3-A 04-1564), α-SMA (abcam #ab5694).

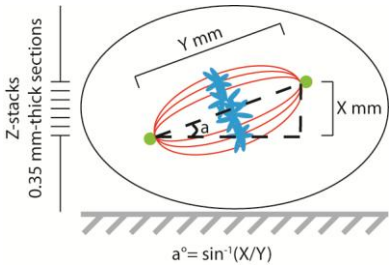

Figure 1. Schematic representation of mitotic spindle angle measurement.

RNA extraction and analysis. Total RNAs were extracted from log-phase cells with TRIzol (Ambion #15596018), according to the manufacturer's instructions. Quantitative real-time PCR analysis was performed with SuperScript III One-Step SYBR Green kit (Invitrogen #11746). The amplification reaction was done using the StepOne Plus system (Applied Biosystem) and the cycling conditions are reported in Table 1. To ensure specificity of amplification, melting curve analysis was performed. Relative gene expression levels were determined using calculated concentration values, normalized to ERCC Spike-In Control RNA (Ambion #4456740). Primers used to detect each gene product were designed using *Universal ProbeLibrary Assay Design Center* (Roche) or Primer3 (http://biotools.umassmed.edu/bioapps/primer3_www.cgi).

For microarray experiments, 500 ng of each sample of RNA were processed to generate labeled cRNAs following the Illumina TotalPrep RNA amplification Kit (Ambion #AMIL1791) protocol. cRNA concentration was quantified and subjected to quality control on Agilent Bioanalyzer (Agilent Technologies #554 G2943CA) and hybridized to MouseRef-8 v2 BeadChip Arrays (Illumina #1128893).

Temperature	Time	Cycling
50°C	15 min	1x
95°C	5 min	
95°C	15 sec	40 cycles
60°C	30 sec	
From 60°C to 95°C	Melting curve	

Table 1: Cycling conditions for the qRT-PCR amplification

Time-lapse video microscopy. Time-lapse video microscopy and single cell tracking of HMEC WT and HMEC-MYC expressing H2B-mCherry were carried out continuously for 48h at 37° C and 5% CO2 using an Eclipse T*i* fully automated 634 system (Nikon). Images of fluorescent cells were acquired every 20 minutes with 20x Plan Apo λ objective (Nikon) using a LED illumination system combined with a CMOS 636 camera (Andor) for the detection. Single cell tracking was performed using the TTT 637 software and movies were assembled using Image J software.

Microarray analysis. BeadChip Arrays were scanned with HiScan Array Scanner (Illumina) using the iScan Control Software (Illumina). Genes and probes transcript levels were obtained from Illumina Intensity Data (.idat) files, applying quantile normalization and background subtraction implemented by the GenomeStudio Gene Expression Module v1.0 Software (Illumina). All experiments in each condition reported were performed on triplicate biological samples. Cut-offs for up- and down-regulation of gene expression were set to 2 fold change threshold in all the analyses performed.

Computational analysis of gene expression data. Heatmap visualization of differentially expressed genes in the comparison between IMEC WT and MYC was generate by performing a hierarchical clustering analysis of single-microarray replicates (complete linkage, Pearson correlation), using the TM4 MeV v4.9 software.Differentially expressed genes in IMEC WT versus MYC were checked for biological and functional enrichment using the Gene Ontology (GO) based online tool PANTHER Classification System. Geneset Enrichement Analysis (GSEA, http://www.broad.mit.edu/gsea/) was performed on genesets retrieved from both public available databases and indicated papers.

Chromatin immunoprecipitation (ChIP) assay. Each ChIP experiment was performed in at least three independent biological samples. Briefly, cells were crosslinked with 1% formaldehyde for 10 min at RT and the reaction was quenched by glycine at a final concentration of 0.125 M, for 5 min at RT. Cells were lysed in lysis buffer (50 mM Tris-HCl pH 8, 0.1% SDS, 10 mM EDTA pH 8, 1 mM phenylmethyl sulphonyl fluoride (PMSF), protease inhibitor cocktail) and chromatin was sonicated to an average size of 0.1–0.5 kb, using a Branson D250 sonifier (4 cycles of 30 s, 20% amplitude). 50 µg of each sonicated chromatin was incubated O/N at 4°C with 4 µg of indicated antibodies (anti-MYC sc-764 Santa Cruz Biotechnology; anti-trimethyl histone H3 Lys4 07-473 Millipore; anti-monomethyl histone H3 Lys4 8895 Abcam; anti-acethyl histone H3 Lys27 4729 Abcam). Protein G-coupled Dynabeads were blocked O/N at 4°C with 1 mg ml $^{-1}$ sonicated salmon sperm DNA and 1 mg ml $^{-1}$ BSA. Subsequently,

blocked protein G-coupled Dynabeads were added to the ChIP reactions and incubated for 4 h at 4°C. Dynabeads linked to ChIP reactions were then recovered and resuspended in RIPA buffer (10 mM Tris-HCl, pH 8, 0.1% SDS, 1 mM EDTA, pH 8, 140 mM NaCl, 1% DOC Q7 , 1% Triton, 1 mM PMSF, protease inhibitor cocktail). Magnetic beads were sequentially washed five times with ice-cold RIPA buffer, twice with ice-cold RIPA-500 buffer (10 mM Tris-HCl, pH 8, 0.1% SDS, 1 mM EDTA, pH 8, 500 mM NaCl, 1% DOC, 1% Triton, 1 mM PMSF, protease inhibitor cocktail), twice with ice-cold LiCl buffer (10 mM Tris-HCl, pH 8, 0.1% SDS, 1 mM EDTA, pH 8, 250 mM LiCl, 0.5% DOC, 0.5% NP-40, 1 mM PMSF, protease inhibitor cocktail) and once with TE buffer (10 mM Tris-HCl, pH 8, 1 mM EDTA, pH 8, 1 mM PMSF, protease inhibitor cocktail). Crosslinking was then reversed in direct elution buffer (10 mM Tris-HCl, pH 8, 0.5% SDS, 5 mM EDTA, pH 8, 300 mM NaCl) at 65 C O/N. Finally, DNA was purified using SPRI beads, washed twice in EtOH 70% and dissolved in 60 ml of Tris-HCl, pH 8.0. DNA was analysed by quantitative real-time PCR using SYBR GreenER kit (Invitrogen). All experimental values were shown as percentage of input. To take into account background signals, we subtracted the values obtained with a non-immune serum to the relative ChIP signals (anti-mouse IgG CS200621 Millipore).

ChIP-seq library generation and data analysis. Five nanograms of immunoprecipitaded and purified DNA were used to generate ChIP-seq libraries. Briefly, end repair of DNA fragments was achieved by sequential 15 min incubations at 12°C and 25°C with T4 PNK (10 U ml 1), T4 POL (3 U ml 1) and 0.1 mM dNTPs. A-base

addition was performed by incubating end-repaired DNA fragments with Klenow (30 -50 exo, 5 U ml 1) and 167 mM dATP for 30 min at 30°C. Adaptor ligation was achieved by using the NEB Quick ligation kit (M2200L) and perfoming an incubation of 15 min at 25°C. Processed DNA fragments were finally amplified with a thermal cycler for 14 cycles, by using the Agilent PfuUltra II Fusion HS DNA Pol kit (600674). All DNA purification steps between the different enzymatic reactions were performed by using Agencourt AMPure XP SPRI beads (Beckman, A63882). The obtained libraries were subjected to quality control on Agilent Bioanalyzer (Agilent Technologies, G2943CA) before sequencing them with Illumina HiSeq2000. Sequenced reads were aligned to the human genome (GRCh37/hg19) by using Bowtie2 version 2.2.3 and only uniquely mapped reads in the subsequent analyses. In order to find the regions of ChIP-seq enrichment over background, we used different peak caller. For MYC ChIP-seq we used MACS2 (p-value $1x10^{-6}$), while for histone modifications we used SICER V1.1 (window size = 200; gap size = 200; FDR 0.01). The HOMER software command 'getDifferentialPeaks' was used to find ChIP-seq differentially enriched regions between different HMEC samples (cut-offs = 2-fold change and p-value $1x10^{-4}$). The HOMER software command 'annotatePeaks.pl' was used to correlate peaks and enhancer regions to the nearest genes, according to GRCh37/hg19 annotation, and to count the number of tags from different sequencing experiments on those regions. Tag counts were then used to produce heatmaps with TM4 MeV v4.9 software. Annotated genes were checked for

biological and functional enrichment using both the GO based online tool PANTHER and GSEA, with genesets retrieved from both public available databases and indicated papers. Venn diagrams were generated using the online tool BioVenn (http://www.cmbi.ru.nl/cdd/biovenn/). Tag density plots around the center of enhancers regions were generated with the ngsplot 2.47 command ngs.plot.r and raw data were plotted on GraphPad Prism (http://www.graphpad.com/scientific-software/prism/). Normalized BigWig tracks of ChIP-seq experiments were generated with bedtools 2.24.0 and the bedGraphToBigWig program and visualized in IGVTools version 2.3.26. Motifs enrichment analysis was performed with the online tool Analysis of Motif Enrichment (AME) of the MEME suite v4.11.2. In all analysis reported data are normalized by per million mapped reads (RPM).

Flow cytometry analysis (FACS). For single cell sorting of GFP ^{high} and GFP ^{low} cells, HMEC transduced with 7xTcf-eGFP//SV40-PuroR (7TGP) were acquired at a BD FACS Aria III sorter (BD Bioscieces). Cells with a GFP signal >10^3 were sorted as GFP ^{high}, while cells with GFP signal <10^2 were sorted as GFP ^{low} cells.

Figures legend

Figure 1. MYC alters cell polarity and mitotic spindle orientation in mammary luminal epithelial cells

(A) Western Blot analysis of c-MYC in HMEC WT and HMEC-MYC; β-ACTIN was used as loading control. (B) Phase contrast photographs showing the morphology of confluent HMEC WT and HMEC-MYC. Scale bar, 200 µm. (C) Immunofluorescence analysis of β-Catenin and Phalloidin on HMEC WT and HMEC-MYC. Scale bar, 10 µm. (D) qRT-PCR analysis of *E-Cadherin* and *β-Catenin* on HMEC WT and HMEC-MYC. Relative transcript levels are normalized on Spike-in. Data are means +/- SEM (n=6). (*P<0.05; Student's t test). (E) Western blot analysis of β-Catenin, E-Cadherin and Pan-Cadherin on HMEC WT and HMEC-MYC; β-ACTIN was used as loading control. Protein quantification from Western Blot analysis. Data are means +/- SEM (n=3). (F) (G) Immunofluorescence analysis of ϒ-TUBULIN on metaphasic and telophasic HMEC WT and HMEC-MYC. Scale bar, 10 µm. White line represents mitotic spindle axes. Average spindle angle and spindle angle frequency of HMEC WT and HMEC-MYC cell divisions are represented. (***P<0.001; Student's t test). (H) Time-lapse sequence of HMEC-MYC cell division in different focal planes. Z stack, 1 µm. (J) Schematic representation of HMEC WT to HMEC-MYC transition showing altered cell polarity and mitotic spindle disorientation.

Figure 2. MYC inhibits the transcriptional program of mature luminal epithelial cells

(A) Upper panel, gene expression plot of all genes, showing up- and down-regulated genes in the comparison HMEC WT versus HMEC-MYC (log2 fold change cutoff = ± 1, indicated by solid horizontal grey lines). Lower panel, heat map of all differentially expressed genes between triplicate microarray experiments of HMEC WT and HMEC-MYC. (B) Gene Ontology analysis of differentially regulated genes between HMEC WT and HMEC-MYC (n=3). (C) Gene set enrichment analysis of mature luminal and luminal progenitor cells gene signature in HMEC WT versus HMEC-MYC (n=3). (D) qRT-PCR analysis of *GATA3* and *ESR1* on HMEC WT and HMEC-MYC. Relative transcript levels are normalized on Spike-in. Data are means +/- SEM (n=6). (E) ChIP-qPCRs for MYC, H3K4me3, H3K27ac and H3K4me1 at *GATA3* promoter and *ESR1* intronic enhancer in HMEC WT and HMEC-MYC. Data are means +/- SEM (n=3). A schematic showing the localization of *GATA3* and *ESR1* PCR amplicons is represented. (F) Gene set enrichment analysis of genes regulated by enhancer regulatory elements bound by luminal lineage transcription factors in HMEC WT versus HMEC-MYC (n=3).

Figure 3. Sustained MYC overexpression confers stem cell-like traits

(A) Phase contrast photographs showing HMEC WT and HMEC-MYC cultured in low adhesion conditions at day 6. Scale bar, 100 µm. (B) Spheres formation efficiency (SFE) of HMEC WT and HMEC-MYC cultured in low adhesion conditions at day 6 of 4 subsequent passages (n=6). (*P<0.05; ***P<0.001; Student's t test). (C) Area

(μm^2) of mammospheres formed by HMEC WT and HMEC-MYC cultured in low adhesion conditions at day 6 of 4 subsequent passages (n=6). Boxes encompass the 25th to 75th percentiles; whiskers extend to 10th and 90th percentiles; the central horizontal bar indicates median fold change, the black cross indicates the mean. (**P<0.01; ***P<0.001; Student's t test). (D) Percentage of cells with high Aldehyde dehydrogenase isoform 1 (ALDH1) in HMEC WT and HMEC-MYC cultured in low adhesion conditions at day 6. Data are means +/- SEM (n=3). (***P<0.001; Student's t test). (E) Single cell spheres formation efficiency (SFE) of HMEC WT, -MYC, -$PIK3CA^{H1047R}$, -P53DD and –RAS. Data are means +/- SEM (n=3). (F) Serial single cell spheres formation efficiency (SFE) of HMEC-MYC, HMEC-MYC-derived 1° Spheres (M1) and 2° Spheres (M2). Single cell-derived clones were obtained at the indicated time. Data are means +/- SEM (n=3). (*P<0.05; **P<0.01; Student's t test). (G) Immunofluorescence for basal (KRT14 and α-SMA) and luminal (KRT8 and ESR1) markers on undifferentiated and differentiated M2. Scale bar, 50 µm. (H) Gene ontology analysis of differentially regulated genes between HMEC-MYC and M2 (n=3). (I) Gene set enrichment analysis of the core embryonic stem cells (ESCs) gene module in HMEC-MYC versus M2 (n=3). (J) Schematic representation of HMEC-MYC cultured in adherence conditions and HMEC-MYC-derived mammospheres, enriched for cells with self-renewing capacity.

Figure 4. MYC induces an alternative epigenetic program in mammary epithelial cells

(A) Barplot showing the genomic distribution of MYC peaks on indicated features in WT, MYC and M2 HMEC. (B) Heatmap showing the dynamic behavior of MYC (left) and H3K4me3 (center) normalized ChIP-seq signals over 4458 MYC bound TSS in WT, MYC and M2 HMEC. The gene expression of relative genes is reported on the right. RPM = reads per million. (C) Gene ontology analysis of genes bound by MYC on their TSS, showing relative enriched biological processes, molecular function and pathways. (D) Identification of modulated enhancers among WT, MYC and M2 HMEC. In the upper panel, the venn diagram shows the overlap of the total H3K4me1 ChIP-seq peaks between WT, MYC and M2 HMEC. In the lower panel, selected identified putative enhancers regions marked by H3K4me1, were analyzed for their enrichment in H3K27ac histone mark in the comparisons WT vs MYC (left) and MYC vs M2 (right), leading to identification of modulated and unchanged enhancers. (E) Heatmap showing the dynamic behavior of H3K4me1 and H3K27ac histone marks and MYC normalized ChIP-seq signals over identified modulated enhancers (2170, 2067 and 5848 enhancers enriched for H3K27ac in WT, MYC and M2 HMEC, respectively). The gene expression of relative associated genes is reported on the right. Relevant genes belonging to different groups are indicated. RPM = reads per million. (F) Gene ontology analysis of genes associated to modulated enhancers, showing relative enriched pathways.

Figure 5. Activation of de novo enhancers drives oncogenic pathways

(A) On the left, heatmap showing the differential gene expression profile of genes associated to M2 *de novo* enhancers, ranked by decreasing fold change in the M2 vs HMEC-MYC comparison. On the right, the heatmap shows the fold change of MYC ChIP-seq signal on only the M2 *de novo* enhancers associated to genes induced at least two fold in M2 with respect to HMEC-MYC. (B) Gene ontology analysis of genes associated to M2 *de novo* enhancers and transcriptionally induced in M2 vs HMEC-MYC, showing relative enriched biological processes and pathways. (C) Venn diagram showing the overlap between M2 *de novo* enhancers-associated genes, which are either transcriptionally induced or bound by MYC, with at least a twofold change in M2 with respect to HMEC-MYC. (D) Heatmap showing the dynamic behavior of MYC and H3K27ac normalized ChIP-seq signals over identified enhancers regions whose associated genes are transcriptionally induced in M2 with respects to HMEC-MYC (159 and 724 enhancers with either increased MYC binding in M2 or not, respectively). The gene expression of relative associated genes is reported. Relevant genes belonging to different groups are indicated. RPM = reads per million. (E-F) Tag density plots showing the average profile of H3K27ac and MYC normalized ChIP-seq signals in WT, MYC and M2 HMEC, centered on enhancers regions associated to genes which are either only transcriptionally induced (E) or both transcriptionally induced and gained MYC binding (F) in M2 with respect to HMEC-MYC. The yellow box indicates a 2 kb

region around the center of the enhancers, in which the MYC binding enrichment in M2 is seen and which were used for following motif discovery analysis. Window size is ±10 kb. (G) Tables depicting transcription factors binding motifs enrichment at enhancers associated to genes which are either only transcriptionally induced (upper table) or both transcriptionally induced and gained MYC binding (lower table) in M2 with respect to HMEC-MYC, with relative p-values.

Figure 6. Reactivation of Wnt pathway supports MYC-induced stem cell features

(A) qRT-PCR analysis of Wnt pathway receptors and co-receptors (*FZD1*, *FZD8*, *LRP5* and *LRP6*) and antagonists (*DKK1* and *SFRP1*) on HMEC WT, HMEC-MYC, 1°-, 2°- and 3° Spheres. Relative transcript levels are normalized on Spike-In. Data are means +/- SEM (n=3). (*P<0.05; **P<0.01; ***P<0.001; Student's t test). (B) FACS analysis showing GFP signal and median fluorescence intensity (MFI) of HMEC-MYC-7TGP cultured in low adhesion conditions at passage 1 (P1) and passage (P2). (C) Left panel shows FACS analysis of GFP signal of HMEC-MYC-7TGP cultured in low adhesion conditions at passage 2 (P2). Gates on total population, GFP ^{high} (>10^3) and GFP ^{low} (<10^2) cells are represented. Right panel shows FACS analysis of dye retention profiles from total, GFP ^{high} and GFP ^{low} populations. The number of recorded events for each gate and percentages representing GFP ^{high} and GFP ^{low} cell populations respect to the total are reported. (D) Schematic representation of GFP ^{high} and GFP ^{low} cells sorting from HMEC-MYC-7TGP, which gave rise to GFP ^{high}- and

GFP ^{low}-derived 1° Spheres. GFP ^{high}-derived 1° Spheres underwent to a second single cell sorting of GFP ^{high} and GFP ^{low} cells, which gave rise to GFP ^{high}- and GFP ^{low}-derived 2° Spheres. Representative FACS analysis showing GFP signal and median fluorescence intensity (MFI) of sorted HMEC-MYC-7TGP and GFP ^{high}-derived 1° Spheres are reported. (E) Left panel shows single cell spheres formation efficiency (SFE) of GFP ^{high} and GFP ^{low} cells, sorted from HMEC-MYC-7TGP, which gave rise to 1° Spheres (M1). Median fluorescence intensity (MFI) of GFP ^{high}- and GFP ^{low}-derived M1 is represented. Right panel shows single cell SFE of GFP ^{high} and GFP ^{low} cells, sorted from GFP ^{high}-derived M1, which gave rise to 2° Spheres (M2). MFI of GFP ^{high}- and GFP ^{low}-derived M2 is represented. Data are means +/- SEM (n=3). (F) Gene set enrichment analysis of mammary stem cells (MaSCs) gene signature in freshly sorted GFP ^{high} and GFP ^{low} cells (n=3). (G) Gene set enrichment analysis (GSEA) showing lung, bone and brain metastatic signatures in freshly sorted GFP ^{high} and GFP ^{low} cells (n=3).

Figure 7. MYC-induced reprogramming favors the onset of TICs

(A) Phase contrast photographs showing the morphology of HMEC WT, -MYC, -PIK3CA^{H1047R} and -MYC-PIK3CA^{H1047R}. Scale bar, 100 µm. (B) Single cell spheres formation efficiency (SFE) of HMEC WT, -MYC, -PIK3CA^{H1047R} and -MYC-PIK3CA^{H1047R}. Data are means +/- SEM (n=3). (**P<0.01; ***P<0.001; Student's t test). (C) Phase contrast photographs showing colonies formed by HMEC-MYC, -PIK3CA^{H1047R} and -MYC-PIK3CA^{H1047R} in soft-agar. Scale bar, 100 µm. HMEC-MYC, -PIK3CA^{H1047R} and -MYC-PIK3CA^{H1047R} spheres formation efficiency (SFE) are shown in the graph. Data are means +/- SEM (n=9).

(*P<0.05; Student's t test). (D) Size of tumors following injection of $2x10^6$ HMEC-MYC-PIK3CA^{H1047R} cells in mouse mammary fat pad. Data are mean tumor size +/- SEM (n=4). (*P<0.05; ***P<0.001; Student's t test). (E) H&E staining of tumors grown after injection of HMEC-MYC-PIK3CA^{H1047R} cells in mouse mammary fat pad. Scale bar, 500 µm the image on the left and 200 µm the magnification on the right. (F) Phase contrast photographs showing the morphology of HMEC-MYC-PIK3CA^{H1047R} and XD cells. Scale bar, 100 µm.

Supplementary figures legend

Supplementary Figure S1.

(A) qRT-PCR analysis of *SLUG*, *SNAIL*, *ZEB1*, *ZEB2* and *TWIST* on HMEC WT and HMEC-MYC. Relative transcript levels are normalized on *GAPDH*. Data are means +/- SEM (n=3). (*P<0.05; **P<0.01; Student's t test).

Supplementary Figure S2.

(A) Gene Ontology (GO) analysis of differentially regulated genes between HMEC WT and HMEC-MYC (n=3). (B) Gene set enrichment analysis (GSEA) of apical junction and mitotic spindle genes in HMEC WT versus HMEC-MYC (n=3). (C) qRT-PCR analysis of mature luminal markers (*MUC1* and *VEGFC*) and luminal progenitor markers (*EIF2S3*, *STAT5A/B* and *LETMD1*) on HMEC WT and HMEC-MYC. Relative transcript levels are normalized on *GAPDH*. Data are means +/- SEM (n=3). (*P<0.05; **P<0.01; Student's t test).

Supplementary Figure S3.

(A) Phase contrast photographs showing HMEC-PIK3CA^{H1047R}, -P53DD and -RAS cultured in low adhesion conditions at day 6. Scale bar, 100 µm. (B) Growth curve of HMEC WT, -MYC, -PIK3CA^{H1047R}, -P53DD and –RAS cultured in low adhesion conditions for 4 subsequent passages. Data are means +/- SEM (n=6). (*P<0.05; ***P<0.001; Student's t test). (C) Spheres formation efficiency (SFE) of HMEC-PIK3CA^{H1047R}, -P53DD and -RAS cultured in low adhesion conditions at day 6 of 4 subsequent passages (n=6). (**P<0.01; ***P<0.001; Student's t test). (D) Area (µm^2) of mammospheres formed by HMEC-PIK3CA^{H1047R}, -

P53DD and -RAS cultured in low adhesion conditions at day 6 of 4 subsequent passages (n=6). Boxes encompass the 25th to 75th percentiles; whiskers extend to 10th and 90th percentiles; the central horizontal bar indicates median fold change, the black cross indicates the mean. (**P<0.01; ***P<0.001; Student's t test). (E) Single cell spheres formation efficiency (SFE) of HMEC WT, -MYC, -PIK3CA^{H1047R}, -P53DD and -RAS cultured in mammospheres medium/2% Matrigel. (**P<0.01; Student's t test). (F) Single cell spheres formation efficiency (SFE) of primary HMEC WT, -MYC, -P53DD, and -MYC-P53DD. Data are means +/- SEM (n=3). (**P<0.01; ***P<0.001; Student's t test). (G) Gene set enrichment analysis (GSEA) of Wnt and HIPPO pathway genes in HMEC-MYC versus 2° Spheres (n=3). (H) Gene set enrichment analysis (GSEA) showing the gene activity of the three embryonic stem cells (ESCs) modules (MYC module, PcG module and core module) in HMEC-MYC versus 2° Spheres (n=3).

Supplementary Figure S4.

(A) Notched boxplot showing the distribution of expression values of genes bound by MYC at their TSS in WT, MYC and M2 HMEC, as indicated. The horizontal black lines and black crosses indicate the median and the average of each distribution, respectively. The boxes extend from the 1st to 3rd quartile and the Tukey method was used to plot whiskers. (B) Notched boxplots showing the distribution of expression values of genes associated to enhancers enriched for H3K27ac in WT, MYC or M2 HMEC, as indicated. The horizontal black lines and black crosses indicate the median and the average of each distribution, respectively. The boxes extend from the 1st to 3rd

quartile and the Tukey method was used to plot whiskers. (C) Barplots showing gene ontology analysis of genes associated to enhancers enriched for H3K27ac in WT (red bars), MYC (blue bars) or M2 (cyano bars) HMEC, Relative enriched biological processes and molecular functions are reported. (D) Venn diagrams showing the amount of enhancers associated genes, which are either induced at least two fold (left) or not (right) in the comparison MYC versus M2 HMEC, which gain MYC binding (at least two fold increment) in mammospheres. The total number of genes belonging to each group and the percentage of genes which gained MYC binding are reported. The enrichment of genes marked by increased MYC binding at their enhancers among M2 induced genes, with respect to un-induced, is associated to a pval = 8.7E-06, as calculated by hypergeometric test.

Supplementary Figure S5.

(A-D) Genomic snapshots showing the epigenetic landscape and MYC binding at relevant genes associated to modulated enhancers. TFAP2C and ITGB1 are shown as representative examples of genes associated to enhancer down-regulation between WT and MYC HMEC (A-B), while SOX9 and WWTR1 represent examples of genes related to activated *de novo* enhancers in M2 HMEC (C-D). Light grey vertical bars indicate enhancer regions. Red bars indicate multiple binding sites for GATA3/ESR1/FOXA1/ZNF1, while cyano bars indicates DNase hypersensitive sites which posses multiple unspecific transcription factor binding sites (data from ENCODE). The physical interaction of each TSS with enhancer regions is indicated by the curved lines as indicated by previously published ChIA-PET data. The

x axis corresponds to genomic location, while the y axis corresponds to ChIP-seq signal density normalized to sequencing depth.

Supplementary Figure S6.

(A) Matrigel invasion assay on HMEC-MYC, -PIK3CA^{H1047R} and -MYC-PIK3CA^{H1047R} cells. Data are means +/- SEM (n=4). (*P<0.05; ***P<0.001; Student's t test). (B) Immunohistochemical staining for cytokeratins 5/6, P63, cytokeratins 8/18, progesterone receptor (PR), estrogen receptor (ER), HER2, VIMENTIN and Ki67 on tumors grown after injection of HMEC-MYC-PIK3CA^{H1047R} cells in mouse mammary fat pad. Scale bar, 200 µm. (C) Spheres formation efficiency (SFE) of HMEC-MYC, -PIK3CA^{H1047R} and -MYC-PIK3CA^{H1047R} in soft-agar. Data are means +/- SEM (n=9). (*P<0.05; Student's t test).

Figures

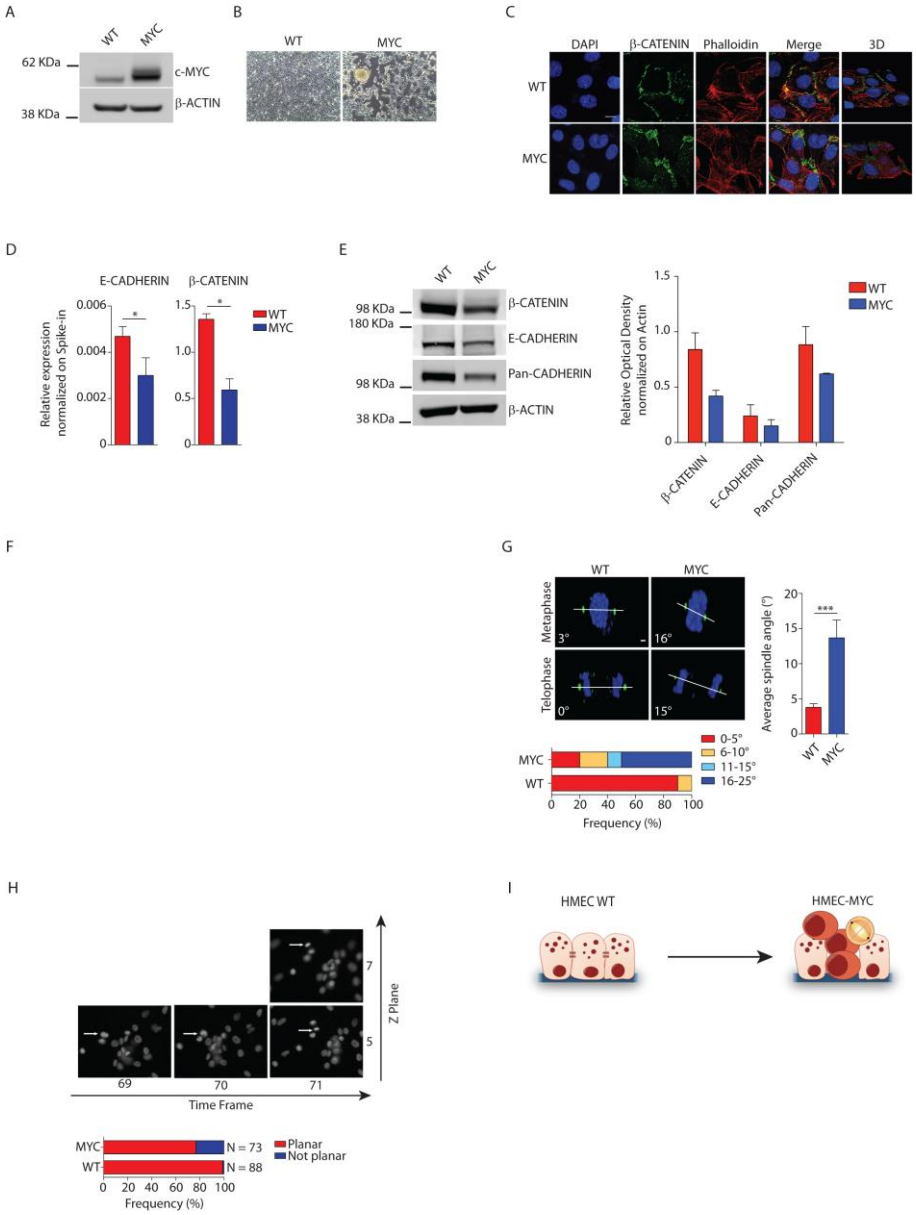

Poli_Figure 1. MYC alters cell polarity and mitotic spindle orientation in mammary luminal epithelial cells

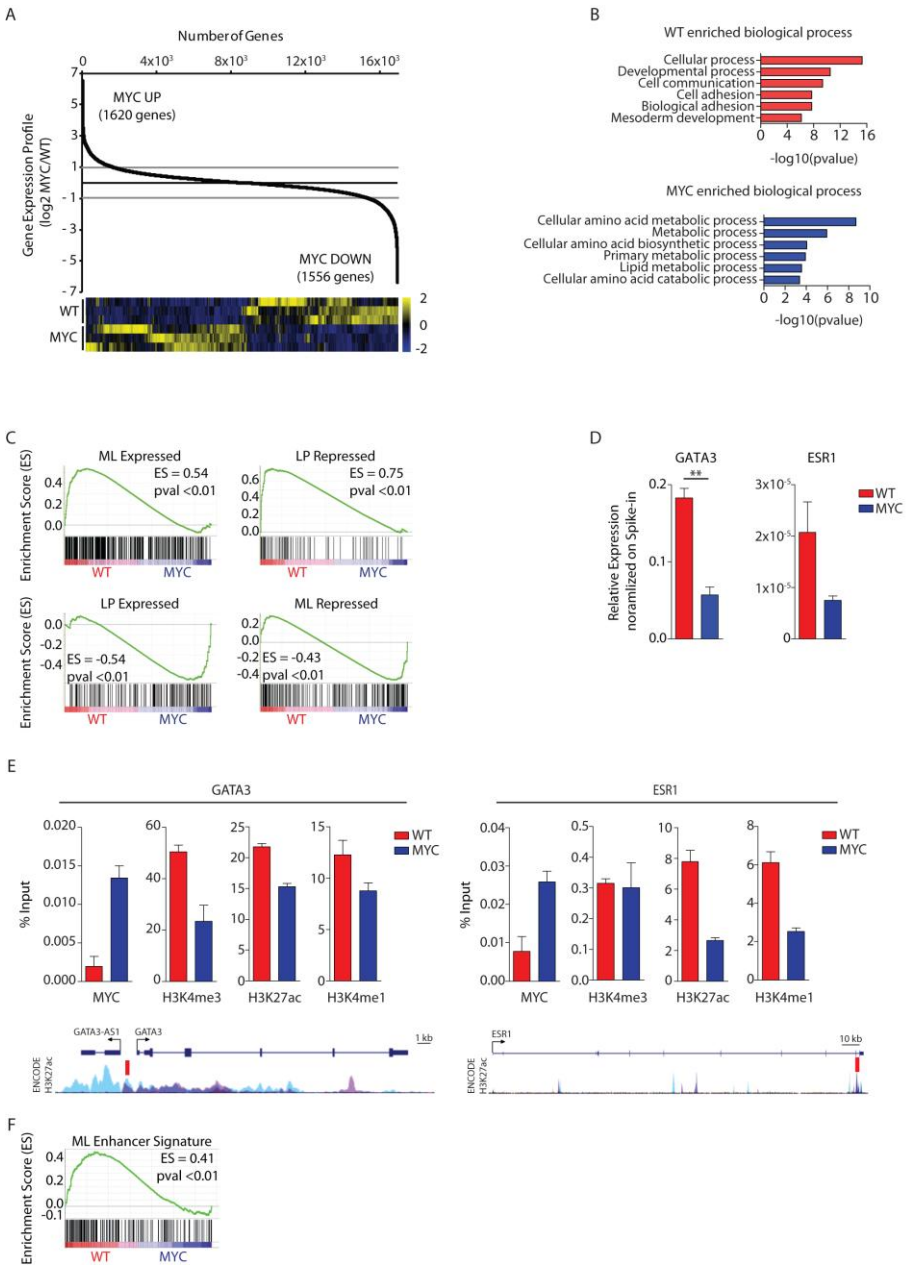

Poli_Figure 2. MYC inhibits the transcriptional program of mature luminal epithelial cells

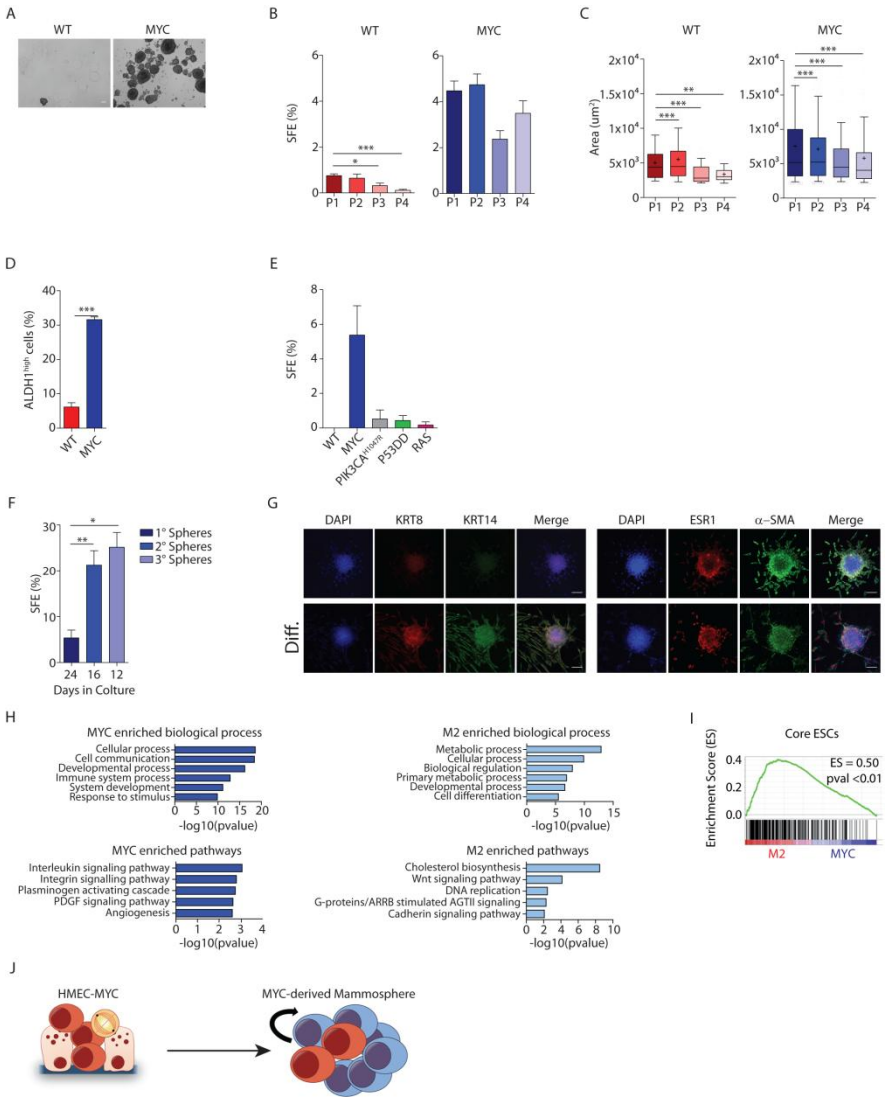

Poli_Figure 3. Sustained MYC overexpression confers stem cell-like traits

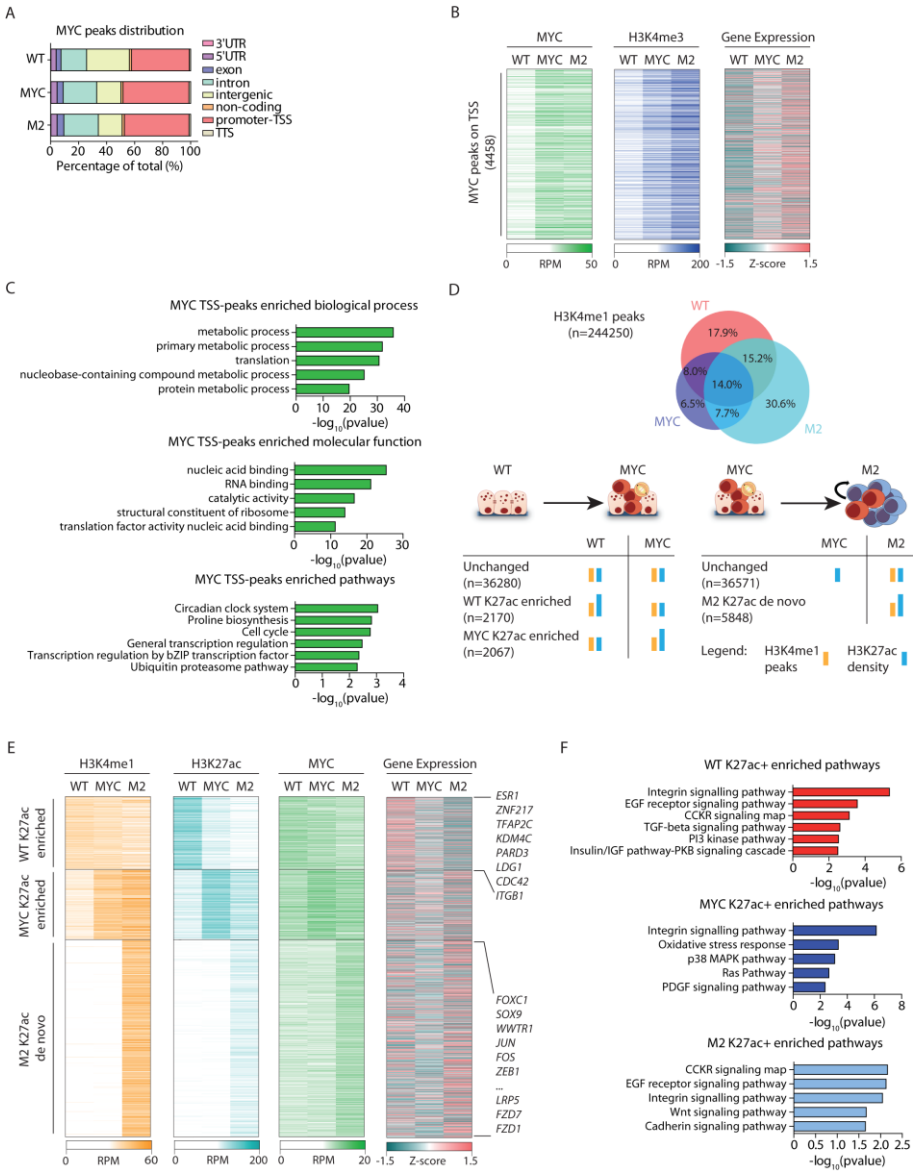

Poli_Figure 4. MYC induces an alternative epigenetic program in mammary epithelial cells

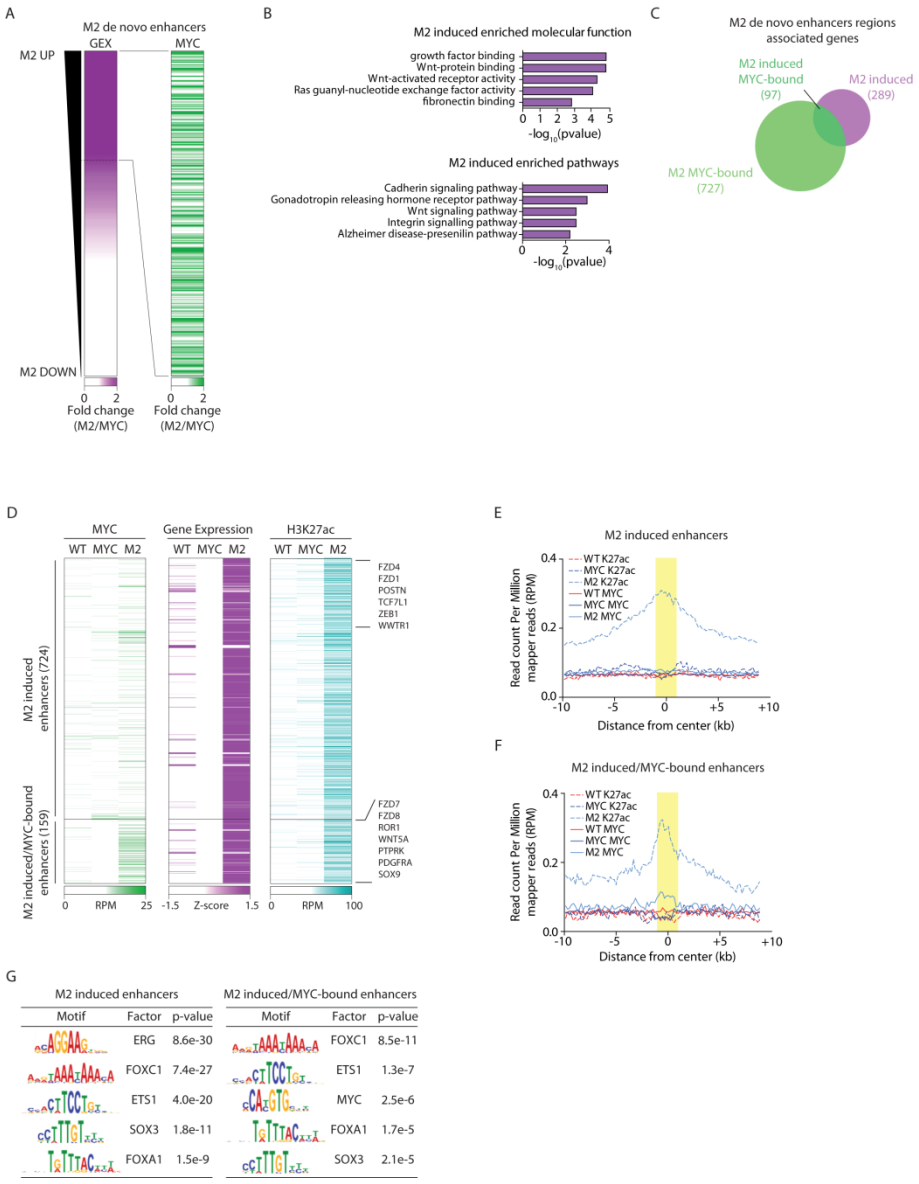

Poli_Figure 5. Activation of de novo enhancers drives oncogenic pathways

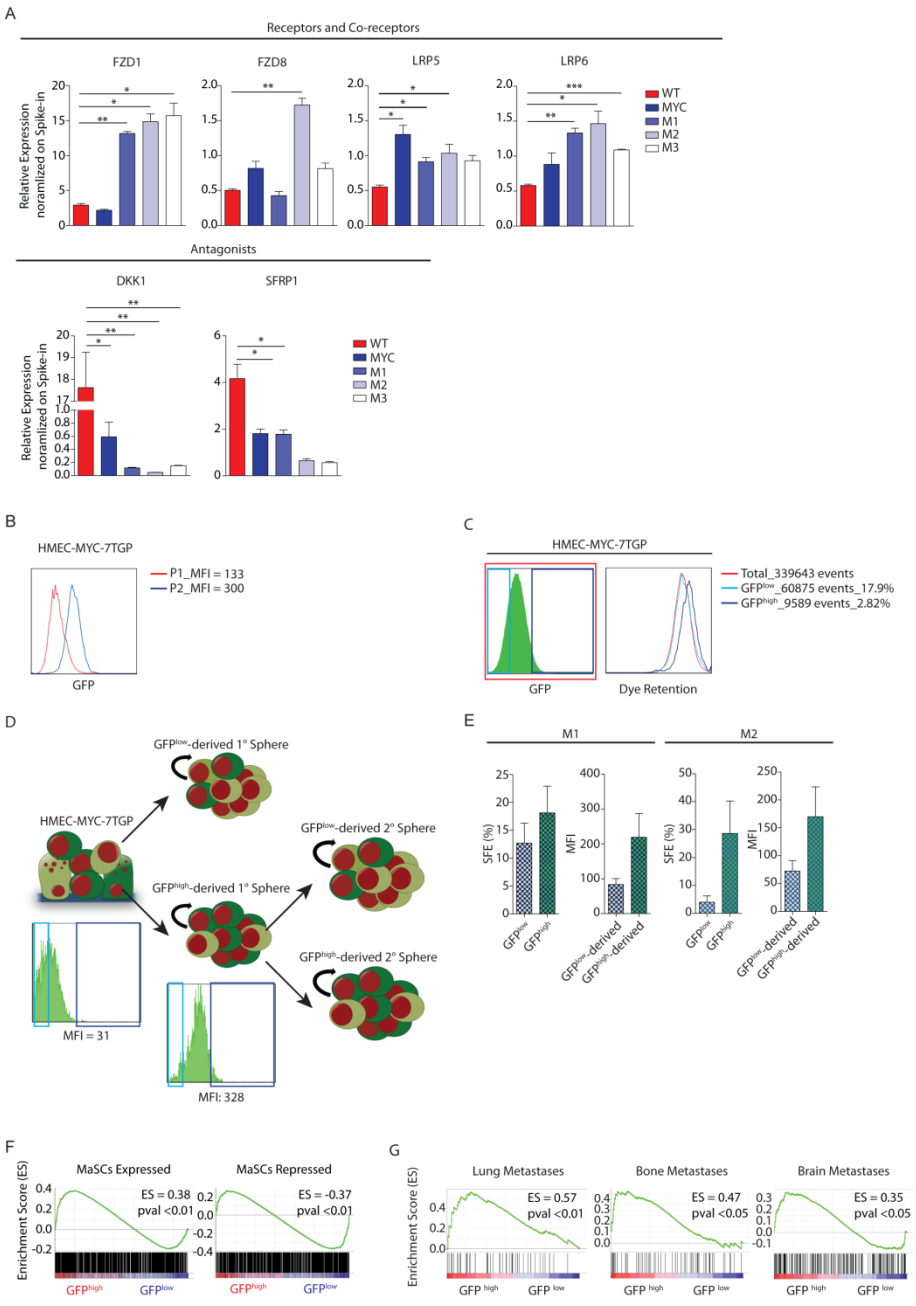

Poli_Figure 6. Reactivation of Wnt pathway supports MYC-induced stem cell features

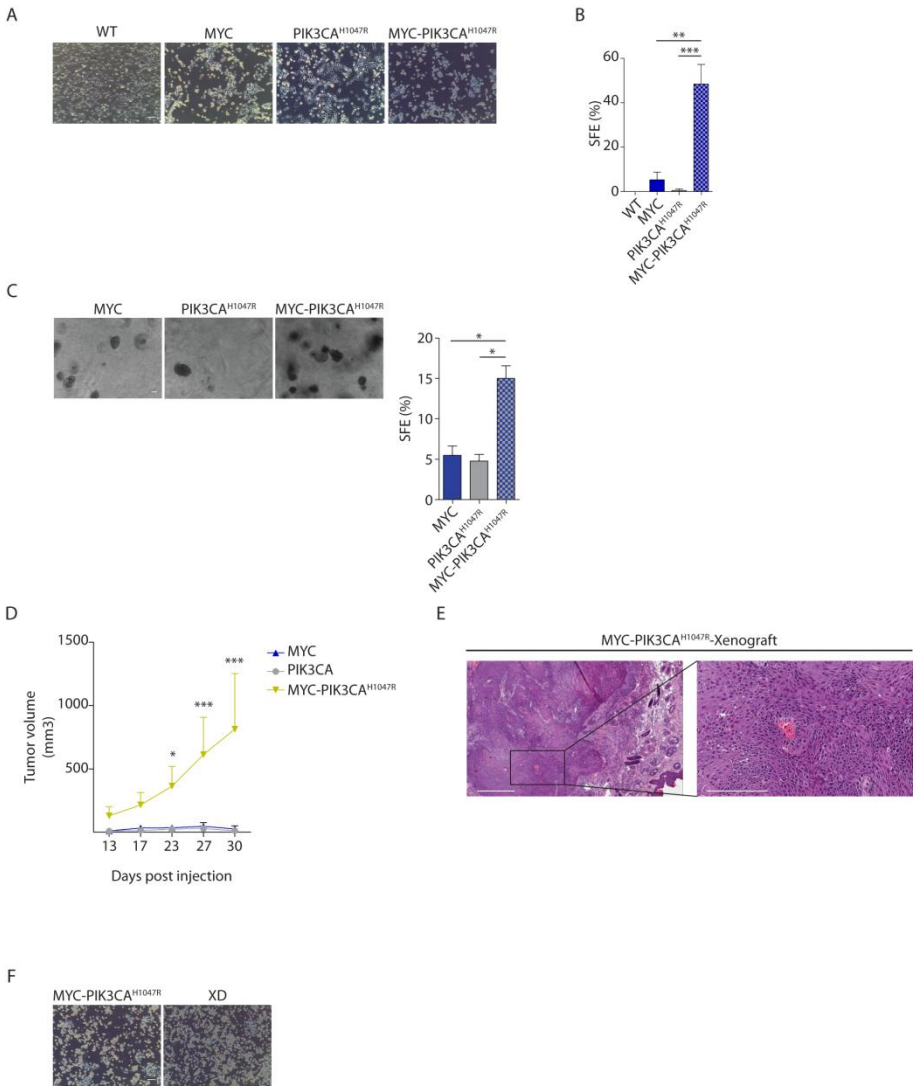

Poli_Figure 7. MYC-induced reprogramming favors the onset of TICs

Supplementary figures

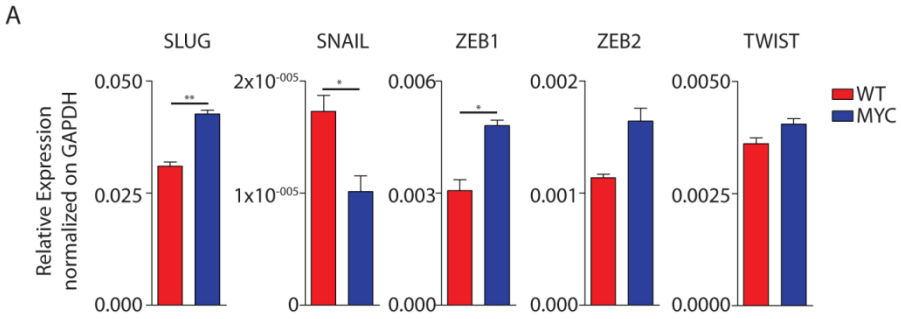

Poli_Supplementary Figure S1

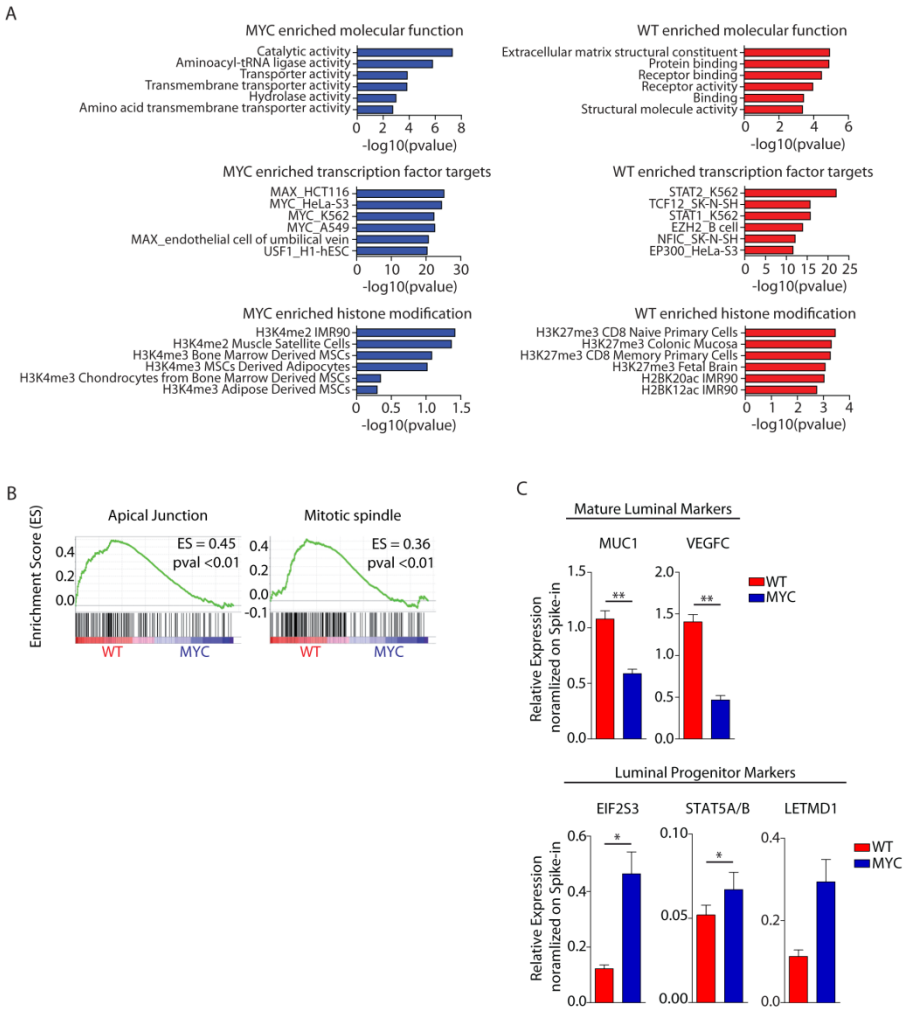

Poli_Supplementary Figure S2

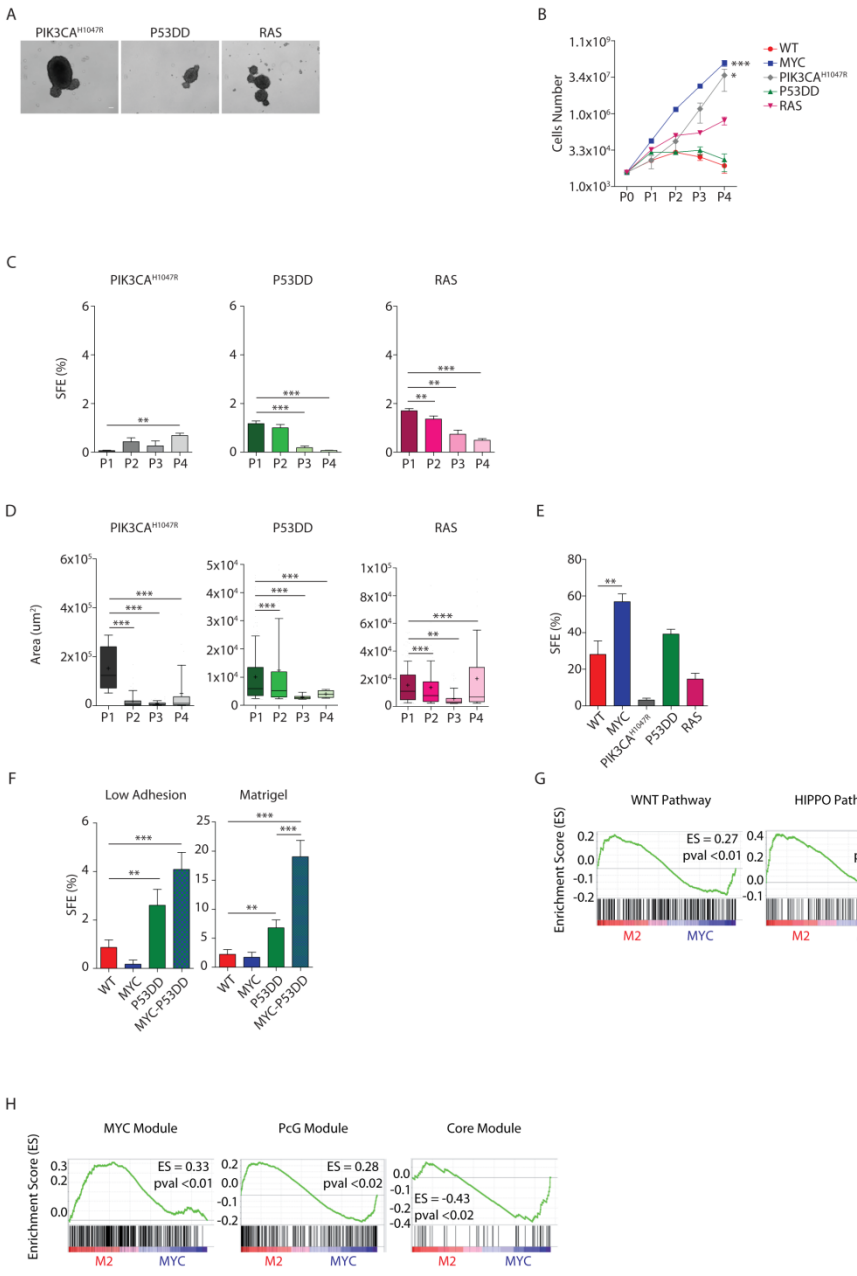

Poli_Supplementary Figure S3

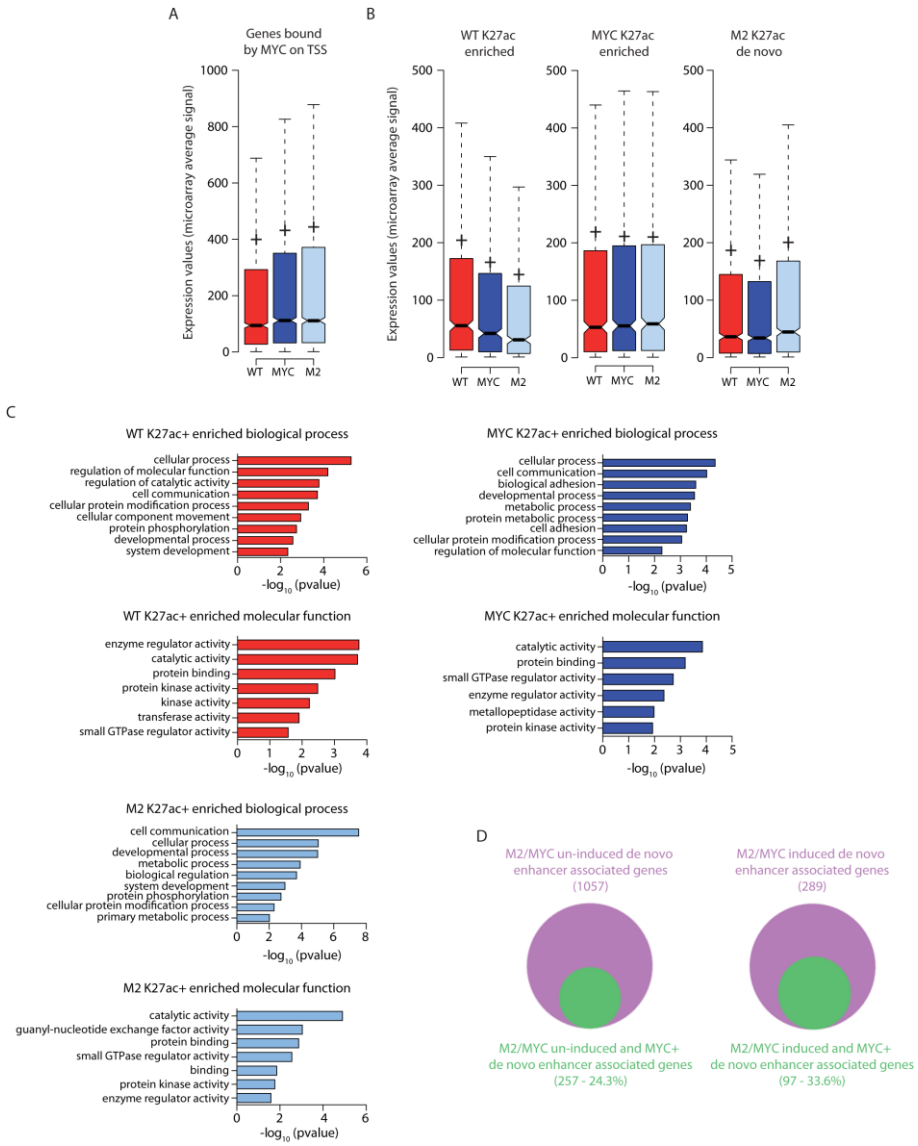

Poli_Supplementary Figure S4

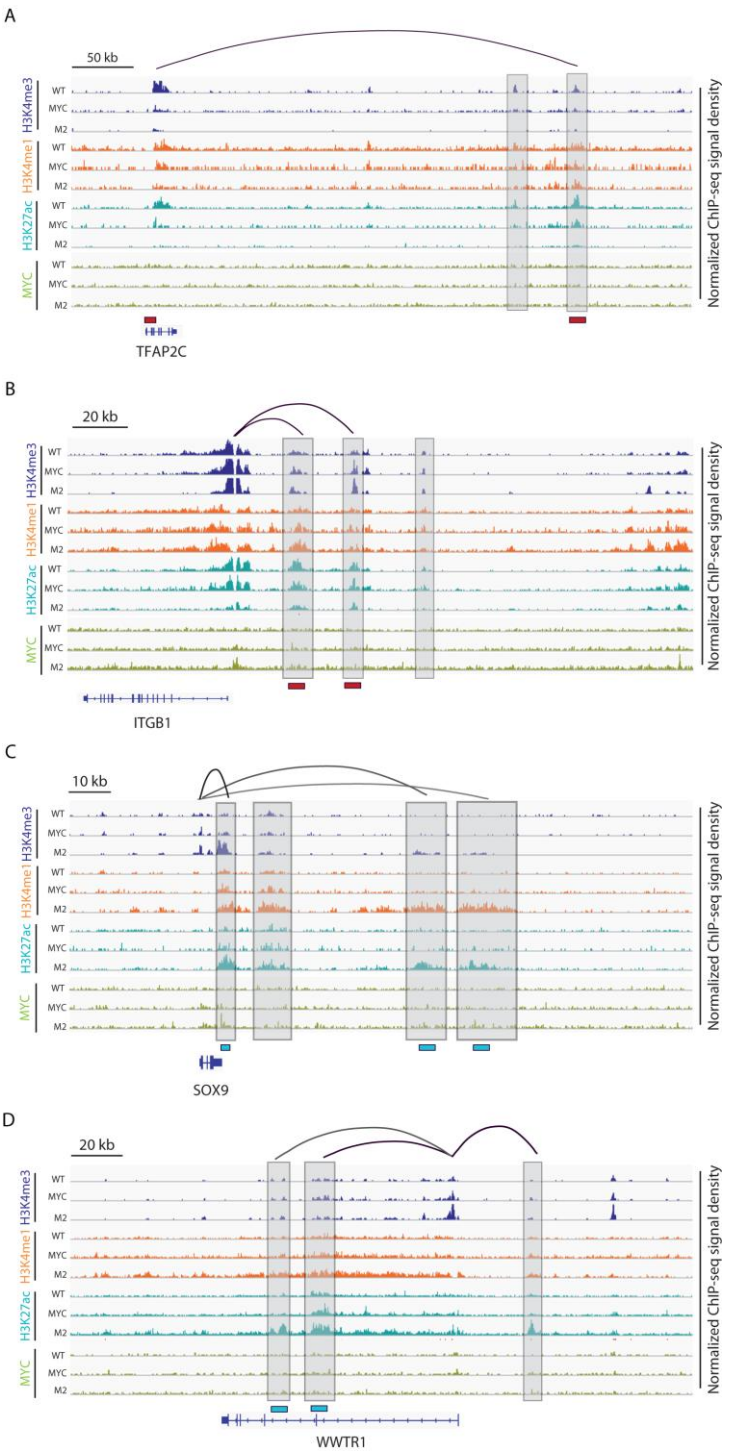

Poli_Supplementary Figure S5

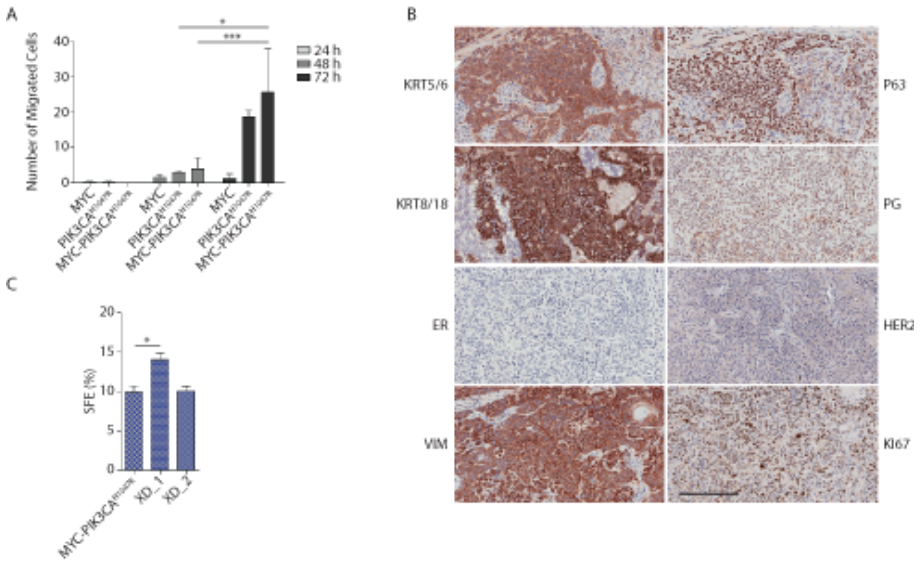

Poli_Supplementary Figure S6

References

Al-Hajj, M., Wicha, M.S., Benito-Hernandez, A., Morrison, S.J., and Clarke, M.F. (2003). Prospective identification of tumorigenic breast cancer cells. Proceedings of the National Academy of Sciences of the United States of America *100*, 3983-3988.

Andrews, J.L., Kim, A.C., and Hens, J.R. (2012). The role and function of cadherins in the mammary gland. Breast cancer research : BCR *14*, 203.

Apostolou, E., and Hochedlinger, K. (2013). Chromatin dynamics during cellular reprogramming. Nature *502*, 462-471.

Asselin-Labat, M.L., Sutherland, K.D., Barker, H., Thomas, R., Shackleton, M., Forrest, N.C., Hartley, L., Robb, L., Grosveld, F.G., van der Wees, J., *et al.* (2007). Gata-3 is an essential regulator of mammary-gland morphogenesis and luminal-cell differentiation. Nature cell biology *9*, 201-209.

Barker, N., Ridgway, R.A., van Es, J.H., van de Wetering, M., Begthel, H., van den Born, M., Danenberg, E., Clarke, A.R., Sansom, O.J., and Clevers, H. (2009). Crypt stem cells as the cells-of-origin of intestinal cancer. Nature *457*, 608-611.

Bonnet, D., and Dick, J.E. (1997). Human acute myeloid leukemia is organized as a hierarchy that originates from a primitive hematopoietic cell. Nature medicine *3*, 730-737.

Brambrink, T., Foreman, R., Welstead, G.G., Lengner, C.J., Wernig, M., Suh, H., and Jaenisch, R. (2008). Sequential expression of pluripotency markers during direct reprogramming of mouse somatic cells. Cell stem cell *2*, 151-159.

Buganim, Y., Faddah, D.A., and Jaenisch, R. (2013). Mechanisms and models of somatic cell reprogramming. Nature reviews Genetics *14*, 427-439.

Calo, E., and Wysocka, J. (2013). Modification of enhancer chromatin: what, how, and why? Molecular cell *49*, 825-837.

Cancer Genome Atlas, N. (2012). Comprehensive molecular portraits of human breast tumours. Nature *490*, 61-70.

Chaffer, C.L., Marjanovic, N.D., Lee, T., Bell, G., Kleer, C.G., Reinhardt, F., D'Alessio, A.C., Young, R.A., and Weinberg, R.A. (2013). Poised chromatin at the ZEB1 promoter enables breast cancer cell plasticity and enhances tumorigenicity. Cell *154*, 61-74.

Chandriani, S., Frengen, E., Cowling, V.H., Pendergrass, S.A., Perou, C.M., Whitfield, M.L., and Cole, M.D. (2009). A core MYC gene expression

signature is prominent in basal-like breast cancer but only partially overlaps the core serum response. PloS one *4*, e6693.

Charafe-Jauffret, E., Ginestier, C., Iovino, F., Wicinski, J., Cervera, N., Finetti, P., Hur, M.H., Diebel, M.E., Monville, F., Dutcher, J.*, et al.* (2009). Breast cancer cell lines contain functional cancer stem cells with metastatic capacity and a distinct molecular signature. Cancer research *69*, 1302-1313.

Chepelev, I., Wei, G., Wangsa, D., Tang, Q., and Zhao, K. (2012). Characterization of genome-wide enhancer-promoter interactions reveals co-expression of interacting genes and modes of higher order chromatin organization. Cell research *22*, 490-503.

Dang, C.V. (2012). MYC on the path to cancer. Cell *149*, 22-35.

Dang, C.V., O'Donnell, K.A., Zeller, K.I., Nguyen, T., Osthus, R.C., and Li, F. (2006). The c-Myc target gene network. Seminars in cancer biology *16*, 253-264.

DiRenzo, J., Signoretti, S., Nakamura, N., Rivera-Gonzalez, R., Sellers, W., Loda, M., and Brown, M. (2002). Growth factor requirements and basal phenotype of an immortalized mammary epithelial cell line. Cancer research *62*, 89-98.

Dontu, G., Abdallah, W.M., Foley, J.M., Jackson, K.W., Clarke, M.F., Kawamura, M.J., and Wicha, M.S. (2003). In vitro propagation and transcriptional profiling of human mammary stem/progenitor cells. Genes & development *17*, 1253-1270.

dos Santos, R.L., Tosti, L., Radzisheuskaya, A., Caballero, I.M., Kaji, K., Hendrich, B., and Silva, J.C. (2014). MBD3/NuRD facilitates induction of pluripotency in a context-dependent manner. Cell stem cell *15*, 102-110.

Fagnocchi, L., Mazzoleni, S., and Zippo, A. (2016). Integration of Signaling Pathways with the Epigenetic Machinery in the Maintenance of Stem Cells. Stem Cells Int *2016*, 8652748.

Fagnocchi L., C.A., Hatsuda H., Fasciani A., Mazzoleni S.,, Poli V., B.V., Rossi RL., Reinbold R., Endele M., Schroeder T.,, and Rocchigiani M., S.Z., Oliviero S., Dalton S. & Zippo A. (2016). A Myc-driven self-reinforcing regulatory network

maintains mouse embryonic stem cell identity. Nature communications.

Feinberg, A.P., and Tycko, B. (2004). The history of cancer epigenetics. Nature reviews Cancer *4*, 143-153.

Friedmann-Morvinski, D., Bushong, E.A., Ke, E., Soda, Y., Marumoto, T., Singer, O., Ellisman, M.H., and Verma, I.M. (2012). Dedifferentiation of neurons and astrocytes by oncogenes can induce gliomas in mice. Science *338*, 1080-1084.

Friedmann-Morvinski, D., and Verma, I.M. (2014). Dedifferentiation and reprogramming: origins of cancer stem cells. EMBO reports *15*, 244-253.

Gebhardt, A., Frye, M., Herold, S., Benitah, S.A., Braun, K., Samans, B., Watt, F.M., Elsasser, H.P., and Eilers, M. (2006). Myc regulates keratinocyte adhesion and differentiation via complex formation with Miz1. The Journal of cell biology *172*, 139-149.

Ginestier, C., Hur, M.H., Charafe-Jauffret, E., Monville, F., Dutcher, J., Brown, M., Jacquemier, J., Viens, P., Kleer, C.G., Liu, S.*, et al.* (2007). ALDH1 is a marker of normal and malignant human mammary stem cells and a predictor of poor clinical outcome. Cell stem cell *1*, 555-567.

Hanahan, D., and Weinberg, R.A. (2011). Hallmarks of cancer: the next generation. Cell *144*, 646-674.

Hao, Y., Du, Q., Chen, X., Zheng, Z., Balsbaugh, J.L., Maitra, S., Shabanowitz, J., Hunt, D.F., and Macara, I.G. (2010). Par3 controls epithelial spindle orientation by aPKC-mediated phosphorylation of apical Pins. Current biology : CB *20*, 1809-1818.

Kim, J., Woo, A.J., Chu, J., Snow, J.W., Fujiwara, Y., Kim, C.G., Cantor, A.B., and Orkin, S.H. (2010). A Myc network accounts for similarities between embryonic stem and cancer cell transcription programs. Cell *143*, 313-324.

Koren, S., Reavie, L., Couto, J.P., De Silva, D., Stadler, M.B., Roloff, T., Britschgi, A., Eichlisberger, T., Kohler, H., Aina, O.*, et al.* (2015). PIK3CA(H1047R) induces multipotency and multi-lineage mammary tumours. Nature *525*, 114-118.

Lim, E., Vaillant, F., Wu, D., Forrest, N.C., Pal, B., Hart, A.H., Asselin-Labat, M.L., Gyorki, D.E., Ward, T., Partanen, A.*, et al.* (2009). Aberrant luminal progenitors as the candidate target population for basal tumor development in BRCA1 mutation carriers. Nature medicine *15*, 907-913.

Lin, C.Y., Loven, J., Rahl, P.B., Paranal, R.M., Burge, C.B., Bradner, J.E., Lee, T.I., and Young, R.A. (2012). Transcriptional amplification in tumor cells with elevated c-Myc. Cell *151*, 56-67.

Martin-Belmonte, F., and Perez-Moreno, M. (2012). Epithelial cell polarity, stem cells and cancer. Nature reviews Cancer *12*, 23-38.

Merlos-Suarez, A., Barriga, F.M., Jung, P., Iglesias, M., Cespedes, M.V., Rossell, D., Sevillano, M., Hernando-Momblona, X., da Silva-Diz, V., Munoz, P.*, et al.* (2011). The intestinal stem cell signature identifies colorectal cancer stem cells and predicts disease relapse. Cell stem cell *8*, 511-524.

Molyneux, G., Geyer, F.C., Magnay, F.A., McCarthy, A., Kendrick, H., Natrajan, R., Mackay, A., Grigoriadis, A., Tutt, A., Ashworth, A*., et al.* (2010). BRCA1 basal-like breast cancers originate from luminal epithelial progenitors and not from basal stem cells. Cell stem cell *7*, 403-417.

Mueller, S.O., Clark, J.A., Myers, P.H., and Korach, K.S. (2002). Mammary gland development in adult mice requires epithelial and stromal estrogen receptor alpha. Endocrinology *143*, 2357-2365.

Nie, Z., Hu, G., Wei, G., Cui, K., Yamane, A., Resch, W., Wang, R., Green, D.R., Tessarollo, L., Casellas, R*., et al.* (2012). c-Myc is a universal amplifier of expressed genes in lymphocytes and embryonic stem cells. Cell *151*, 68-79.

Nishi, M., Sakai, Y., Akutsu, H., Nagashima, Y., Quinn, G., Masui, S., Kimura, H., Perrem, K., Umezawa, A., Yamamoto, N*., et al.* (2014). Induction of cells with cancer stem cell properties from nontumorigenic human mammary epithelial cells by defined reprogramming factors. Oncogene *33*, 643-652.

Overcast, W.B., Zhang, J., Zynger, D.L., and Tozbikian, G.H. (2016). Impact of the 2013 ASCO/CAP HER2 revised guidelines on HER2 results in breast core biopsies with invasive breast carcinoma: a retrospective study. Virchows Archiv : an international journal of pathology.

Palaskas, N., Larson, S.M., Schultz, N., Komisopoulou, E., Wong, J., Rohle, D., Campos, C., Yannuzzi, N., Osborne, J.R., Linkov, I*., et al.* (2011). 18F-fluorodeoxy-glucose positron emission tomography marks MYC-overexpressing human basal-like breast cancers. Cancer research *71*, 5164-5174.

Rahl, P.B., Lin, C.Y., Seila, A.C., Flynn, R.A., McCuine, S., Burge, C.B., Sharp, P.A., and Young, R.A. (2010). c-Myc regulates transcriptional pause release. Cell *141*, 432-445.

Rais, Y., Zviran, A., Geula, S., Gafni, O., Chomsky, E., Viukov, S., Mansour, A.A., Caspi, I., Krupalnik, V., Zerbib, M*., et al.* (2013). Deterministic direct reprogramming of somatic cells to pluripotency. Nature *502*, 65-70.

Ray, P.S., Bagaria, S.P., Wang, J., Shamonki, J.M., Ye, X., Sim, M.S., Steen, S., Qu, Y., Cui, X., and Giuliano, A.E. (2011). Basal-like breast cancer defined by FOXC1 expression offers superior prognostic value: a retrospective immunohistochemical study. Annals of surgical oncology *18*, 3839-3847.

Ray, P.S., Wang, J., Qu, Y., Sim, M.S., Shamonki, J., Bagaria, S.P., Ye, X., Liu, B., Elashoff, D., Hoon, D.S*., et al.* (2010). FOXC1 is a potential prognostic biomarker with functional significance in basal-like breast cancer. Cancer research *70*, 3870-3876.

Reya, T., and Clevers, H. (2005). Wnt signalling in stem cells and cancer. Nature *434*, 843-850.

Sabo, A., Kress, T.R., Pelizzola, M., de Pretis, S., Gorski, M.M., Tesi, A., Morelli, M.J., Bora, P., Doni, M., Verrecchia, A.*, et al.* (2014). Selective transcriptional regulation by Myc in cellular growth control and lymphomagenesis. Nature *511*, 488-492.

Schepers, A.G., Snippert, H.J., Stange, D.E., van den Born, M., van Es, J.H., van de Wetering, M., and Clevers, H. (2012). Lineage tracing reveals Lgr5+ stem cell activity in mouse intestinal adenomas. Science *337*, 730-735.

Schneider, A., Peukert, K., Eilers, M., and Hanel, F. (1997). Association of Myc with the zinc-finger protein Miz-1 defines a novel pathway for gene regulation by Myc. Current topics in microbiology and immunology *224*, 137-146.

Schroeder, A., Herrmann, A., Cherryholmes, G., Kowolik, C., Buettner, R., Pal, S., Yu, H., Muller-Newen, G., and Jove, R. (2014). Loss of androgen receptor expression promotes a stem-like cell phenotype in prostate cancer through STAT3 signaling. Cancer research *74*, 1227-1237.

Schwitalla, S., Fingerle, A.A., Cammareri, P., Nebelsiek, T., Goktuna, S.I., Ziegler, P.K., Canli, O., Heijmans, J., Huels, D.J., Moreaux, G.*, et al.* (2013). Intestinal tumorigenesis initiated by dedifferentiation and acquisition of stem-cell-like properties. Cell *152*, 25-38.

Shehata, M., Teschendorff, A., Sharp, G., Novcic, N., Russell, I.A., Avril, S., Prater, M., Eirew, P., Caldas, C., Watson, C.J.*, et al.* (2012). Phenotypic and functional characterisation of the luminal cell hierarchy of the mammary gland. Breast cancer research : BCR *14*, R134.

Shen, H., Xu, W., Guo, R., Rong, B., Gu, L., Wang, Z., He, C., Zheng, L., Hu, X., Hu, Z.*, et al.* (2016). Suppression of Enhancer Overactivation by a RACK7-Histone Demethylase Complex. Cell *165*, 331-342.

Singh, A.M., and Dalton, S. (2009). The cell cycle and Myc intersect with mechanisms that regulate pluripotency and reprogramming. Cell stem cell *5*, 141-149.

Southall, T.D., Davidson, C.M., Miller, C., Carr, A., and Brand, A.H. (2014). Dedifferentiation of neurons precedes tumor formation in Lola mutants. Developmental cell *28*, 685-696.

Sridharan, R., Tchieu, J., Mason, M.J., Yachechko, R., Kuoy, E., Horvath, S., Zhou, Q., and Plath, K. (2009). Role of the murine reprogramming factors in the induction of pluripotency. Cell *136*, 364-377.

Stadtfeld, M., Maherali, N., Breault, D.T., and Hochedlinger, K. (2008). Defining molecular cornerstones during fibroblast to iPS cell reprogramming in mouse. Cell stem cell *2*, 230-240.

Taddei, I., Deugnier, M.A., Faraldo, M.M., Petit, V., Bouvard, D., Medina, D., Fassler, R., Thiery, J.P., and Glukhova, M.A. (2008). Beta1 integrin deletion from the basal compartment of the mammary epithelium affects stem cells. Nature cell biology *10*, 716-722.

Takahashi, K., and Yamanaka, S. (2006). Induction of pluripotent stem cells from mouse embryonic and adult fibroblast cultures by defined factors. Cell *126*, 663-676.

Valent, P., Bonnet, D., De Maria, R., Lapidot, T., Copland, M., Melo, J.V., Chomienne, C., Ishikawa, F., Schuringa, J.J., Stassi, G.*, et al.* (2012). Cancer stem cell definitions and terminology: the devil is in the details. Nature reviews Cancer *12*, 767-775.

Van Keymeulen, A., Lee, M.Y., Ousset, M., Brohee, S., Rorive, S., Giraddi, R.R., Wuidart, A., Bouvencourt, G., Dubois, C., Salmon, I.*, et al.* (2015). Reactivation of multipotency by oncogenic PIK3CA induces breast tumour heterogeneity. Nature *525*, 119-123.

Visvader, J.E. (2011). Cells of origin in cancer. Nature *469*, 314-322.

Visvader, J.E., and Lindeman, G.J. (2012). Cancer stem cells: current status and evolving complexities. Cell stem cell *10*, 717-728.

Vita, M., and Henriksson, M. (2006). The Myc oncoprotein as a therapeutic target for human cancer. Seminars in cancer biology *16*, 318-330.

Wang, J., Ray, P.S., Sim, M.S., Zhou, X.Z., Lu, K.P., Lee, A.V., Lin, X., Bagaria, S.P., Giuliano, A.E., and Cui, X. (2012). FOXC1 regulates the functions of human basal-like breast cancer cells by activating NF-kappaB signaling. Oncogene *31*, 4798-4802.

Whyte, W.A., Bilodeau, S., Orlando, D.A., Hoke, H.A., Frampton, G.M., Foster, C.T., Cowley, S.M., and Young, R.A. (2012). Enhancer decommissioning by LSD1 during embryonic stem cell differentiation. Nature *482*, 221-225.

Zhao, B., Tumaneng, K., and Guan, K.L. (2011). The Hippo pathway in organ size control, tissue regeneration and stem cell self-renewal. Nature cell biology *13*, 877-883.

Zhou, B.B., Zhang, H., Damelin, M., Geles, K.G., Grindley, J.C., and Dirks, P.B. (2009). Tumour-initiating cells: challenges and opportunities for anticancer drug discovery. Nature reviews Drug discovery *8*, 806-823.

Zimdahl, B., Ito, T., Blevins, A., Bajaj, J., Konuma, T., Weeks, J., Koechlein, C.S., Kwon, H.Y., Arami, O., Rizzieri, D.*, et al.* (2014). Lis1 regulates asymmetric division in hematopoietic stem cells and in leukemia. Nature genetics *46*, 245-252.

Conclusions and perspectives in translational medicine

Cancer cells are characterized by increased genomic heterogeneity compared to normal cells. In some cancers, driver mutations in key oncogenes can be targeted therapeutically to inhibit cancer cell growth or induce apoptosis. In the context of breast cancer therapy, the development of specific strategies for each of the major pathologic subtypes of breast cancer has improved outcomes for many breast cancer patients. In these tumor-specific approaches, ER/PR^{+} breast cancers are treated with hormonal therapies and cancers with *HER2* gene amplification are treated with HER2-targeting agents. Nevertheless, in cancers with no detected driver mutations, such as triple-negative breast cancers (TNBCs), the main therapeutic approach is still cytotoxic chemotherapy (Lehmann et al., 2011) (Metzger-Filho et al., 2012) (Vaz-Luis et al., 2014). Compared to ER/PR^{+} breast cancers, TNBCs are characterized by higher genetic complexity, as indicated by a higher rate of somatic mutations, gene amplifications and deletions (Cancer Genome Atlas, 2012).

MYC amplification is among the most common genetic alterations observed in cancer genomes and a key regulatory feature of TNBCs (Cancer Genome Atlas, 2012). Many transgenic mouse studies have provided evidence that deregulated expression of MYC is sufficient to drive tumorigenesis in a number of tissues (Adams et al., 1985; Chesi et al., 2008; Leder et al., 1986). In addition, de-activation of MYC in established, MYC-induced transgenic tumors is

able to promote rapid tumor regression (Arvanitis and Felsher, 2006). These observations suggested that MYC also participates in tumor maintenance and might be a good therapeutic target. Nevertheless, strategies based on the direct inhibition of MYC interactions with cofactors or DNA, through the use of small molecules, failed (Nair and Burley, 2003). It is also necessary to consider that, given its pleiotropy, systemically inhibition of MYC function might induce serious side effects by affecting proliferation of normal tissues. For these reasons, strategies to modulate MYC oncoprotein in cancer have remained elusive.

An alternative strategy, recently investigated in a number of studies, is the targeting of MYC function through small molecules inhibitors of the transcriptional machinery. MYC transcription is globally associated with increase of open chromatin marks, including H3K4me3 and H3K27ac at promoter regions. Moreover, MYC recruits the positive transcription elongation factor P-TEFb, which phosphorylates and increases the processivity of RNA Pol II, leading to expression of growth promoting genes (Bouchard et al., 2004; Eberhardy and Farnham, 2001; Rahl et al., 2010). Histone acetylation allows the assembly of higher-ordered transcriptional complexes, by recruiting coactivator proteins endowed with one or more acetyl-lysine-binding domains, called “bromodomains” (Dhalluin et al., 1999; Haynes et al., 1992). Members of the bromodomain and extraterminal (BET) subfamily of bromodomain proteins (BRD2, BRD3 and BRD4) are able to associate with acetylated chromatin and facilitate transcriptional activation by increasing the recruiting of

transcriptional activators (LeRoy et al., 2008; Rahman et al., 2011). In particular, BRD4 is involved in the control of transcriptional elongation by RNA polymerase II (RNA Pol II), through recruitment of P-TEFb. Two recently developed bromodomain inhibitors, JQ1 and iBET, selectively bind to the amino-terminal bromodomains of BET proteins, preventing their recruitement to target genes (Nicodeme et al., 2010) (Filippakopoulos et al., 2010). This limits the binding of P-TEFb and RNA Pol II, decreases histone acetylation and transcription, prompting cell cycle arrest and cellular senescence (Figure 1).

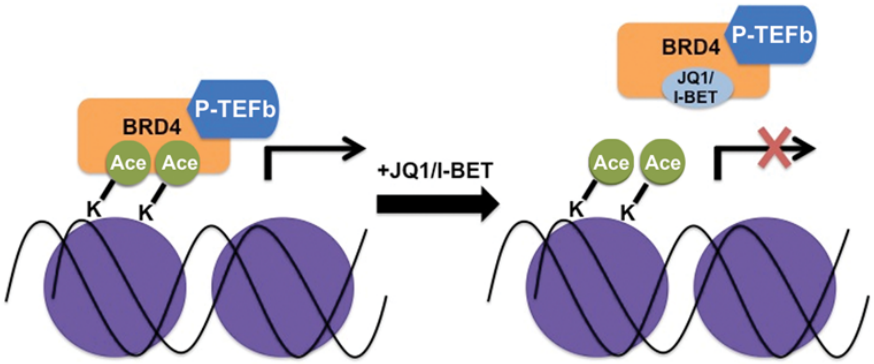

Figure 1. BRD4 interaction with acetylated histones activates gene expression. JQ1 or iBET binding to BRD4 prevents this interaction, leading to repression of BRD4 transcriptional targets (Popovic and Licht, 2012).

Treatment with JQ1 or iBET has exploited the dependence of a range of mouse model tumors on the transcription of *MYC* oncogene, rendering these cancers sensitive to *MYC* transcriptional inhibition (Dawson et al., 2011) (Delmore et al., 2011) (Mertz et al., 2011) (Zuber et al., 2011) (Ott et al., 2012). MYC inhibition occurs as a

consequence of BRD4 depletion at the level of enhancer regulatory elements that drive *MYC* expression (Delmore et al., 2011). Down-regulation of *MYC* transcription is then followed by genome-wide silencing of MYC-dependent target genes. Notably, although BRD4 is expressed in almost all human cells, *MYC* transcriptional inhibition is selective and mice are reasonably tolerant of the level of BET bromodomain inhibition. A possible explanation is that, although BRD4 associates with most active enhancers and promoters, exceptionally high levels of this cofactor occur at enhancer regions associated with *MYC* and other key genes. These genes are often associated to short mRNA and protein half-life and are therefore strikingly dependent on a continuous active transcription, driven by enhancer regulatory regions that are densely occupied by transcription factors and co-factors (Hnisz et al., 2013; Hnisz et al., 2015; Loven et al., 2013). It has been postulated that for this reason, treatment with BET inhibitors causes a preferentially loss of BRD4 and P-TEFb at those enhancers, determining selective inhibition of transcription at associated genes.

In addition to BET inhibitors, also THZ1, a small-molecule inhibitor of cyclin-dependent kinase (CDK) CDK7, has been shown to be effective in inhibiting the growth of several cancers (Chipumuro et al., 2014; Christensen et al., 2014; Kwiatkowski et al., 2014). CDK7 plays a dual role in the regulation of cell cycle progression and transcription. It controls cell-cycle by phosphorilating other CDKs, as a component of the CDK activating kinase (CAK). At the same time, it regulates transcription initiation by phosphorilating RNA Pol II, as

part of the multi-protein basal transcription factor TFIIH (Malumbres, 2014). THZ1 acts by covalently binding to CDK7 and suppressing its kinase activity (Kwiatkowski et al., 2014) (Figure 2).

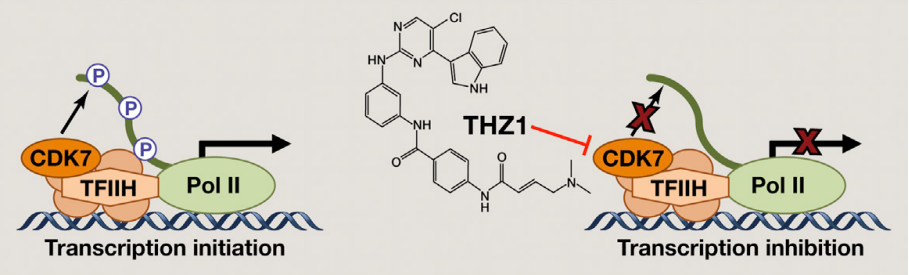

Figure2. THZ1 covalently binds to and inhibits the activity of CDK7, preventing phosphorylation of the C-terminal domain of the largest subunit (RPB1) of RNA polymerase II and inhibiting productive transcription initiation (modified from (Franco and Kraus, 2015)).

More recently, a work conduced on TNBC cell lines and patient-derived tumor samples explored the therapeutic potential of targeting CDK7 in TNBCs (Wang et al., 2015). They observed that TNBC cells, but not ER^+/PR^+ breast cancer cells, are highly dependent on the transcriptional functions of CDK7 and that its inhibition by THZ1 promotes apoptosis. Notably, they provided evidences that TNBC cells are dependent, for their proliferation, on the uninterrupted transcription of a key set of genes whose expression is highly sensitive to inhibition of CDK7 by THZ1. This gene set includes genes encoding for signaling molecules (such as WNT) and transcription factors with established role in breast cancer, including MYC and SOX9. The 40% of these genes was associated with large clustered enhancer regions required to drive high levels of

expression. Similarly to what observed with BET inhibitors treatment, the extraordinary reliance of these enhancer regulatory regions on CDK7, may confer special sensitivity to transcriptional inhibitors like THZ1.

Notably, all reported works show how MYC function in cancer can be counteract by the use of drugs that act up-stream in MYC-induced oncologic cascade, at the level of MYC-associated enhancers. This can be a valid strategy in cases in which *MYC* overexpression is induced by deregulation of up-stream oncogenic signals, but would not ensure inhibition of MYC oncogenic effects in cases of *MYC* amplification or chromosomal translocation. In our work we show how *MYC* overexpression can initiate a process of cell transformation, characterized by re-acquisition of a stem cell-identity, guided through the activation of a subset of *de novo* enhancers. Regulated enhancers were involved in transcriptional activation of genes codifying for transcription factors with established roles in tumorigenesis, as well as components of both canonical and non-canonical WNT signaling (Poli_Figure 5D). About one third of these regulatory elements was specifically bound by MYC (Poli_Figure 5C-G). Furthermore, we observed enrichment for additional transcription factors (FOX- and SOX- family members, ETS1) at MYC-bound enhancers, that could cooperate with MYC in the induction of transcription (Poli_Figure 5G). Further studies will be required to determine whether these observations will translate to chromatin remodeling processes that characterize MYC-guided cell transformation *in vivo*, and whether continuous active transcription

of these regulated genes is mandatory for tumor maintenance. Nevertheless, our findings shed light to the possibility to improve pharmacological treatment of breast cancer cases characterized by *MYC* overexpression, in which a direct targeting of MYC transcription is not possible. Treatment with BET inhibitors or THZ1, would allow to selectively inhibit the activation of those enhancers that lay downstream *MYC* overexpression, either directly bound by MYC or other transcription factors, and that are responsible for orchestrating the activation of oncogenic programs. Preliminary data showed that while treatment with JQ1 inhibitor of ER^+ luminal cells (T-47D) did not have any effect on cell proliferation and viability, treatment of GFP ^{high}-derived M2 cells seriously affected the cell population (Figure 3).

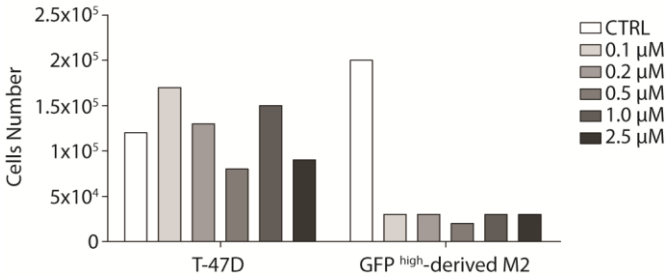

Figure 3. Cells treatment with increasing doses of JQ1 inhibitor.

Moreover, this effect was associated to a strong reduction of WNT signal activation (Figure 4).

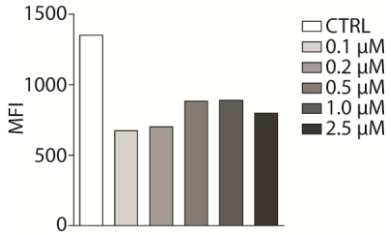

Figure 4. Mean fluorescence intensity (MFI) of GFP ^{high}-derived M2 cells treated with JQ1 inhibitor.

This suggested that pharmacological treatment specifically targeted enhancers responsible for WNT pathway activation, allowing to counteract the stem cell-like phenotype induced by *MYC* overexpression.

References

Adams, J.M., Harris, A.W., Pinkert, C.A., Corcoran, L.M., Alexander, W.S., Cory, S., Palmiter, R.D., and Brinster, R.L. (1985). The c-myc oncogene driven by immunoglobulin enhancers induces lymphoid malignancy in transgenic mice. Nature *318*, 533-538.

Arvanitis, C., and Felsher, D.W. (2006). Conditional transgenic models define how MYC initiates and maintains tumorigenesis. Seminars in cancer biology *16*, 313-317.

Bouchard, C., Marquardt, J., Bras, A., Medema, R.H., and Eilers, M. (2004). Myc-induced proliferation and transformation require Akt-mediated phosphorylation of FoxO proteins. The EMBO journal *23*, 2830-2840.

Cancer Genome Atlas, N. (2012). Comprehensive molecular portraits of human breast tumours. Nature *490*, 61-70.

Chesi, M., Robbiani, D.F., Sebag, M., Chng, W.J., Affer, M., Tiedemann, R., Valdez, R., Palmer, S.E., Haas, S.S., Stewart, A.K.*, et al.* (2008). AID-dependent activation of a MYC transgene induces multiple myeloma in a conditional mouse model of post-germinal center malignancies. Cancer cell *13*, 167-180.

Chipumuro, E., Marco, E., Christensen, C.L., Kwiatkowski, N., Zhang, T., Hatheway, C.M., Abraham, B.J., Sharma, B., Yeung, C., Altabef, A.*, et al.* (2014). CDK7 inhibition suppresses super-enhancer-linked oncogenic transcription in MYCN-driven cancer. Cell *159*, 1126-1139.

Christensen, C.L., Kwiatkowski, N., Abraham, B.J., Carretero, J., Al-Shahrour, F., Zhang, T., Chipumuro, E., Herter-Sprie, G.S., Akbay, E.A., Altabef, A.*, et al.* (2014). Targeting transcriptional addictions in small cell lung cancer with a covalent CDK7 inhibitor. Cancer cell *26*, 909-922.

Dawson, M.A., Prinjha, R.K., Dittmann, A., Giotopoulos, G., Bantscheff, M., Chan, W.I., Robson, S.C., Chung, C.W., Hopf, C., Savitski, M.M.*, et al.* (2011). Inhibition of BET recruitment to chromatin as an effective treatment for MLL-fusion leukaemia. Nature *478*, 529-533.

Delmore, J.E., Issa, G.C., Lemieux, M.E., Rahl, P.B., Shi, J., Jacobs, H.M., Kastritis, E., Gilpatrick, T., Paranal, R.M., Qi, J.*, et al.* (2011). BET bromodomain inhibition as a therapeutic strategy to target c-Myc. Cell *146*, 904-917.

Dhalluin, C., Carlson, J.E., Zeng, L., He, C., Aggarwal, A.K., and Zhou, M.M. (1999). Structure and ligand of a histone acetyltransferase bromodomain. Nature *399*, 491-496.

Eberhardy, S.R., and Farnham, P.J. (2001). c-Myc mediates activation of the cad promoter via a post-RNA polymerase II recruitment mechanism. The Journal of biological chemistry *276*, 48562-48571.

Filippakopoulos, P., Qi, J., Picaud, S., Shen, Y., Smith, W.B., Fedorov, O., Morse, E.M., Keates, T., Hickman, T.T., Felletar, I.*, et al.* (2010). Selective inhibition of BET bromodomains. Nature *468*, 1067-1073.

Franco, H.L., and Kraus, W.L. (2015). No driver behind the wheel? Targeting transcription in cancer. Cell *163*, 28-30.

Haynes, S.R., Dollard, C., Winston, F., Beck, S., Trowsdale, J., and Dawid, I.B. (1992). The bromodomain: a conserved sequence found in human, Drosophila and yeast proteins. Nucleic acids research *20*, 2603.

Hnisz, D., Abraham, B.J., Lee, T.I., Lau, A., Saint-Andre, V., Sigova, A.A., Hoke, H.A., and Young, R.A. (2013). Super-enhancers in the control of cell identity and disease. Cell *155*, 934-947.

Hnisz, D., Schuijers, J., Lin, C.Y., Weintraub, A.S., Abraham, B.J., Lee, T.I., Bradner, J.E., and Young, R.A. (2015). Convergence of developmental and oncogenic signaling pathways at transcriptional super-enhancers. Molecular cell *58*, 362-370.

Kwiatkowski, N., Zhang, T., Rahl, P.B., Abraham, B.J., Reddy, J., Ficarro, S.B., Dastur, A., Amzallag, A., Ramaswamy, S., Tesar, B.*, et al.* (2014). Targeting transcription regulation in cancer with a covalent CDK7 inhibitor. Nature *511*, 616-620.

Leder, A., Pattengale, P.K., Kuo, A., Stewart, T.A., and Leder, P. (1986). Consequences of widespread deregulation of the c-myc gene in transgenic mice: multiple neoplasms and normal development. Cell *45*, 485-495.

Lehmann, B.D., Bauer, J.A., Chen, X., Sanders, M.E., Chakravarthy, A.B., Shyr, Y., and Pietenpol, J.A. (2011). Identification of human triple-negative breast cancer subtypes and preclinical models for selection of targeted therapies. The Journal of clinical investigation *121*, 2750-2767.

LeRoy, G., Rickards, B., and Flint, S.J. (2008). The double bromodomain proteins Brd2 and Brd3 couple histone acetylation to transcription. Molecular cell *30*, 51-60.

Loven, J., Hoke, H.A., Lin, C.Y., Lau, A., Orlando, D.A., Vakoc, C.R., Bradner, J.E., Lee, T.I., and Young, R.A. (2013). Selective inhibition of tumor oncogenes by disruption of super-enhancers. Cell *153*, 320-334.

Malumbres, M. (2014). Cyclin-dependent kinases. Genome biology *15*, 122.

Mertz, J.A., Conery, A.R., Bryant, B.M., Sandy, P., Balasubramanian, S., Mele, D.A., Bergeron, L., and Sims, R.J., 3rd (2011). Targeting MYC dependence in cancer by inhibiting BET bromodomains.

Proceedings of the National Academy of Sciences of the United States of America *108*, 16669-16674.

Metzger-Filho, O., Tutt, A., de Azambuja, E., Saini, K.S., Viale, G., Loi, S., Bradbury, I., Bliss, J.M., Azim, H.A., Jr., Ellis, P.*, et al.* (2012). Dissecting the heterogeneity of triple-negative breast cancer. Journal of clinical oncology : official journal of the American Society of Clinical Oncology *30*, 1879-1887.

Nair, S.K., and Burley, S.K. (2003). X-ray structures of Myc-Max and Mad-Max recognizing DNA. Molecular bases of regulation by proto-oncogenic transcription factors. Cell *112*, 193-205.

Nicodeme, E., Jeffrey, K.L., Schaefer, U., Beinke, S., Dewell, S., Chung, C.W., Chandwani, R., Marazzi, I., Wilson, P., Coste, H.*, et al.* (2010). Suppression of inflammation by a synthetic histone mimic. Nature *468*, 1119-1123.

Ott, C.J., Kopp, N., Bird, L., Paranal, R.M., Qi, J., Bowman, T., Rodig, S.J., Kung, A.L., Bradner, J.E., and Weinstock, D.M. (2012). BET bromodomain inhibition targets both c-Myc and IL7R in high-risk acute lymphoblastic leukemia. Blood *120*, 2843-2852.

Popovic, R., and Licht, J.D. (2012). Emerging epigenetic targets and therapies in cancer medicine. Cancer discovery *2*, 405-413.

Rahl, P.B., Lin, C.Y., Seila, A.C., Flynn, R.A., McCuine, S., Burge, C.B., Sharp, P.A., and Young, R.A. (2010). c-Myc regulates transcriptional pause release. Cell *141*, 432-445.

Rahman, S., Sowa, M.E., Ottinger, M., Smith, J.A., Shi, Y., Harper, J.W., and Howley, P.M. (2011). The Brd4 extraterminal domain confers transcription activation independent of pTEFb by recruiting multiple proteins, including NSD3. Molecular and cellular biology *31*, 2641-2652.

Vaz-Luis, I., Ottesen, R.A., Hughes, M.E., Mamet, R., Burstein, H.J., Edge, S.B., Gonzalez-Angulo, A.M., Moy, B., Rugo, H.S., Theriault, R.L.*, et al.* (2014). Outcomes by tumor subtype and treatment pattern in women with small, node-negative breast cancer: a multi-institutional study. Journal of clinical oncology : official journal of the American Society of Clinical Oncology *32*, 2142-2150.

Wang, Y., Zhang, T., Kwiatkowski, N., Abraham, B.J., Lee, T.I., Xie, S., Yuzugullu, H., Von, T., Li, H., Lin, Z.*, et al.* (2015). CDK7-dependent transcriptional addiction in triple-negative breast cancer. Cell *163*, 174-186.

Zuber, J., Shi, J., Wang, E., Rappaport, A.R., Herrmann, H., Sison, E.A., Magoon, D., Qi, J., Blatt, K., Wunderlich, M.*, et al.* (2011). RNAi screen identifies Brd4 as a therapeutic target in acute myeloid leukaemia. Nature *478*, 524-528.